ASSESSMENT OF LAND USE CHANGE IMPACTS ON HYDROLOGICAL PARAMETERS IN PORSUK RIVER BASIN - TURKEY

A Thesis Submitted to
the Graduate School of
İzmir Institute of Technology
in Partial Fulfilment of the Requirements for the Degree of

MASTER OF SCIENCE

in International Water Resources

by
Khalilullah ZULAL

July 2023
İZMİR

We approve the thesis of **Khalilullah ZULAL.**

Examining Committee Members:

_____
Prof. Dr. Orhan GÜNDÜZ
Environmental Engineering Department, Izmir Institute of Technology

_____
Prof. Dr. Alper BABA
International Water Resources Department, Izmir Institute of Technology

_____
Prof. Dr. Okan FISTIKOĞLU
Civil Engineering Department, Dokuz Eylül University

10 July 2023

_____
Prof. Dr. Orhan GÜNDÜZ
Supervisor, Environmental Engineering Department, Izmir Institute of Technology

_____
Assoc. Prof. Dr. Emre ALP
Co-Supervisor, Environmental Engineering Department, Middle East Technical University

_____
Prof. Dr. Alper BABA
Head of the International Water Resources Department

_____
Prof. Dr. Mehtap EANES
Dean of the Graduate School

ACKNOWLEDGEMENTS

First and foremost, I am grateful to Almighty Allah for his grace and guidance during my studies abroad.

This study was conducted with the partial support provided by the Scientific and Technological Research Council of Turkey (TÜBİTAK), project No. 121R014, in International Water Resources Department, Izmir Institute of Technology.

I would like to express my heartfelt, sincere gratitude to my supervisor Prof. Dr. Orhan Gündüz for his precious guidance, constructive suggestions, and encouragement from the start to the last moment of this research work. I am deeply grateful to my co-supervisor Assoc. Prof. Dr. Emre Alp at the Middle East Technical University (METU) in Ankara for his comments and corrections throughout this work. I would like to thank Assoc. Prof. Dr. Fernando Jaramillo at Stockholm University (SU), whose valuable guidance helped me setup the first steps of building my model at the Physical Geography Department of SU during a six-month exchange fellowship supported by EU Erasmus+ mobility. I am deeply grateful to Izmir Institute of Technology (IYTE), for providing such an outstanding opportunity for international student to feel home and learn at the highest quality.

I would like to thank Mr. Hilmi Angın, Ms. Tülin Angın, Mr. Haluk Hanlıoğlu, and Ms. Rezan Hanlıoğlu, whom I call my second family in Turkey for their invaluable support and inspiration during my stay in Izmir.

I would like to thank my family, especially my mother, sisters, and brothers, for their support and prayers during my studies abroad. Knowing that they are by my side and their presence always give me heart warmth and strength.

Last but not least, I would like to express my deepest gratitude to my very helpful friends here in Izmir and my beloved home country Afghanistan for their never-ending support, inspiration, and encouragement.

ABSTRACT

ASSESSMENT OF LAND USE CHANGE IMPACTS ON HYDROLOGICAL PARAMETERS IN PORSUK RIVER BASIN - TURKEY

Land Use Land Cover (LULC) change is considered to play an essential role in river basin hydrology. Climate change, and increase in urbanization have disrupted the hydrological parameters pattern in Porsuk River Basin (PRB). The current study is aimed to investigate the LULC change impacts on surface runoff, groundwater, evapotranspiration, and lateral flow parameters in the five sub-basins of the PRB under different LULC development scenarios (1990 & 2006) and one climate period (1989-2010) through hydrological modeling. In this study, the Soil and Water Assessment Tool (SWAT) model was utilized to analyze the hydrology of the river basin at watershed scale. The hydrological pattern characterization is based on five discharge gauges monitored by State Hydraulic Works (DSI) in the basin. The Kiranharmani, Parsibey, and Porsuk Ciftligi subbasins, the yearly increase in surface runoff reached 25%, 18%, and 12.91%, respectively, are more affected by landuse changes. The Scenario 2, contrary to Scenario 1, showed a noticeable reduction of groundwater infiltration in all subbasins with exception of Parsibey, due to rapid increased area of residential regions. In comparison to the 1990 LULC, changes in the 2006 LULC have a greater overall impact on hydrological processes in all sub-basins of the PRB. Therefore, it is believed that changes in specific LULC classifications can be linked to the reaction to changes in hydrological processes in a subbasin. Overall, this research is believed to be among the first to be done in the PRB, and the findings are thought to be helpful for water management.

Keywords: CORINE Land Use, Hydrological Parameters, Porsuk River Basin, SWAT

ÖZET

ARAZİ KULLANIM DEĞİŞİKLİĞİNİN HİDROLOJİK PARAMETRELER ÜZERİNDEKİ ETKİLERİNİN DEĞERLENDİRİLMESİ PORSUK NEHRİ HAVZASINDA – TÜRKİYE

Arazi Kullanımı Arazi Örtüsü (AKAÖ) değişikliğinin nehir havzası hidrolojisinde önemli bir rol oynadığı düşünülmektedir. İklim değişikliği, kentleşmedeki artış ve insan kaynaklı faaliyetlerin doğal kaynaklar üzerindeki etkisi Porsuk Havzası'ndaki hidrolojik parametre örüntüsünü bozmuştur. Mevcut çalışmanın amacı, farklı AKAÖ gelişim senaryoları (1990 & 2006) ve bir iklim dönemi (1990 & 2006) altında Porsuk Nehri Havzasının beş alt havzasındaki yüzey akışı, yeraltı suyu deşarjı, evapotranspirasyon ve yanal akış parametreleri üzerindeki AKAÖ değişiminin etkilerini araştırmaktır (1989-2010) hidrolojik modelleme yoluyla. Bu çalışmada, nehir havzasının hidrolojisini havza ölçeğinde analiz etmek için Toprak ve Su Değerlendirme Aracı (SWAT) modeli kullanılmıştır. Hidrolojik patern karakterizasyonu, havzada Devlet Su İşleri (DSİ) tarafından kontrol edilen ve izlenen beş deşarj göstergesine dayanmaktadır. Yüzeysel akıştaki yıllık artışın sırasıyla %25 (40,43 mm), %18 (33 mm) ve %12,91'e (34,21 mm) ulaştığı Kıranharmani, Parsibey ve Porsuk Çiftliği alt havzaları kara- değişiklikleri kullanın. Öte yandan, Senaryo 2, Senaryo 1'in aksine, Parsibey hariç tüm alt havzalarda, hızlı kentleşme ve artan yerleşim alanları nedeniyle yeraltı suyu infiltrasyonunda gözle görülür bir azalma göstermiştir. 1990 AKAÖ ile karşılaştırıldığında, 2006 AKAÖ'deki değişikliklerin Porsuk Nehri havzasının tüm alt havzalarındaki hidrolojik süreçler üzerinde daha büyük bir genel etkisi vardır. Bu nedenle, belirli arazi kullanımı sınıflandırmalarındaki değişikliklerin, bir alt havzadaki hidrolojik süreçlerdeki değişikliklere verilen tepkiyle bağlantılı olabileceğine inanılmaktadır. Genel olarak, bu araştırmanın Porsuk Nehri Havzası'nda yapılacak ilk araştırmalar arasında olduğuna inanılıyor ve bulguların su yönetimine yardımcı olacağı düşünülüyor.

Anahtar Kelimeler: CORINE Arazi Kullanımı, Hidrolojik Parametreler, Porsuk Nehri Havzası, SWAT

To my beloved father

TABLE OF CONTENTS

LIST OF FIGURES

Figure **Page**

Figure **Page**

Figure **Page**

Figure **Page**

LIST OF TABLES

Table **Page**

Table **Page**

LIST OF ABBREVIATIONS

ASTER – Space-borne Thermal Emission and Reflection Radiometer

CORINE - Coordination of information on the environment

DEM – Digital Elevation Model

ENS – Nash-Sutcliffe Efficiency

ETM – Enhanced Thematic Mapper

FAO - Food and Agriculture Organization

GIS – Geographic Information System

HRU – Hydrologic Response Unit

LULC – Land Use and Land Cover

NASA - National Aeronautics and Space Administration

PBIAS - Percent Bias

R^2 – Coefficient of Determination

SWAT – Soil and Water Assessment Tool

CHAPTER 1

INTRODUCTION

1.1. Study Background

The most important natural resource for all organisms is water. Due to the fact that there is a finite supply of water that is not spatially distributed according to population needs, it is crucial to manage water resources effectively in order to meet current demands and preserve sustainability. Planning and managing land use is strongly tied to ensuring the long-term viability of water resources since changes in land use are correlated with changes in water availability via pertinent hydrological processes (Guo et al., 2008). Environmental resources are under much pressure due to current global trends, including population growth and economic expansion, which frequently result in rising food consumption (Aghsaei et al., 2020; Grey et al., 2014). According to Aghsaei et al. (2020); (Anand et al., 2018), these developments cause changes in land use and land cover (LULC), which have a significant impact on hydrological processes. Global land-use patterns in river basins have undergone major changes as a result of the ongoing spread of human development. The result has been a significant alteration of the biological, energetic, and hydrological processes on the surface of the globe (Kalnay & Cai, 2003). The effects of changing land use on the planet's resources, the environment, and the likelihood of sustainable development are the main concerns of this widely debated scientific issue (Vorosmarty et al., 2000). Such influences on hydrological processes are seen in changes in the supply-and-demand relationship of water resources on a watershed scale, which will have a profound impact on the ecology, environment, and economy. Therefore, it will be critical for the planning, management, and sustainable development of water resources to have a more thorough knowledge of how land-use changes affect the hydrological processes in the watershed (DeFries & Eshleman, 2004). Studies on the effects of land-use changes on those hydrological processes had made little progress and were only seriously set up after the worldwide adoption of the LUCC plans (Bewket & Sterk, 2005).

Different types of land cover have varying values for albedo, abrasion length, root levels, and leaf area, which have an effect on the interactions between the land surface and atmosphere by influencing temperature, humidity, wind speed, and precipitation (Wei & Zhang, 2010; Yan et al., 2018). Different moisture at the surface, heat, and momentum fluxes will emerge from variations in these interactions as a result of changes in land use (Lee & Berbery, 2012; Sertel et al., 2010). To ascertain how much these changes may impact regional, nationwide, and worldwide climate and hydrological processes, it is crucial to consider the spatial distribution, magnitude, extent, and position of land cover changes.

Changes in land cover may impact a watershed's overall health and functionality (Miller et al., 2002). Surface discharge, evapotranspiration, lateral flow, and groundwater recharge are just a few of the land cover change-induced hydrological processes that can affect a watershed's runoff and ultimately vary the timing and volumes of surface flow. Modest boosts in urban growth may increase surface runoff because urbanization reduces infiltration, affecting streamflow and aquifer recharge. As a result, it is important to quantify how urbanization affects streamflow when creating mitigation strategies to deal with anthropogenic influences on watershed processes. Furthermore, by reducing roughness and increasing albedo, deforestation may reduce evapotranspiration, which may result in changes to precipitation patterns and intensity (Costa et al., 2003). Urbanization alters the watershed's surface runoff sensitivity due to changes in the evapotranspiration rate, surface roughness, and geographic distribution of vegetation.

The Soil and Water Assessment Tool (SWAT) (Neitsch et al., 2011), a distributed hydrologic model, was used in this work to assess the effects of LULC modifications on hydrological processes at five different watershed scales for the Porsuk River basin. The model was updated with 1990 and 2006 CORINE LULC maps, soil maps, and digital elevation models. To quantify the effects of various LULC changes, such as urbanization and agricultural area conversions, on the actual evaporation, infiltration, surface runoff, and groundwater flow in a water supply catchment and to analyze which components are more sensitive to various LULC changes, spatial distributions of LULC classes within the sub-basin level were evaluated.

1.2. Problem Statement

Porsuk River basin encompasses in two rapidly growing populated provinces, Eskişehir and Kütahya, respectively. The dense urbanization in the last two decades after the 1980s has had various impacts on resource bases, especially on residential spot expansion, deforestation, and agricultural lands. The water balance in this region has been troubled. As a result, there is a clear need for hydrological approaches and tools that can evaluate the impact of changing LULC on a watershed's hydrologic response, such as surface runoff, evapotranspiration, groundwater infiltration, etc. Spatially distributed modeling can offer means that can be used for sustainable management of water resources.

1.3. Research Objective

The main objective of this study is to analyze the two different land use and land cover (CORINE 1990 and 2006) change impacts on the four specific hydrological processes (surface runoff, evapotranspiration, groundwater recharge, and lateral flow) utilizing Soil and Water Assessment (SWAT) model and geographic information systems (GIS) techniques. The specific objectives of the study are listed as follows:

1. To extract and produce the CORINE land use and land cover maps of the Porsuk River basin for 1990 and 2006.
2. To figure out the most essential sensitive flow parameters
3. To setup the SWAT model
4. To conduct calibration and validation of the SWAT model.
5. To assess the SWAT model performance
6. To analyze the changes in hydrological processes due to land cover/use change

1.4. Research Questions Addressed

The above objectives are addressed within the following research questions.

1. How is the Soil and Water Assessment Tool's (SWAT model) ability towards the simulation of surface runoff, groundwater, evapotranspiration, and lateral flow parameters in the basin between CORINE 1990 and 2006 land use patterns?
2. To what extend the CORINE 1990 and 2006 land use changes impact the hydrological processes (surface runoff, groundwater, evapotranspiration, and lateral flow) in the basin?

CHAPTER 2

LITERATURE REVIEW

With urbanization, land use and land cover (LULC) changes frequently involve the conversion of forests and agricultural areas to rangelands and urbanized areas. Increases in impermeable surfaces caused by urban expansion frequently result in hydrologic change and deterioration of water quality at local scales (Dunne & Leopold, 1978; Paul & Meyer, 2001; Rose & Peters, 2001).

Urbanization replaces forest or agricultural lands, which increases impervious surfaces to often create local economic growth within a watershed. In order to prevent flooding damage associated with reduced infiltration, hydrologic researchers are concerned about the increased quantity of runoff since mid-1900s (Brabec et al., 2002). To further provide a better knowledge of land use change, further researches have been conducted towards the investigation of the ratio of pervious land use and impervious surface in connection to the context of current land use (Brabec et al., 2002). Impervious surfaces, such as parking lots, roadways, and rooftops generate high runoff, raise the total volume, induce peak discharge to emerge early, and increase the frequency of flooding by preventing infiltration of precipitation (Coutu & Vega, 2007). This describes how shifting hydrological processes make a watershed more hydrologically active due to increased level of development.

In general, land use changes result in less natural open spaces and typically more impervious surfaces like parking lots, roadways and residential neighborhoods (Leopold, 1968). A watershed's hydrology degrades due to modified hydrological status caused by increased impermeable surfaces, thus affecting streamflow characteristics, increasing runoff volumes, and time to peaks (Coutu & Vega, 2007). Decreasing a watershed’s response time to a precipitation event worsens the flooding conditions (USDA, 2000). An increase in the area of settlements and construction activities in a watershed makes drought and flooding a major issue. In order to successfully execute sustainable strategies for the management of water and land resources, decision- and policy-makers must have a thorough understanding of the effects of LULC change on watersheds.

2.1. Land Use Change and Hydrological System

LULC modifications have been made since the beginning of human history. They reshaped the landscape and changed the hydrologic regimes all over the planet. Understanding the consequences of LULC change in highly changed watersheds has become more critical since industrial LULC change has risen in frequency and magnitude over the past few decades. A typical example of a dynamic shift in land cover is clearing vegetation for grazing or farming or the regrowth of planted woods (Watson et al., 2014).

More and more people are becoming aware of the issues with water quantity and quality brought on by changes in land cover and climate, which are the main causes of hydrological fluctuations (Arceo, 2017; Arceo et al., 2018; Li et al., 2021; Zhang et al., 2018). Resource managers must comprehend how these various components interact to ensure water security because a constantly expanding population depending on a resource that is susceptible to the effects of LULC change is likely to experience detrimental consequences on water availability.

A watershed is a region of land where precipitation (rainfall and snowmelt) flow into a network of streams with just one outlet point. Watersheds offer the water supplies needed by species at all trophic levels for household, agricultural, and ecological maintenance. As precipitation returns to the ocean, where the majority of evaporation in the water cycle starts, it is through runoff, infiltration, and evaporation and transpiration inside watersheds that the water cycle is completed (Gleick, 1996).

By geographic information systems (GIS) based hydrologic modeling, the complexities of watersheds, particularly the interconnectedness of land-cover change and climate, and the hydrologic cycle are made simpler. Each watershed and the associated parameters are unique due to the nonlinear behaviors of numerous hydrological processes (climate, land-cover change, etc.) (Zhang et al., 2018).

The perpetual movement of water through the various elements of the Earth's climate system is reflected in the hydrologic cycle (Figure 2.1). Seas, the atmosphere, and the earth's surface all collect water. Throughout various phases, water moving between these basins is crucial to the climate system. Both the sea and the surface of the earth release water vapor into the air, where it circulates as humidity across the surface of the world. In the form of sleet, snow, hail, and rain, the water vapor eventually condenses into the atmosphere and returns to the earth. This precipitation may fall into open water

bodies, be gathered and absorbed by vegetation, and then transform into surface flow or groundwater recharge. Water that has permeated the land's surface may seep into the deep places and turn into a source of groundwater storage before eventually resurfacing as streamflow or mixing with saltwater in coastal regions. The water cycle is finished when the water returns to the ocean in this final stage and eventually evaporates (Pagano & Sorooshian, 2002).

The water cycle and changes in land use are intricately related. A comprehensive strategy for managing water resources is necessary because of the rise in freshwater demand brought on by meteorological and LULC variations (Zeng et al., 2012). The amount of natural areas that can absorb water decreases as impervious land increases, which in turn affects river discharge within a watershed (Leopold, 1968). The frequency of unexpected floods is increased by these impermeable surfaces and climate variations. Due to the variability in land use, soil, and topography, it is difficult to accurately quantify the effects of rural and urban changes in land use on the hydrological response of a watershed. Water quality and quantity are determined mainly by processes including evaporation, transpiration, interception, and surface runoff, and LULC is considered a key component in hydrological models (Hörmann et al., 2005).

Watershed modeling has developed beyond physical processes to describe socioeconomic as well as environmental interplay at an accessible price and within a specified timeframe as a result of improvements in data collecting and management (Ali Mirchi et al., 2010). Hydrologic modeling tools' production of data on catchment runoff related to peak discharge, runoff volume, and the timing of peak discharge occurrence will aid in effective flood preparedness. Distributed hydrologic models, as opposed to conventional lumped hydrologic models, give more physically meaningful information that is important to assist planning and policy decisions through flood prediction, early warning systems, and potential disaster distribution.

Because it involves several hydrological domains (saturated, unsaturated, overland, etc.), understanding the mechanisms of hydrological modeling in a watershed is one of the most challenging tasks. In fact, there are numerous flow mechanisms that may be distinguished, such as Horton overland flow, which happens when precipitation intensity exceeds soil infiltration capacity and causes water to pool on the ground's surface. Horton overland flow typically occurs in dry and semiarid environments during periods of heavy rainfall and sparse vegetation. Saturation overland flow, on the other hand, is another type of flow that happens when the soil is completely saturated as a result

of the groundwater level rising to the surface of the land. Moist overland flows are common in wet places. Stream flows occur when water flowing over the land progressively transforms into a tiny stream. Finally, as water comes to the catchment water drainage system, channel flow develops.

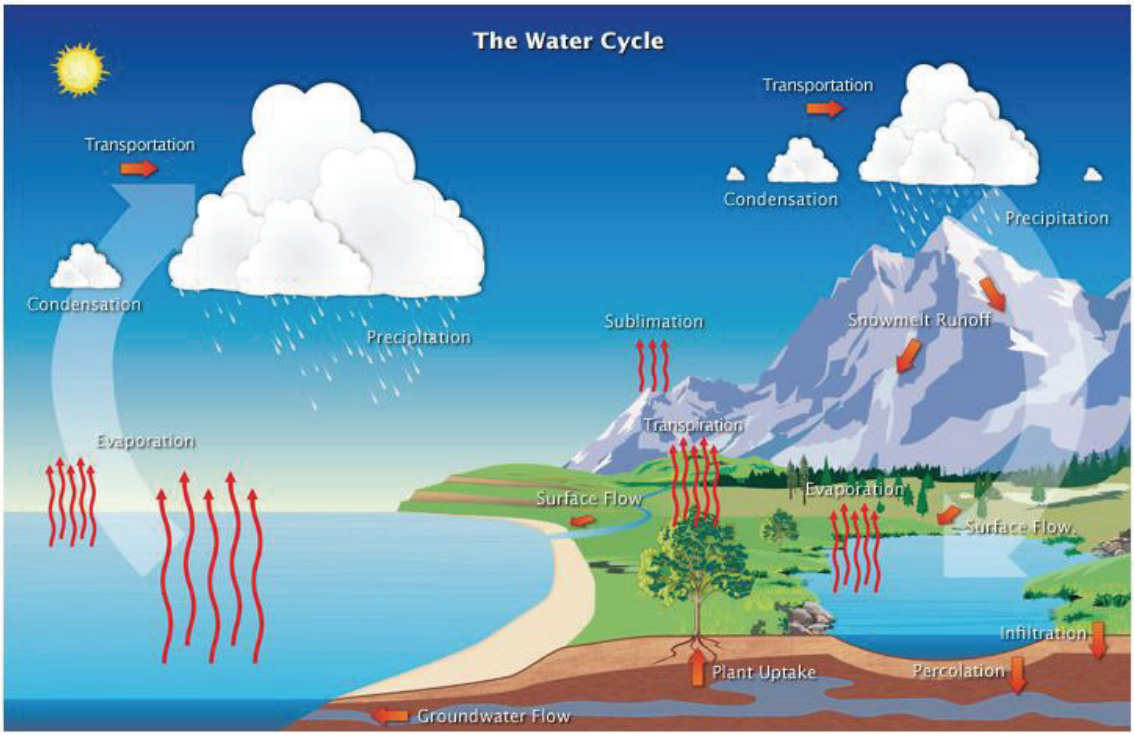

Figure 2.1. Hydrological Water Cycle (NOAA National Weather Service)

Based on the findings of (Arnold Jr & Gibbons, 1996; Paul & Meyer, 2001; Rose & Peters, 2001; Schueler & Galli, 1992), the impervious cover has historically been acknowledged as one of the most crucial factors in assessing the effects of urbanization on hydrology. With the removal of natural vegetation, the growing impermeable cover associated with urbanization influences the channel formation of the stream, the temperature of the water, and the quality of the streamflow. Typically, runoff is accepted to double if the impervious surface area is increased by 10–20% (Paul & Meyer, 2001). As seen in (Figure 2.2.), total runoff could increase by around five times in a region with 75% to 100% impermeable cover (Arnold Jr & Gibbons, 1996; Paul & Meyer, 2001).

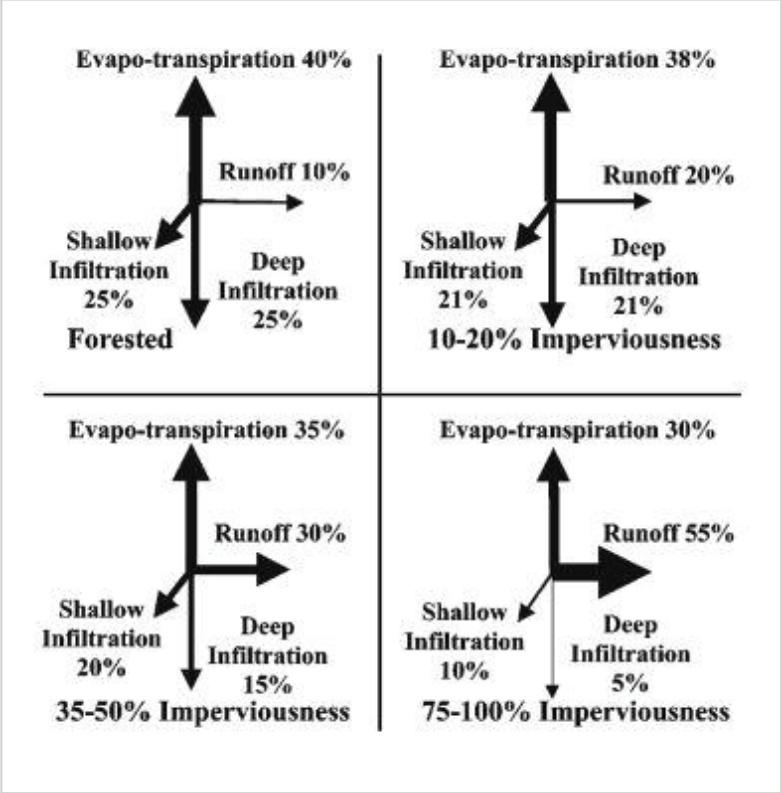

Figure 2.2. Diagram showing how hydrologic flows are predicted to fluctuate under various surface coverings (arnold & gibbons 1996).

2.2. Peak and Base Flow Changes

Urbanization and climatic changes alter hydrological patterns by raising runoff, peak discharge, flow volumes, and flood frequency while decreasing seepage, base flow, and delay time. More impermeable lands would come from growing urbanization, which would worsen flood events. Climate change and land use changes may have a negative impact on the hydrological cycle and the frequency of high flows (floods) and shallow flows (droughts) (Arnold Jr & Gibbons, 1996; Dougherty et al., 2007; Hollis, 1975; Ogden et al., 2011; Smith et al., 2005). These changes could have a negative impact on urban infrastructure as well as ecosystems in tropical regions. Changes in land use, especially the growth of metropolitan areas, can worsen surface runoff. (Du et al., 2012).

The impact of land use alterations on the hydrological responsiveness of watersheds has been investigated by numerous scholars. For instance, (Emam et al., 2015) evaluated the impact of changes in land use on surface water discharge in the Razan-

Ghahavand watershed in Iran using the Soil and Water Assessment Tools (SWAT) model. (Li & Wang, 2009) investigated the impacts of changes in land use and land cover on surface water discharge in the Dardenne Creek watershed in St. Louis, Missouri, USA using a Long-Term Hydrologic Impact Assessment (L-THIA) model. Using the Hydrologic Modeling System (HEC-HMS), (Du et al., 2012) created an integrated modeling system to assess the consequences of urbanization on peak flow events in the Qinhuai River watershed in Jiangsu Province, China. According to Wang and Cai (2009), groundwater utilization for agricultural, commercial, and residential uses are a major factor in the decline of the base flow in urbanized watersheds. Land cover changes, which are indirect human interferences, also have an impact on peak flow.

2.3. Hydrological Modeling in Runoff studies

The most crucial tools for studying the effects of LULC change on water resources are hydrological models, which are among the various ways that are accessible to comprehend and address water-related difficulties (Lundin et al., 2000). The research on watersheds has become more effective with the incorporation of contemporary modeling methods and GIS data. Spatial modeling as well as simulation for flood surveillance and projection, have improved thanks to the use of satellite observational data with greater resolution, increased computer power, and enhanced GIS database management (A Mirchi et al., 2010). When taking into account factors like the types of soil, surface roughness, and infiltration ability of the soil, surface runoff volume and distribution are directly related to land usage (Hörmann et al., 2005). These variables serve as inputs for a hydrologic model that generates information.

Understanding how data and models relate to one another is a crucial foundation for modeling. With the help of geographic information systems and powerful pre- and post- processors for hydrological models, today's technology and computers can provide users with a collaborative modeling environment. Global breakthroughs in remote sensing, coupled with modeling and data integration, are producing new sources of knowledge.

Modeling is often used to investigate how LULC affects the hydrologic system. For instance, runoff from the surface in the Dardenne Creek Basin in Missouri and

immediate runoff as a result of LULC in the Richland Creek Watershed in Illinois were investigated using the Long-Term Hydrologic Impact Assessment (L-THIA) and the EPA Storm Water Management Model (SWMM) (Li and Wang, 2009). The Soil and Water Assessment Tool (SWAT) (Arnold et al., 1998) is another model that is used to simulate the response of watersheds to various precipitation and agricultural nutrient inputs. SWAT is a semi-distributed hydrological model that can simulate hydrology, agricultural yield, and nutrient fluxes simultaneously. While modeling for land use and runoff mostly focuses on short-term storm events with an emphasis on peak flows and floods, climate modeling mainly considers long-term scenarios.

Rainfall-runoff analysis is another application of watershed modeling. The rainfall and runoff modeling analysis are clustered into three main groups, which are; distributed, semi-distributed, and lumped models. Distributed modeling represents the spatial and temporal variables that control the conversion of precipitation into runoff with the aim of improving the simulation of the hydrological processes of a watershed. Distributed hydrologic models specifically take into account the many processes and geospatial changes throughout a watershed. These models make an effort to characterize the spatial heterogeneity of hydrologic parameters, and they use these data to examine the processes of rainfall-runoff at specific sites inside a hydrological basin (Smith, 1993). In semi-distributed modeling, the spatially variable factors or conditions are essentially represented in a semi-distributed manner as a set of sub-basins with standardized properties (Vieux et al., 2004). It reflects all hydrologic simulations in which there are numerous sub-basins that make up the watershed. Sub-basins are not gridded, and uniform infiltration and theoretical surface transformation techniques are used, as well as average precipitation for each sub-basin (Paudel, 2010). Finally, in the case of lumped modeling, models assume that the soil, vegetation, and land use patterns within a watershed are all the same. This is a key premise since the infiltration characteristics along a watershed are typically averaged and controlled by the soil and land use. Constructing deductions from the average precipitation allows for the computation of runoff for the drainage basin. This runoff is transformed using a unit hydrograph idea in conventional lumped models to calculate the overall stream flow at the basin outflow. A lumped model is a mathematical formulation that treats a watershed as a relatively homogeneous unit.

2.4. Soil and Water Assessment Tool (SWAT) Applications around the Globe

The Soil and Water Assessment Tool (SWAT) is a river basin model with semi-distributed, continuous-time steps (Arnold et al., 2012). Watershed-scale hydrological process analysis has made extensive use of SWAT. This model was created to assess the long-term effects of climate change and land management techniques on the water in vast and intricate watersheds with a range of soil types, land uses, and management circumstances (Arnold et al., 1998). The water balance equation that the model's hydrological components is built on processes including precipitation, surface runoff, water yield, ET, lateral flow, percolation, and groundwater flow (Arnold et al., 1998). Some of the sample applications of SWAT model around the world are as follows:

2.4.1. USA

The study by Chien et al. (2013) aims to evaluate the potential impacts of climate change on future streamflow (2051-2060 and 2086-2095) for the Rock River Illinois River, Kaskaskia River, and Wabash River, watersheds in the Midwestern United States, primarily in Illinois. The distributed hydrologic model, the Soil and Water Assessment Tool (SWAT), is calibrated and validated using distributed streamflow data (1978-2009). The SWAT streamflow simulations were driven by forecasts from nine worldwide climate models under a maximum of three IPCC Special Report on Emissions Scenarios (SRES) scenarios to evaluate the possible effects of climate change on future water supplies (A1B, A2, and B1). In this study, they found that model validation depicted enough spatial and temporal predictions of streamflow and suggested several site calibration approach to more precisely predict the spatial alteration in the catchment hydrology.

The studies by (Cherkauer & Sinha, 2010); Hay et al. (2011); (Jha et al., 2006; Kang & Ramírez, 2007) in the Midwestern United States examined the effects of future climate projections form GCM downscaled simulations on the water resources. The four above studies have done on lake Michigan of the Michigan state, Naches and Sprague rivers in Washington & Oregon states, Mississippi river in Minnesota & Wisconsin states,

and South Platte river basin in Colorado state. The above four studies emphasize on understanding of how future climate changes may alter the hydrology of the interested river basins in the USA.

In another study in the USA, In the Racoon River watershed, Schilling et al. (2008) found that enhanced perennial vegetation improved annual ET while decreasing water output. In this research which has been conducted within SWAT model and ArcMap, three basic scenarios for LULC change were analyzed, as well as three scenario variations, including an increase in maize area in the catchment and two scenarios, including land expansion employing summer and cool winter grasses for ethanol biofuel. the authors found that the results of the modeling were congruent with historical observations. Increased maize output reduces yearly ET while increasing water yield.

In the aspects of SWAT model calibration and validation studies in the USA, Santhi et al. (2001) successfully calibrated and validated a SWAT model for sediment and nutrient simulations for the Bosque River watershed in Texas, with an area of 4300 km2 characterized by pasture, range, and row crop land uses. This study examines the validity of calibration and validation at two different points along the North Bosque River, Hico and Valley Mills. Stream calibration was carried out from 1960 to 1998. Calibration of sediment and nutrients was performed at Hico from 1993 to 1997, and at Valley Mills from 1996 to 1997. For 1998, model validation was carried out. To validate model predictions, periodic plots and measurements of statistical significance were used.

2.4.2. Europe

SWAT model has widely been applied for different purposes in European countries in recent years after the model has been developed.

(Glavan et al., 2013) evaluated the influence of past land use patterns on hydrological processes and the accessibility of water supply and retention for people and wildlife under present climate conditions in Slovenia. Furthermore, the authors explained

how this information could be utilized to anticipate or improve future land management alternatives, as well as serve as an outline for subsequent water and land administration. For the research sites, that are two small-scale Slovenian basins (Reka and Dragonja), the study included digitized historical maps of land use from 1787, 1827, 1940, and 1984, as well as a digital land use map from 2009.

In another study, (Shukla et al., 2023) have utilized SWAT model to assess the LULC alterations effects on the amount of runoff in Rur basin, Germany. In this work, the model was calibrated between 2000 and 2010, against the observed data at three catchments (Monschau, Stah, and Linnich) then validated between 2011 and 2015. The hydrological model's performance was evaluated using statistical indicators which include the percentage bias (PBAIS), coefficient of determination (R2), r-value, and p-value.

In an extensive study by (Koltsida et al., 2023), SWAT model was used to assess the discharge simulation and administrative decisions using daily and hourly precipitation data time scale in a mixed containing land use Kifisos subbain, Greece. The research was conducted to observe the effects of rainfall data resolution on the performance of the model. The model outputs were calibrated and validated using SWAT-CUP program for the years of 2018 and 2019, respectively. The results in this study, showed that the model in daily timescale performs better compared to subdaily. The performance indicators were found to be $R^2 = 0.87$, NSE = 0.86, and PBIAS = 4.2 %; and $R^2 = 0.63$, NSE = 0.6, and PBIAS = 11.7 % for daily and subdaily timescale, repectively.

2.4.3. Asia

Water scarcity and groundwater shortage is becoming a crucial issue for the developing countries, including Afghanistan, in the southwest of Asia. In a comprehensive research study by (Hussainzada & Lee, 2021), the authors have endeavored to evaluated and assess the water loss in northern Afghanistan, Balkhab river basin using SWAT model. The model has been conducted based on monthly timespan to simulate the surface runoff. The findings in this study have shown a well behaved performance by the model having a Nash-Sutcliff efficiency (NSE) values of 0.52, 0.83,

0.40, and 0.57; R2 values of 0.70, 0.86, 0.67, and 0.80; and percent bias (PBIAS) values of 23.4, −8.5, 23.4, and 17.5 in the four subbasins, namely, Rabat-i-Bala, Pul-i-Baraq, Doshqadam, and Nazdik-i-Nayak during calibration and good validation statistics.

In a study by (Ghoraba, 2015) in Simly Dam watershed, part of Saon river basin Pakistan, SWAT model was utilized to simulate the discharge flow and evaluated the monthly timescale volume income water to Simly dam. In this study, model was calibrated between 1990 – 2001 and validated between 2002 – 2011. Based on the study findings, the model depicted a good enough performance during both phases, calibration and validation, respectively. The model performance was assessed using Coefficient of Determination (R^2) and Nash and Sutcliffe Efficiency (NSE) having 95% and 84% during calibration and 84% and 80% in validation period.

Another study using SWAT model in the continent of Asia is conducted by (McGinn et al., 2021) in Myanmar. This research focused to investigate the LULC change impacts on water resources of Chindwin river basin over two decades from 1999 to 2019. Apart from the physical data, this work includes interviews which shows that widespread side of SWAT application. The detections by the model in LULC changes are a downfall in forest field of 2%, an increase in rangeland (0.38%) which is a shrink in forest area and decrease of 2.1% in agricultural land of the region in two decades. Additionally, based on the fact that the forest area got decreased, evapotranspiration had seen reduction in volume.

2.4.4. Africa

The study by Diriba (2021) aimed to analyze the surface discharge/runoff by Soil and Water Assessment Tool model in Dabus catchment, Ethiopia. Dribia (2021) simulated surface discharge/runoff using meteorological data from (1987-2016). The findings demonstrate that during both calibration and validation, there was a solid correlation between observed and simulated streamflow. The watershed's simulated annual mean surface runoff was 690.84 mm. The maximum yearly surface runoff was found in the watershed's southeast region. Consequently, this work demonstrates that the

Dabus watershed may be modeled using the SWAT hydrological model for improved evaluation and modeling of the hydrological processes.

Another study by (Mengistu et al., 2022) have used SWAT model in Gilgel Gibe watershed in East Africa. The authors have used the model to assess the factors that impact the hydrological parameter of the watershed utilizing three different type of LULC data from years of 2000, 2010, and 2020 produced from Landsat processed images. This study evaluated the impacts of the above determined LULCs on surface runoff and groundwater recharge. The study concluded that SWAT model's ability to perform satisfactorily and it showed reasonable results with R2 and NSE greater than 0.84.

To investigate the effects of various land use classes on variations in the hydrological components, a combined strategy utilizing a SWAT model and partial least squares regression (PLSR) was used by Twisa et al. (2020). Throughout the research period, the main land use changes that affected the hydrology constituents in the basin were the extension of agricultural land, the growth of the building space and grassland, and the reduction of the natural forests and woods. For improved strategic and operational decisions in the utilization of the basin's resources, these findings offer decision-makers and stakeholders baseline data on land and water resources.

2.4.5. Australia

Globally, simulating the effects of changing land use on water balance has been done extensively using the Soil and Water Assessment Tool (SWAT) model. The original SWAT model, however, performs poorly when attempting to estimate the leaf area index (LAI) of various types of vegetation for tropical regions. (Zhang et al., 2020) used an enhanced SWAT model with weed growth calibrated from MODIS LAI data. This work aimed to predict the effects of several changes in land use scenarios (deforestation, afforestation, and urbanization) on the water balance. For forest-evergreen, range-grass and urban land uses, a substantial positive correlation between yearly rainfall and total runoff (r 0.94) was found. Under the same rainfall, terrain slope, and soil texture conditions, forest-evergreen land use often generated smaller total drainage than range-grasses and urban land use. Moreover, under the same circumstances, urban land use

commonly generated larger water flow and so less horizontal drainage and underground water than forest-evergreen and range-grasses.

2.5. SWAT Applications in Turkey

2.5.1. General Applications in Turkey

A study by Cuceloglu et al. (2017) evaluated Istanbul's water resources' water budget components that used a high-resolution hydrological modeling approach. The Soil and Water Assessment Tool (SWAT), a continuous-time, semi-distributed, and process-based model, was used in this study to model Istanbul's water resources and the watersheds nearby. The model was calibrated and validated utilizing the SUFI-2 algorithm for the years 1977 to 2013 at 25 monitoring stations using the SWAT-CUP application. The findings showed that Istanbul had a 3.5 billion m^3 annual blue-water potential, while on the other side, its green-water flow and storage were 2.9 billion m^3 and 0.7 billion m^3, respectively. The model emphasized the city's water potential in the current environment and provides information on how it was distributed spatially throughout the area. This study served as a solid foundation for future research on better water resource management techniques, water quality, climate change studies, and other socioeconomic scenario analyses in the area.

In a study by Bucak et al. (2018), the biggest lake in the Mediterranean basin, Lake Beyşehir, was selected to examine the effects of climate change and different land use scenarios on the dynamics of freshwater ecosystems in the Mediterranean and the services they offer using SWAT model. In the beginning, the outputs were connected from the catchment models to the two distinct processed-based lake models, PCLake and GLM-AED, and tested scenarios using five general circulation models, two representation concentration pathways, and three different land use scenarios. This allowed the authors to take into account the numerous sources of uncertainty. Hydraulic and nutrient loads from the catchment to the lake were expected to drop significantly in the future under climate change and land development scenarios. Results also indicated that future cyanobacterial abundance might limit ecosystem services related to drinking

water and harm ecosystem integrity. The ecosystem services provided by the lake as a source of water for agriculture and drinking water may also be harmed by prolonged durations of diminished hydraulic stresses from the watershed and increased evaporation.

The Soil and Water Assessment Tool hydrologic model was used in a study by Sertel et al. (2019) to examine the effects of land use alterations on watershed parameters and hydrological processes in the Buyukcekmece Watershed of Istanbul Metropolitan City, Turkey. After finishing calibration operations under gauge-data sparse conditions, the SWAT model was tested for two distinct scenarios for the 40 years between 1973 and 2012. For the first case, 1990 LULC with meteorological data between 1973-2012 were utilized. For the second case, 2006 LUCL with the same meteorological data of the first scenario was used to study the effects of landscape parameters on hydrological pattern behavior. According to the study, under identical climatic factors, changes in land cover/use, particularly urbanization, had a significant impact on hydrological dynamics, with changes in actual transpiration, base flow, runoff, percolation, and soil water primarily caused by changes in urban and agricultural areas.

In the Seyhan River Basin of Turkey, in a work by El-Sadek and Irvem (2014), the outcomes of employing three separate kinds of land cover datasets through the soil and water assessment tool (SWAT) model to simulate stream flow and sediment output were examined and compared to the observed data. The coordination of information on the environment dataset (CORINE; CLC2006), the global land cover characterization (GLCC) dataset and the GlobCover datasetweare the three land cover datasets that were used. The findings implied that the monthly runoff and sediment simulations from the Seyhan River basin showed very little sensitivity to the LULC datasets with varied spatial resolutions and from different time periods.

In a work by Koycegiz and Buyukyildiz (2019), streamflow along the Arşamba River's headwater in Turkey's Konya Closed Basin was simulated using a semi-distributed soil and water assessment tool (SWAT) model. The SWAT model was first calibrated using the sequential uncertainty fitting-2 (SUFI-2) approach. Also, the outcomes of the radial-based neural network (RBNN) and support vector machines are contrasted with those of the SWAT model (SVM). The Nash-Sutcliffe efficiency coefficient (NSE) and determination coefficient (R^2) values for the SWAT model at the

calibration stage were both 0.787 and 0.779, respectively, but these values were substantially lower at the validation stage (R^2 = 0.508 and NSE = 0.502). The authors found that AI models produce highly accurate findings but only offer discharge outputs. The SWAT model was suitable for addressing physical issues connected to hydrological processes, such as snowmelt, soil moisture, and groundwater. This model can also be used to determine how land use and cover changes will affect hydrologic fluxes.

The study by Cuceloglu and Ozturk (2019) evaluated the viability of simulating streamflow at numerous gauges in the mountainous Black Sea catchment using the Climate Forecasting System Reanalysis (CFSR) and local climate data. Additionally, the model's use of the altitudes band was examined for applicability. As a hydrological simulator, SWAT is employed. Using SWAT-CUP and the Sequential Uncertainty Fitting (SUFI-2) technique, calibration and uncertainty analysis were carried out using monthly streamflow data from six different hydrometric stations that were situated at various altitudes. In comparison to the local dataset, the results showed that the CFSR dataset offered pretty sensible agreements between both the simulation and the actual streamflow at the monitoring stations.

Cüceloğlu et al. (2021) examined the hydrological elements of a basin in Turkey in order to determine the impact of employing two alternative LULC datasets. The research region is the 621 km^2 drainage area of the Omerli Basin, which covers one of Istanbul's major drinking water reservoirs. This groundbreaking study uses the SWAT model at the sub-basin level to assess and contrast the effects of the CORINE and LANDSAT 7 ETM LULC data used in hydrological modeling. In terms of runoff from the surface and real evapotranspiration, it was discovered that several LULC datasets produced results that were quite similar in the Omerli basin. However, variable spatial distribution was discovered, especially in populated sub-basins. LANDSAT 7 ETM data, despite having a coarser land-use classification, allowed for the discovery of various LULC categorizations with a better spatial resolution, which led to varied model results, particularly in the urbanized sub-basins.

2.5.2. Applications in Porsuk River Basin

In the only study conducted in the Porsuk river basin by Güngör and Göncü (2013), the Soil and Water Assessment Tool is used to model the hydrology of the Lower Porsuk River Watershed in Turkey in order to identify the best water management practices. Data retrieved from two monitoring sites were used for the calibration and validation processes. The model is set for the period 1978–2009, and while the calibration period was the 1998–2004 period, the validation period has included the entire period. The authors have utilized the SWAT-CUP as the uncertainty program. After the model run in multiple iterations, the upstream Esenkara station's monthly Nash-Sutcliffe and R^2 performance indices have been 0.74 and 0.88 for the calibration period and 0.87 and 0.87 for the validation period, respectively. Near the watershed outlet at the Kiranharmani station, values of 0.59 and 0.72 for the calibration period and 0.44 and 0.56 for the validation period, respectively, were recorded. Upstream of Eskisehir, the SWAT model has performed well but, at the watershed outflow, the model has performed poorly due to unknown irrigation abstraction quantities. Data availability has also been hampered by the inadequacy of observing stations on the main channel and its tributaries. Performance indicators, however, showed that the catchment between the Porsuk River and the Eskisehir has been adequately calculated. This result can give decision-makers a tool to accurately anticipate the water resources that Eskisehir will have access to.

CHAPTER 3

DESCRIPTION OF THE STUDY AREA

3.1. Location

Porsuk River Basin is one of the main sub-basins of the Sakarya River Watershed. It is located in the Central Anatolia Region. Porsuk River reaches Sakarya by passing through the provinces of Kütahya and Eskişehir. The Porsuk River basin is located between 29°38'-31°59' east longitudes and 38°44'- 39°99' north latitudes in northwest Anatolia and covers an area of 10 825.19 km². The basin has a width of 202 km in the east-west direction and 135 km in the north-south direction and is the most important branch of the Sakarya River with a length of 448 km. The annual average natural flow is estimated around 15.47 m3/s with average annual precipitation height of 466.4 mm/year. Table 3.1 provides further information regarding the general outlook of the basin. The Porsuk River is the main drainage unit of the basin and arises from the skirts of Murat Mountain in Kütahya. After passing Kütahya province center, the Porsuk River, first receives the Kunduzlar Stream and then the Kargın Stream. Afterwards, its slope decreases until it joins Sakarya River. Porsuk River continues to flow through the middle of Eskişehir city in the west-east direction, taking Sarısu Stream. After the city center, the branches that join the Porsuk until it mingles with Sakarya are short, and have comparably low flow rates. (Güngör, 2011).

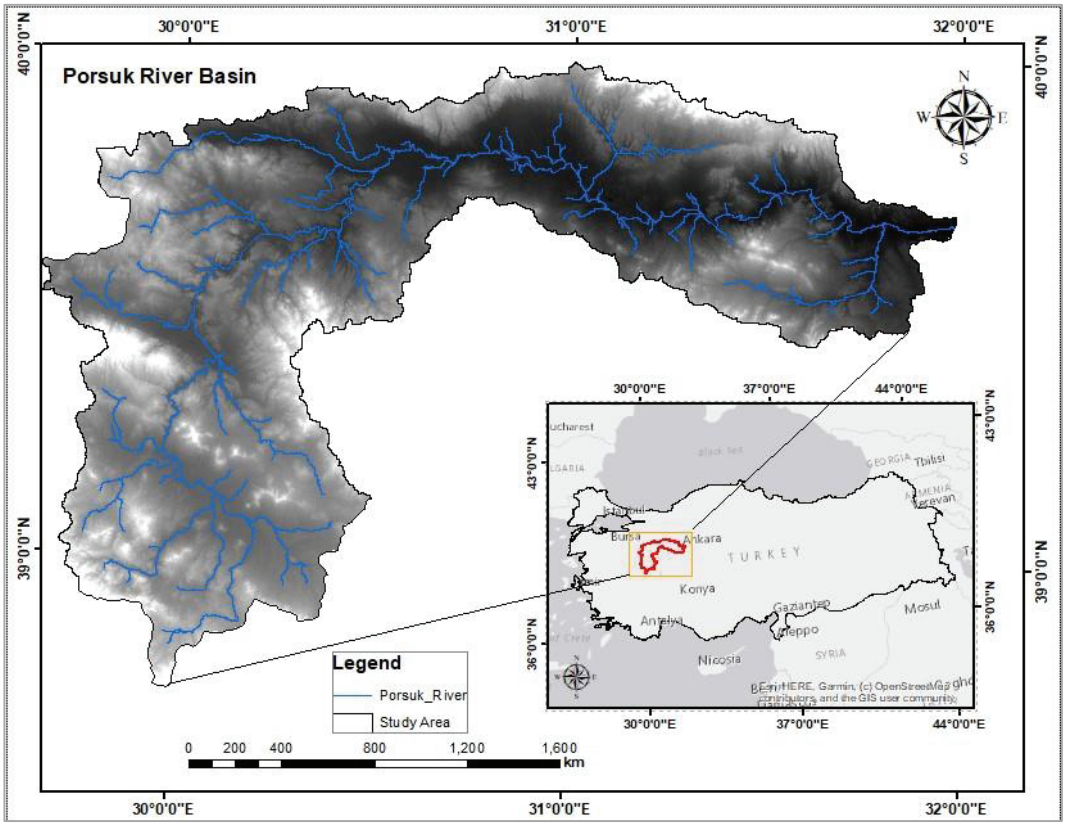

Figure 3.1. Location of the Study Area

Table 3.1. Porsuk River Basin General Characteristic Values

Drainage Area	km²	10 825
Average Altitude	m	1050.80
Population (2012)	person	1 002 397
Municipality Population (2012)	person	930 614
Ratio of Municipality Population to Total Population	%	0.93
Annual Average Natural Flow	hm³	487.85
Annual Average Natural Flow	m³/s	15.47
Annual Average Yield	L/s/km²	1.43
Average Annual Precipitation Height	mm	466.44
Annual Average Flow Height	mm	45.1
Flow / Precipitation Rate	%	9.7

3.2. Climate

Porsuk Stream and its basin are on the threshold of Inner Western Anatolia, in the transition zone from the moderate climate of the Western Black Sea, Aegean, and Marmara regions to the continental climate of Central Anatolia. It has a unique climate where winters are harsh, long, and rainy; summers are hot and dry. In winter and summer, the temperature differences between day and night are quite high. In the basin, the Central Anatolian precipitation regime is generally dominant. The rainy seasons of the basin, which are slightly longer than the Central Anatolian continental climate, coincide with the winter and spring months. It is seen that precipitation decreases especially towards the east. In Eskişehir Station, which was put into operation in 1929 and is one of the stations with the longest rainfall observation in the basin, the average annual total precipitation was calculated to be 368.4 mm. The average annual precipitation at Kütahya Station, which was put into operation in 1929, was calculated to be 555.6 mm. The stations with the longest temperature observations in the Porsuk Dam Basin are Eskişehir and Kütahya. Kütahya station, which has data since 1932, has an average temperature of 10.7°C. In addition, the annual average temperature of Eskişehir Station, which is located downstream of the Porsuk Dam and has data since 1929, is 11.0°C. According to the monthly average values, the coldest month of the year is January, with an average temperature of -2°. From mid-December to mid-February, there are very cold days and frosts during which the temperature values ranged between -10°C to -25°C. The hottest days are experienced in June, July and August. The highest temperature ranges from 30° to 40°. Large temperature differences occur between day and night temperatures in the region.

CHAPTER 4

DATASET SETTING

The SWAT model needs a digital elevation model, a soil map, a land use map, and meteorological data consisting of solar radiation, temperature, precipitation, wind, and relative humidity for the modeling of hydrological processes in a watershed. The sources from which the necessary information was gathered are listed in Table 4.1.

4.1. Digital Elevation Model (DEM) Data

At a spatial resolution of 1 arc-second (30m), the Terra Advanced Space-borne Thermal Emission and Reflection Radiometer (ASTER) Global Digital Elevation Model (GDEM) Version 3 (ASTGTM) offers a global digital elevation model (DEM) of terrestrial areas on Earth with a resolution of 30x30 meters (ASTER, 2023). DEMs mostly come raw with several voids, which necessitates, a void filling operation before any analysis. The DEM of the Porsuk River Basin was downloaded from the USGS website and was observed that it contained many voids, which was unsuitable for further analysis. The raster file was reanalyzed and all voids were filled by using the ArcGIS “fill sinks” option. The DEM data was later transformed to the projected coordinate system required by the SWAT model to avoid errors that occurs during the watershed delineation procedure.

In this study, after loading the void-filled DEM file into the ArcGIS 10.7 and Spatial Analysis environment, the DEM of the Porsuk River Basin (study area) was extracted by Mask Tool. The relevant study area DEM was then projected to UTM zone 36 (WGS-1984). Projected DEM is used for the delineation of the catchment, generation of basins, rivers, flow accumulation, slope analysis, etc. Based on the DEM analysis, the Porsuk River Basin covers 10825 km^2 of the area with an elevation ranging from 657 m to 2173 m above means sea level.

Table 4.1. Datasets used in SWAT model

Data Name	Source	References
DEM	ASTER DEM	http://asterweb.jpl.nasa.gov/
Land Use	CORINE (1990; 2006)	http://land.copernicus.eu/pan-european/corine-land-cover
Soil Data	FAO Digital Soil Map of the World (DSMW)	https://www.fao.org/soils-portal/data-hub/soil-maps-and-databases/faounesco-soil-map-of-the-world/en/
Meteorological Data	NASA (POWER)	https://power.larc.nasa.gov/data-access-viewer/
Discharge Data	DSI &EIE (Government Water Affairs)	
ArcMap 10.7.1	Izmir Institute of Technology	
ArcSWAT 2012	Texas A&M University	

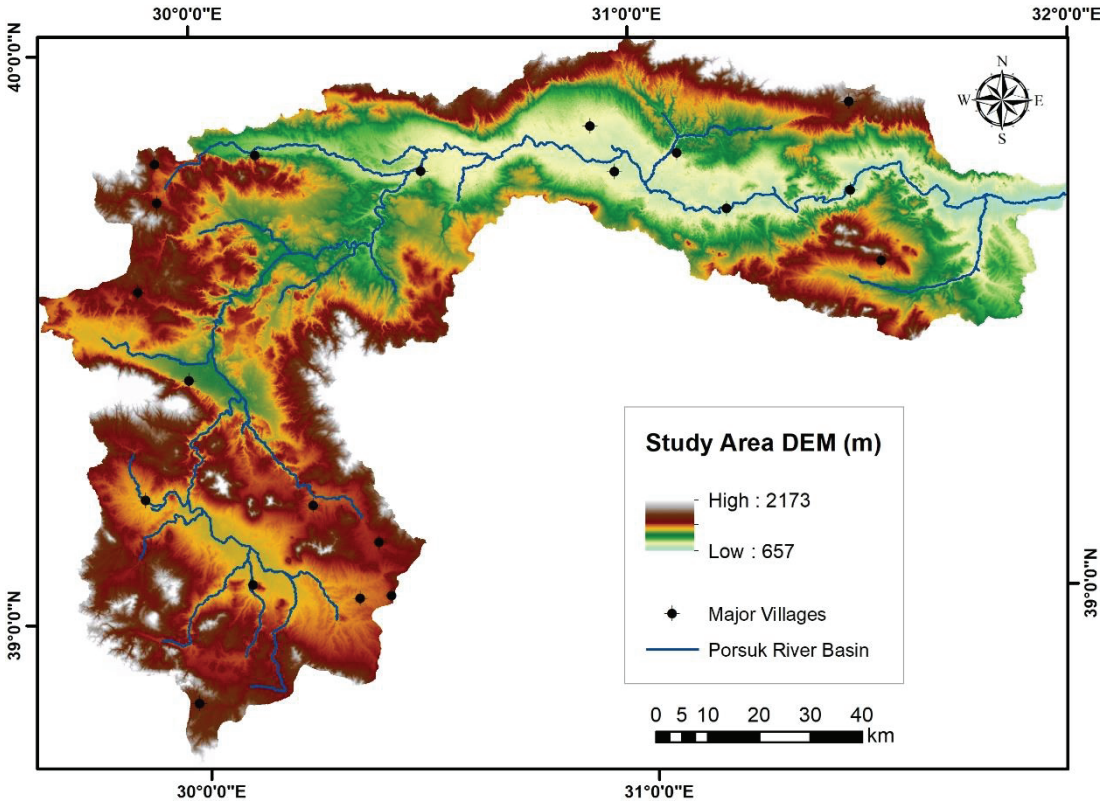

Figure 4.1. Study Area

4.2. Land Use/Land Cover Data

The LULC map is an important physical dataset for the SWAT model's runoff and infiltration simulations. Figure 4.2 displays the LULC map utilized in this investigation for the year 1990 with a resolution of 100 meters. Data from the Coordination of Information on the Environment (CORINE) were utilized to define the LULC map for the SWAT model. Established in 1985, CORINE is a program with the objectives of collecting environmental data in Europe, ensuring the coordinating of data collection organizations, and evaluating the accuracy of the data collected. Among the various data types created by CORINE is the LULC map (EU_CORINE, 2022). SWAT Model requires the land use/land cover to be in ESRI GRID or feature class formats. At least 95% of the modeled area must be covered by the land use/land cover map. The land use and land cover map categories must be classed into the SWAT database of plant/land cover types. Table 4.2 lists the LULC's areas and SWAT codes. One could claim that non-arable agricultural lands and range shrub lands make up the majority of the LULC in the watershed.

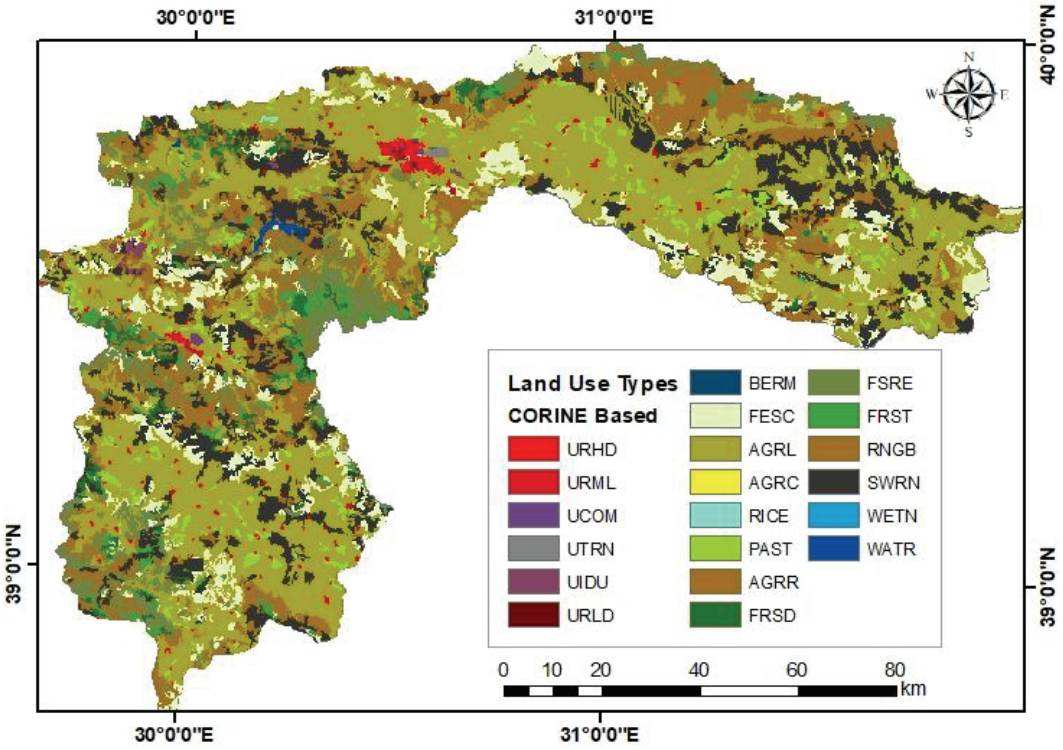

Figure 4.2. CORINE Land Use Land Cover Map of the Study Area (the year 1990)

After the CORINE land use data was extracted according to the obtained watershed boundaries, the CORINE data definitions were classified to resemble the SWAT land use definitions.

To make the region compatible with all geographic datasets, 1990 and 2006 dated CORINE LCLU maps of the area were acquired and geometrically rectified. Since major LCLU changes began to take place in Turkey towards the end of the 1980s and land cover status remained consistent between 1970 and 1990, the year 1990 was crucial for this research. Moreover, between 1990 and 2006, the region's terrain saw considerable modifications (Figure 4. 3).

To be compatible with the SWAT hydrological model class definitions, these LCLU maps were divided into 16 separate land cover classes. Due to the 44 different LCLU classes in the CORINE system, some LCLU classes were combined to produce new 20-class LCLU maps of the study region. For instance, the artificial surface class in CORINE contains 11 distinct subclasses, including continuous urban fabric, discontinuous urban fabric, industrial or commercial units, road and rail networks, and related land, port regions, airport, etc. In order to create the Urban Area class, every one of these factors considered sub-level classes were combined. Dryland Cropland and Pasture and Irrigated Cropland and Pasture classes were developed using a similar methodology.

Table 4.2. LULC classes derived for years 1990 and 2006

CORINE CODE	CLASS NAME	SWAT CODE	SWAT CLASS	1990 (km^2)	2006 (km^2)	DIFF (km^2)	1990 (%)	2006 (%)	DIFF (%)
212	Permanently irrigated land	AGRC	Small Grains	0.4	1122.84	1122	0.0	10.52	10.52
211	Non-irrigated arable land	AGRL	Agricultural Land Generic	4611.11	3434.1	-1177	43.19	32.16	-11.03
243	Agricultural Land-Row Crops	AGRR	Row Crops	440.1	540.6	100.5	4.12	5.1	0.98
141	Green Urban Areas	BERM	Bermuda Grass	2.95	2.46	-0.49	0.03	0.02	-0.01
321	Natural Grass Land	FESC	Tall Fescue	935.17	910.23	24.94	8.76	8.53	-0.23
311	Broad-leaved forest	FRSD	Deciduous Forest	223.12	255.07	31.95	2.09	2.39	0.3
313	Mixed Forest	FRST	Forest-Mix	211.9	222.59	10.69	2.0	2.08	0.08
312	Coniferous Forest	FRSE	Evergreen Forest	753.7	736.57	-17.13	7.0	6.90	-0.1
231	Pastures	PAST	Pasture	329.32	302.94	-26.38	3.1	2.84	-0.26
213	Rice Fields	RICE	Rice	3.85	3.86	0.01	0.04	0.04	0
132	Dump Sites	RNGB	Range Shrub-land	1447.16	1701.16	254	13.81	15.93	2.12
333	Sparsely Vegetated Areas	SWRN	Bare Rock	1495.6	1146.46	-349.14	13.80	10.74	-3.06
121	Industrial Units	UCOM	Urban Commercial	15.01	32.51	17.5	0.14	0.30	0.16
131	Mineral Extraction Sites	UIDU	Urban Industrial	36.11	61.99	25.88	0.34	0.58	0.24

(cont. on next page)

Table 4.2 (cont.)

CORINE CODE	CLASS NAME	SWAT CODE	SWAT CLASS	1990 (km2)	2006 (km2)	DIFF	1990 (%)	2006 (%)	DIFF (%)
111	Continuous Urban Fabric	URHD	Urban High Density	30.43	42.92	12.49	0.29	0.40	0.11
133	Construction Sites	URLD	Residential, Low Density	1.36	6.91	5.55	0.01	0.06	0.05
112	Discontinuous Urban Fabric	URML	Urban Medium Density	124.93	105.37	-19.6	1.17	0.99	-0.18
122	Road and rail networks and associated land	UTRN	Urban Transportation	8.52	14.37	5.85	0.08	0.13	0.05
512	Water Bodies	WATR	Water	27.38	28.77	1.39	0.26	0.27	0.01
411	Inland Marshes	WETN	Wetland-Non-Forested	1.8	4.37	2.57	0.02	0.04	0.02

4.3. Soil Data

In this study, the Food and Agriculture Organization (FAO) Digital Soil Map of the World (DSMW) data is used, and the general information on the soil data at the boundaries of the study area is given in Table 4.2. The soil map was downloaded with a scale of 1:5.000.000 from the Food and Agriculture Organization of the United Nations (FAO) website (http://www.fao.org/geonetwork/srv/en/metadata.show%3Fid=14116). Then it was converted into SWAT data format having five types of soils, as seen in Figure 4.3. The soil map must be in one of the following formats: shape file, feature class, or ESRI GRID. Additionally, the created soil map was projected based on WGS-1984 / UTM Zone 36. The created soil map is reclassified right after it is coupled with the database using a look-up table readable by the SWAT model. At a minimum, 95% of the modeled area must be covered by the soil map. The SWAT soil dataset must be associated with the categories listed in the soil map. By utilizing the ArcSWAT edit database tool or transferring SWAT soil files, the user can add new soil types and their associated properties to the SWAT soil database (.sol).

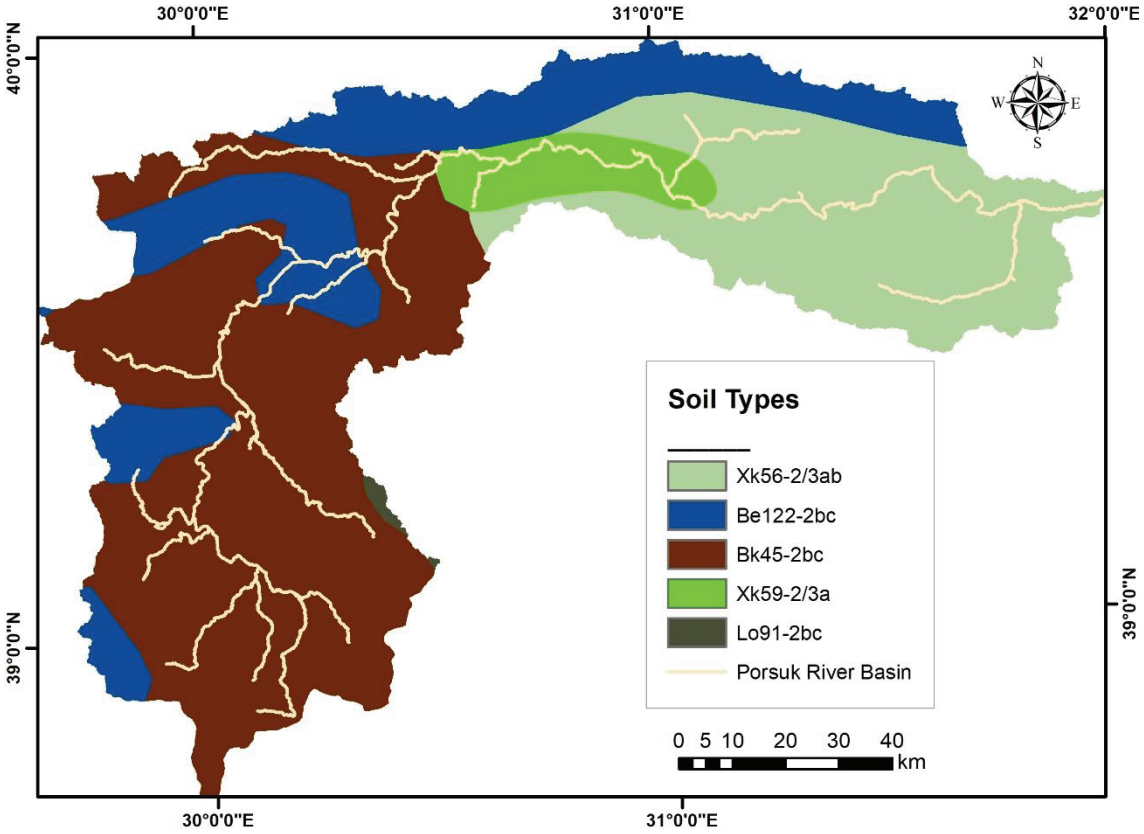

Figure 4.3. Soil Map of Porsuk River Basin

Table 4.3. FAO Soil Data Classification

Soil Type Code	Soil Texture	Area (km^2)	Percentage (%)
Be122-2bc	Schist; limestone shale	2292.07	21.15
Bk45-2bc	Schist; limestone marl	5193.96	47.93
Lo91-2bc	Andesite; granite; schist	33.0828	0.305
Xk56-213a	Clay; marl; lime	2765.28	25.52
Xk59-2/3a	Silt-clay sediment	553.111	5.104

Based on the above classifications, Bk45-2bc covers 47.93 percent, Xk56-213a covers 25.52 percent, Be122-2bc covers 21.15 percent, Xk59-2/3a covers 5.104 percent, and Lo91-2bc covers around 0.305 percent of the Porsuk River Basin soil type.
Table 4.4 provides further information regarding the soil texture, hydrologic group, and percentages of the soil combinations.

Table 4.4. Soil Texture Combination

Soil Type	Hydrologic Group	Texture	Clay %	Silt %	Sand %	Rock %
Be122-2bc	C	LOAM	22	36	42	0
Bk45-2bc	C	LOAM	22	40	39	0
Xk56-2/3ab	D	LOAM	27	40	33	2
Xk59-2/3a	D	CLAY-LOAM	30	37	33	1.8
Lo91-2bc	D	LOAM	22	34	44	0

4.4. Weather Data

A crucial component of the SWAT model inputs is meteorological data. Accurate meteorological dataset collection is an essential step in producing a representative simulation. Temperature and precipitation are the two main meteorological variables that are a must to input datasets. The model may generate additional variables like solar radiation, wind speed, and relative humidity based on temperature and precipitation data, or the user can import these variables. The model needs a table with the latitude, longitude, and elevation of weather stations adjacent to the project area for the location of the weather generator gage. Moreover, SWAT is able to produce any missing data using the information provided. Although the record need not start on the initial day of the simulation, meteorological datasets must hold data for the whole simulation duration. SWAT can search the file for the file's start date. The user may simply run the model for various time periods after submitting the data for an extended period of time.

SWAT asks for daily or sub-daily weather data, including precipitation, minimum and maximum temperature. When using measured data, the model needs a temperature measurement location table, much like it does for the precipitation file, to supply the positions of the gages. The daily minimum and maximum temperatures for a meteorological station are stored using the temperature data. Before beginning the simulations, one temperature data recording must be produced for each place mentioned in the temperature measurement location table as a temperature gage.

After preparing the datasets for temperature and precipitation, the SWAT model requires datasets for solar radiation, wind speed, and relative humidity as inputs. The number of gages utilized in a simulation is not constrained by the model, though. As a result, a simulation's data file could have many gage data sets. The total daily amounts of solar radiation reaching the ground that was measured at a particular station are stored in solar radiation data, which holds the same for the wind speed dataset.

In the case of relative humidity data, SWAT also requires daily data to calculate the potential evapotranspiration and stress of water on plant growth using two common methods: Penman-Montheith, and Pristley-Taylor, respectively. Similarly, the model allows the user to have multiple monitoring stations providing that the location and the names are written in the look-up table. In this study, although there are several stations

available within the research area (Figure 4.4), none of them had proper daily data to cover the simulation period 1989 – 2010.

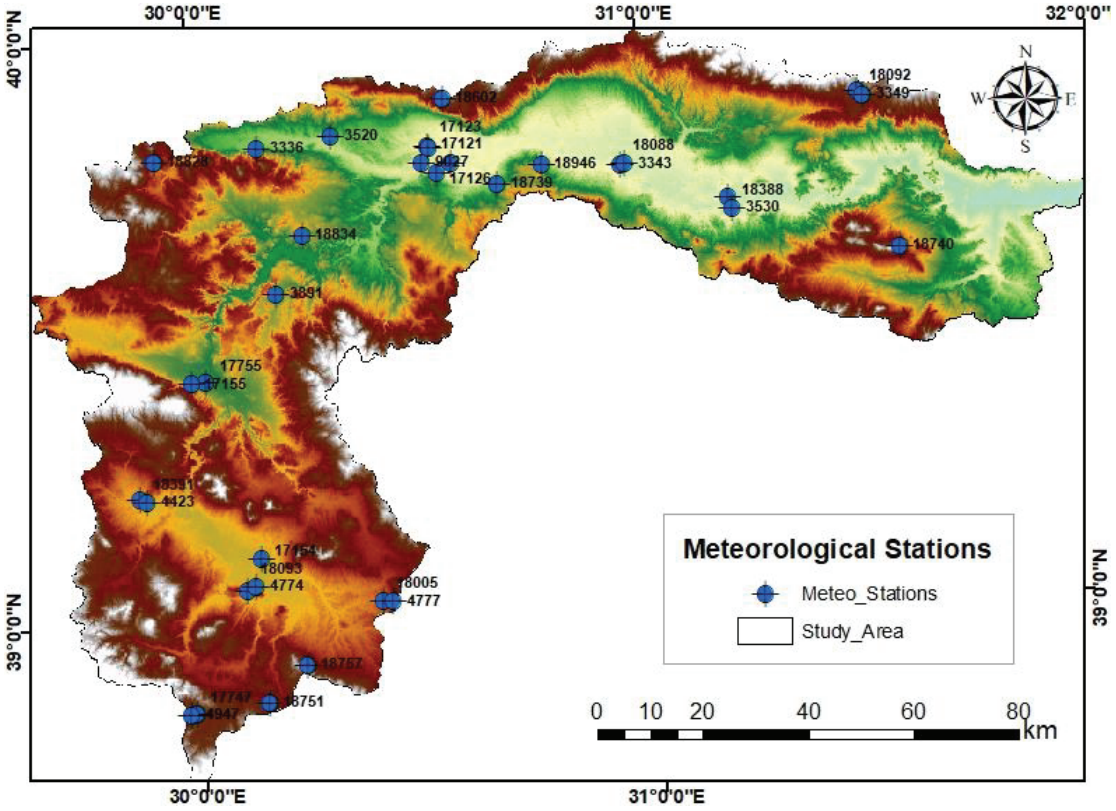

Figure 4.4. Meteorological stations in Porsuk River Basin

The available data had a lot of missing parts, and the gap was big between years of the recording. Thus, the open-source data form PowerNASA (POWER | Data Access Viewer (nasa.gov)) was used instead (Figure 4.5).

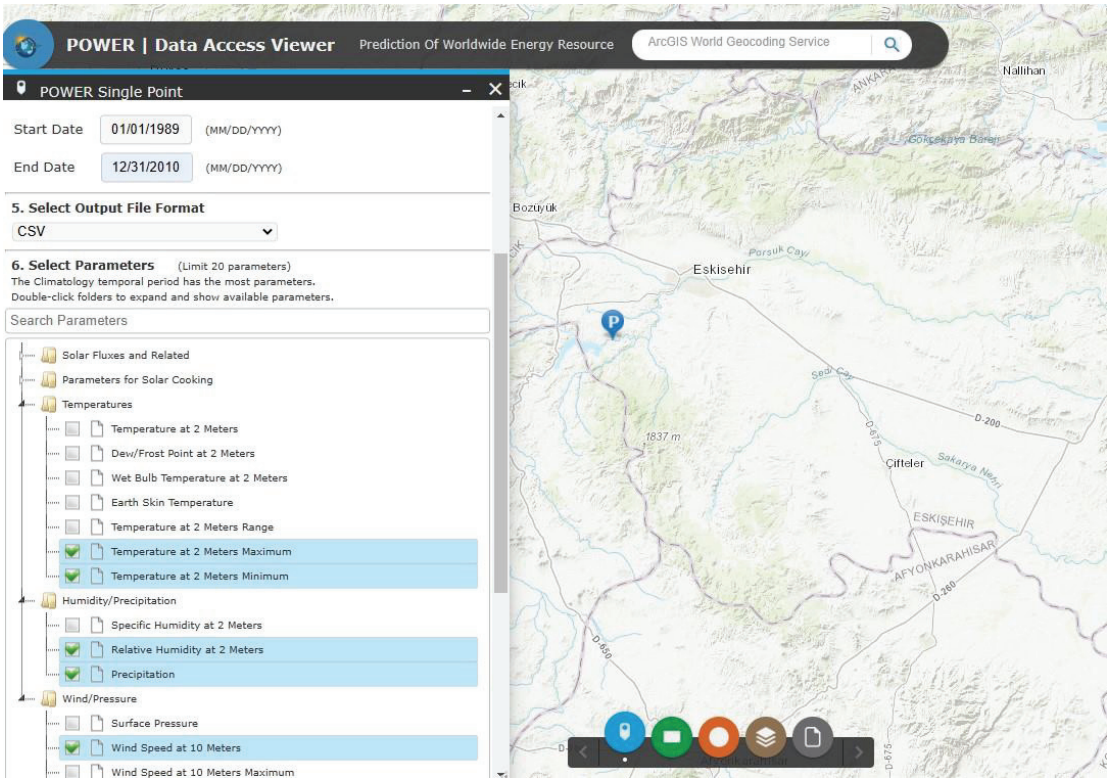

Figure 4.5. Weather Data (PowerNASA Website)

4.5. Hydrological Data

In the study region, there are flow observation stations run by the State Hydraulic Works (DSI) and the Electrical Works Survey Administration (EIE). To calibrate the model, data from 5 separate observation stations was employed. Getting complete data for all time intervals for every station, though, would not always be achievable. Thus, the monthly flow data of the flow observation stations Kiranharmani (E12A051), Parsibey (D12A215), Porsuk Dam Outlet Point (D12A034), Porsuk Ciftligi (D12A033), Murat Ciftligi (D12A055) stations were taken into consideration between the modeling years, in accordance with the land cover information year, and determined according to the time intervals for which continuous data are available.

The locations of the present observation stations that are employed in the calibration and validation process are depicted in Figure 4.5. Information on the current observation sites utilized for model calibration can be found in Table 4.5.

Table 4.5. Available Hydrological Stations

Hydro. Station Name	Station No.	Latitude	Longitude	Data Coverage Period
Kiranharmani	E12A051	31.964481	39.672822	1989-2010
Parsibey	D12A215	31.160572	39.688764	1989-2010
Porsuk Dam Outlet	D12A034	30.278506	39.634988	1989-2010
Porsuk Ciftligi	D12A033	30.032827	39.343504	1989-2010
Murat Ciftligi	D12A055	30.014981	39.030843	1989-2010

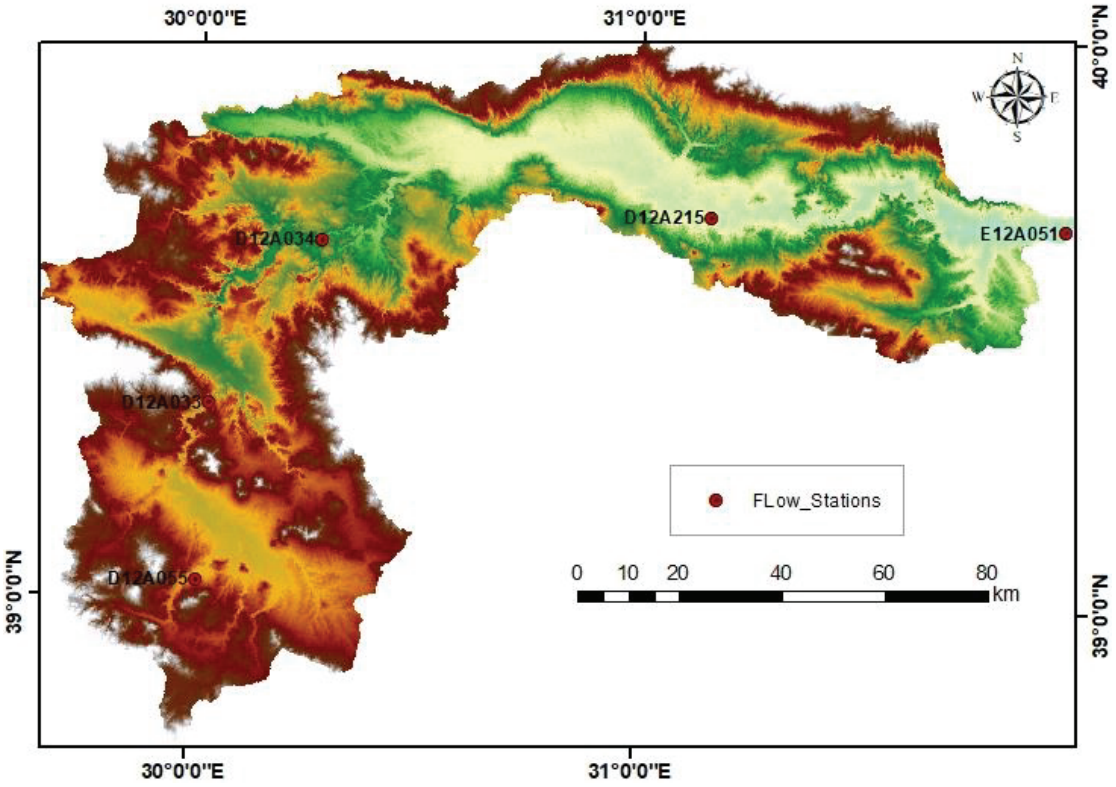

Figure 4.6. Flow Monitoring Stations in Porsuk River Basins

CHAPTER 5

THE SWAT MODEL

5.1. Model Description

The Soil & Water Assessment Tool (SWAT) model is a physical model and was developed by the U.S. Department of Agriculture and Agriculture Research Service (USDA). The model is implemented in Arc GIS, which can incorporate several publicly accessible geographic data to reflect the watershed's properties precisely. The model uses a daily time step and is physical-based, semi-distributed, and continuous time (Neitsch et al., 2011). It aims to simulate persistent overland flow, sediment output, and nutrient depletion from a region's watershed (Arnold, 2010). It was created to make long-term predictions of water, sediment, and agrochemical yields in vast, intricate catchments with a range of land uses, land covers, and soil conditions.

In the SWAT model, the hydrological simulation is divided into two main phases. The watershed land areas in the first section represent the water delivered to the channels along with sediments, nutrients, and pesticides. The water's behavior in the channels leading from tributaries to the watershed exit is covered in the second section (Cibin et al., 2010).

With SWAT, evapotranspiration, infiltration, percolation, flow formation, nutrient cycling, and transport for each hydrological unit can be simulated. The basic input data set of the SWAT model is topography, land use, soil, and climate data. With the SWAT model, the model output can be obtained on a daily, monthly, and annual basis. It uses topography to split the basin into several sub-basins and then further separates each sub-basin into hydrologic response units (HRUs), which are a special combination of soil, land-use, slope, and land management (Neitsch et al., 2011)

The watershed boundary is defined by the model using a digital elevation model (DEM), and the watershed is then divided into several sub-watersheds and hydrologic response units (HRUs) that have comparable land use, slope, and soil characteristics (Arnold et al., 2012). Hydrological Response Units (HRUs) are the smallest spatial unit of the model, and a standard HRU identification approach is based on user-specified

thresholds for all similar watersheds within a sub-basin. It groups land uses, soils, and slopes (Teshager et al., 2016). The model's outputs include yields for sediment, nutrients, pesticides, groundwater, lateral flow, and surface runoff.

5.2. Hydrologic Cycle

To express spatially varied distribution with regard to soil type, land cover, and basin slope, SWAT utilizes hydrologic response units (HRUs). The hydrological parameters from the preceding section are run twice using the SWAT model.

In the SWAT hydrological model, each sub-basin of a basin or watershed is further divided into Hydrologic Response Units (HRUs), which are made up of distinctive combinations of the land cover, soils, and slope. Each HRU's water, sediment, and nutrient budgets are assessed and simulated before being combined for all of the sub-basins. SWAT simulates hydrological processes using its land phase and water phase systems (Neitsch et al., 2011). For the currently under investigation Porsuk River Basin, the SWAT land phase was considered. The amount of water, sediment, and nutrient loading into the main channel in each sub-basin is controlled by the land phase.

Equation 5.1. 's water balance equation, which incorporates components for daily precipitation runoff, evapotranspiration, percolation, and return flow, is used in the model to forecast the hydrology at each HRU (Neitsch et al., 2011).

$$SW_t = SW_0 + \sum_{i=1}^{t} \left(R_{day} - Q_{surf} - E_a - W_{seep} - Q_{gw} \right) \tag{5.1}$$

where t shows the time in days, SW_t is the final soil water content (mm), SW_0 is the initial water content of soil (mm), R_{day} is the rainfall on day (mm), Q_{surf} is the amount of surface runoff (mm), E_a is the amount of evapotranspiration (mm), W_{seep} represents the amount of water entering the vadose zone from the soil profile (mm) and Q_{gw} is the flow return amount (mm). SWAT's water balance in a circular schematic pattern is represented in Figure 5.1.

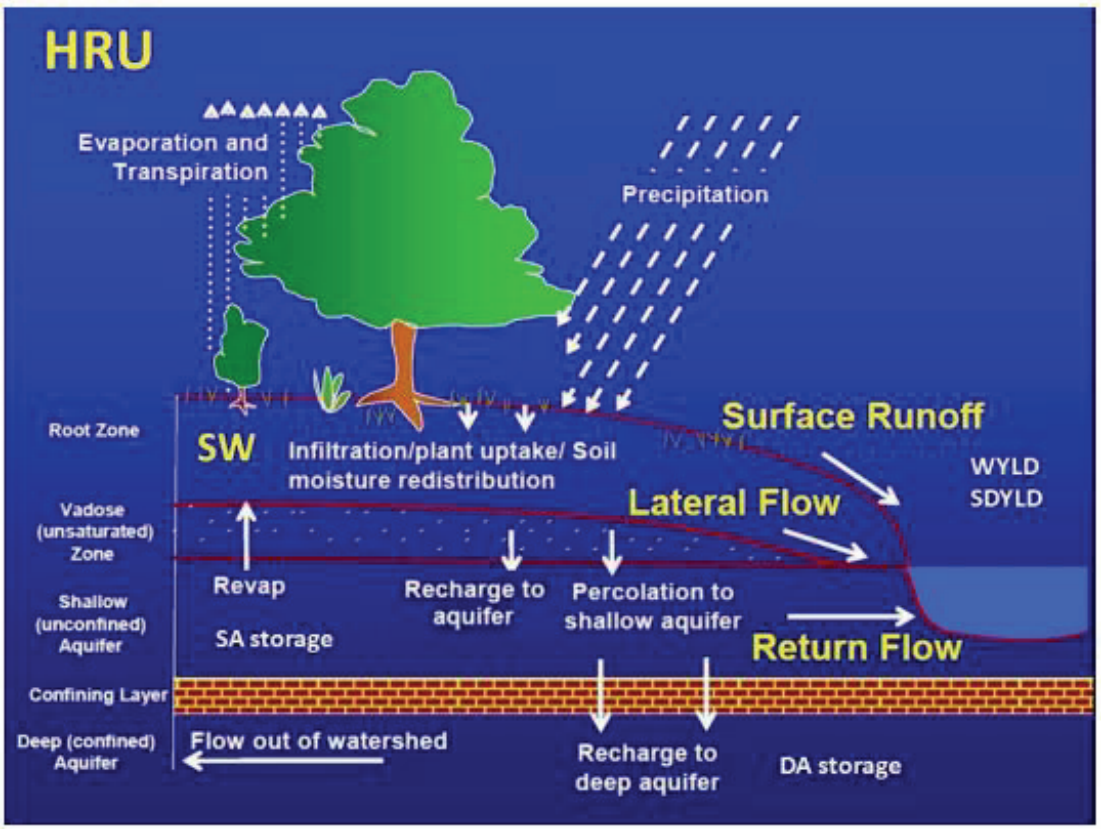

Figure 5.1. SWAT hydrological output parameters schematic pattern (Taken from Srinivasan, 2009)

5.2.1. Surface Runoff

Surface runoff occurs when rainfall fills all of the soil's pore space, and the moisture content of the soil exceeds its field capacity. To determine the surface runoff, the SWAT model employs the soil conservation system (SCS) and the Green and Ampt infiltration method (Rallison and Miller 1982). The surface runoff is determined empirically using the SCS approach. The SCS approach primarily depends on soil hydrological groups and land use/cover:

$$Q_{surf} = \frac{(R_{day} - 0.2S)^2}{(R_{day} + 0.8S)} \quad (5.2)$$

where Q_{surf} is the daily surface runoff (mm), R_{day} is the rainfall amount on day I (mm) and S is the retention parameter (mm). if $R_{day} > 0.2S$; otherwise Qsurf = 0. The retention

parameter S and the lateral flow prediction using the SWAT model are declared in the equation below:

$$S = 25.4\left(\frac{100}{CN} - 10\right)\# \tag{5.3}$$

where CN shows the curve number, and S is the drainable amount of water of the soil in a unit area of saturated thickness with the unit of (mm/day).

There are three antecedent moisture conditions (AMC) under the SCS definition:

I. Dry (AMC-1)
II. Average Moisture (AMC-2)
III. Wet (AMC-2)

of which, AMC-1 is counted as the lowest value that the curve number (daily) can presume in dry situations. AMC is the initially existing amount of moisture in the soil at the very start of the rainfall-runoff schedule.

AMC-1 and AMC-3 are calculated for curve numbers using the following equations:

$$CN_1 = CN_2 - \frac{2000 - 20CN_2}{100 - CN_2 + \exp[2.533 - 0.0636(100 - CN_2)]}\# \tag{5.4}$$

$$CN_3 = CN_2 * \exp[0.00673(100 - CN_2)] \tag{5.5}$$

where CN1 represents AMC-1 (moisture condition I), CN2 represents AMC-2 (moisture condition II), and CN3 represents AMC-3 (moisture condition III) in a respective manner.

The curve number approach was used in PRB to predict surface runoff for the four hydrologic soil groups and 20 LULC classes. The FAO website served as the source for the soil group input (Table 4-3). The assigned curve numbers are listed in Table 5-1 and were determined based on values published by (Hjelmfelt et al., 2004; Westenbroek et al., 2010).

Table 5.1. Curve Numbers

No	LULC	Hydrological Group of Soil			
		A	B	C	D
1	Agricultural Land-Close-grown	62	71	88	91
2	Agrıcultural Land Generic	72	81	88	91
3	Row Crops	45	53	67	72
4	Bermuda Grass	25	66	77	83
5	Tall Fescue	39	61	74	80
6	Deciduous Forest	62	71	88	83
7	Forest-Mix	43	65	76	82
8	Evergreen Forest	45	66	77	83
9	Pasture	39	61	74	80
10	Rice	62	71	88	91
11	Range Shrub-land	36	60	73	79
12	Bare Rock	36	60	73	79
13	Urban Commercial	57	72	81	86
14	Urban Industrial	57	72	81	86
15	Urban High Density	98	98	98	98
16	Residential, Low Density	77	85	90	92
17	Urban Medium Density	81	88	91	93
18	Urban Transportation	98	98	98	98
19	Water	100	100	100	100
20	Wetlands-Non-Forested	98	98	98	98

5.2.2. Lateral Flow

The lateral flow modeling method used by the SWAT model is the kinematic storage model created by Sloan in 1983. The patterns of flow in the accumulated percolated water just above the impervious surface are equal to the impervious boundary according to the kinematic wave approximation of lateral flow. The SWAT model uses the following equation to determine how much lateral flow is present.

$$Q_{latl} = 0.024 * \left(\frac{2 * S_{watr} * K * Sin\alpha}{\emptyset * L}\right) \# \quad (5.6)$$

where Q_{latl} is lateral flow (mm/day), S_{watr} is the amount of water of saturated soil in a unit area (mm/day), K is the saturated (wet) hydraulic conductivity (mm/h), L is the length of flow (m), ∅ is the value of porosity and Sinα is the land slope.

5.2.3. Ground Water

According to Neitsch et al. (2005), the saturated zone of groundwater is divided into two regions: those with high conductivity and those with low conductivity. Large numbers of macro-pores and coarse-grained particles are present in areas with high conductivity, which facilitates the easy movement of water. Fine particles with a high concentration of mesopores and micro-pores, which slow down water movement, make up the poor conductivity zone.

SWAT model partitions the groundwater into two main systems, shallow and deep aquifer systems, respectively. The following water balance equation is utilized in the SWAT model in shallow aquifers:

$$Q_{shl} = Q_{shl,i-1} + W - Q_g - W_r - W_{pump} \quad (5.7)$$

where (in shallow aquifers) Q_{shl} is water amount stored on day i (mm), $Q_{shl,i-1}$ is the amount of water in previous day (mm), W is the amount of recharge infiltrating to shallow aquifer (mm), W_r is the amount of water reaching the soil zone (mm) and W_{pump} is the amount of pumped water from aquifer (mm).

The following water balance equation is utilized in the SWAT model in deep aquifers:

$$Q_{deep} = Q_{d,i-1} + W_d - W_{pd}\# \quad (5.8)$$

where (in deep aquifers) Q_{deep} represents the amount of water reaching the aquifer (mm), $Q_{d,i-1}$ represents the amount of water reaching the aquifer in previous day (mm), W_d represents the infiltrated amount water from above layer (shallow aquifer) into deep aquifer (mm) and W_{dp} represents the pumped amount of water down the deep aquifer (mm).

5.3. Evapotranspiration (ET)

In the current study, the FAO-recommended Penman-Monteith method has been used. It is considered one of the best approaches for calculating evapotranspiration. This method is arranged to estimate the amount of potential evapotranspiration from hypothetical vegetation with an assumed height of 0.12m to 10m.

$$ET = \left(\frac{0.408 * \triangle * (Rn - G) + \Upsilon * \frac{900}{T + 273} * u(es - ea)}{\triangle + \Upsilon (1 + 0.34u)} \right) \quad (5.9)$$

where Rn represents net radiation (MJ/m^2/d), G represents ground heat density (MJ/m^2/d), Υ represents psychometric constant (kPa/°C), T represents air temperature (°C), u represents wind speed (m/s), $\triangle$ represents saturation vapor pressure slope (kPa/°C), e_s represents saturation vapor pressure (kpa), and e_a is actual vapor pressure.

CHAPTER 6

MODEL SETUP

In chapter 6, the step-by-step processes of setting a SWAT Model and then RUN is discussed with a flowchart given in Figure 6.1. In dataset preparation Chapter 4, all the required input data are discussed in detail. The prepared data in SWAT readable format are enquired into the model for the simulation processes of the Porsuk River Basin.

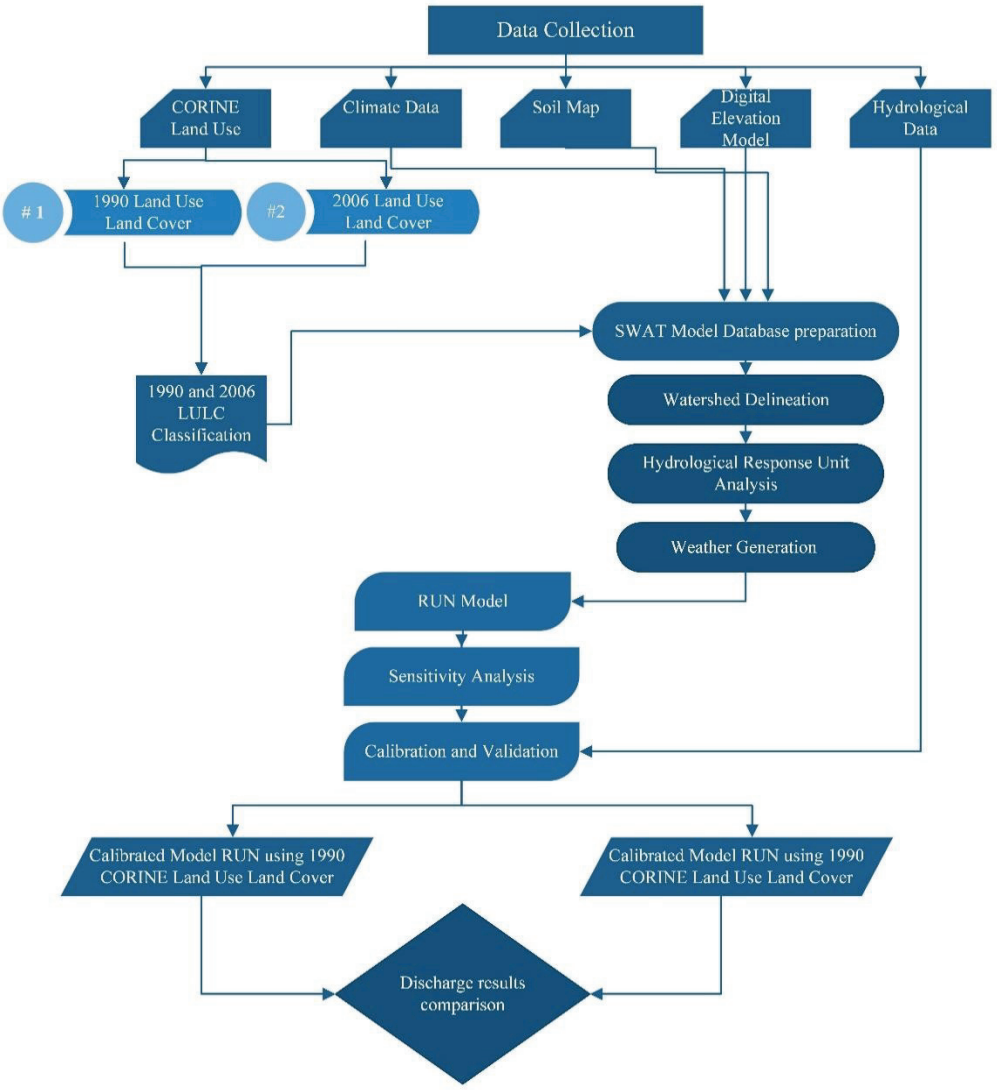

Figure 6.1. Methodology flowchart.

6.1. SWAT Model Setup and Installation

Before setting up the model and installation processes, the user needs to check the software SWAT model machine requirements to stop any errors. In this study, the analysis has been conducted using the SWAT2012 model in an ArcGIS 10.1 version licensed by Izmir Institute of Technology.

The post-SWAT2012 installation is to install the SWAT Editor and SWAT-Check for further processes. After every SWAT2012 installation, a folder is created in the addressed path with the name ArcSWAT, including the SWAT2012 database. This database is prepared for studies within the United States of America (USA). Suppose the new user's study area is other than the USA. In that case, the user must edit the SWAT2012.mdb database, which comes in a Microsoft Access file, by importing data such as Land Cover types, soil types, etc., into the original SWAT2012.mdb database.

To start a SWAT project, the first step is to activate the ArcSWAT plugin on the ArcGIS software screen. To do this, the ArcSWAT option must be selected using the Toolbars menu, as shown in Figure 6.2.

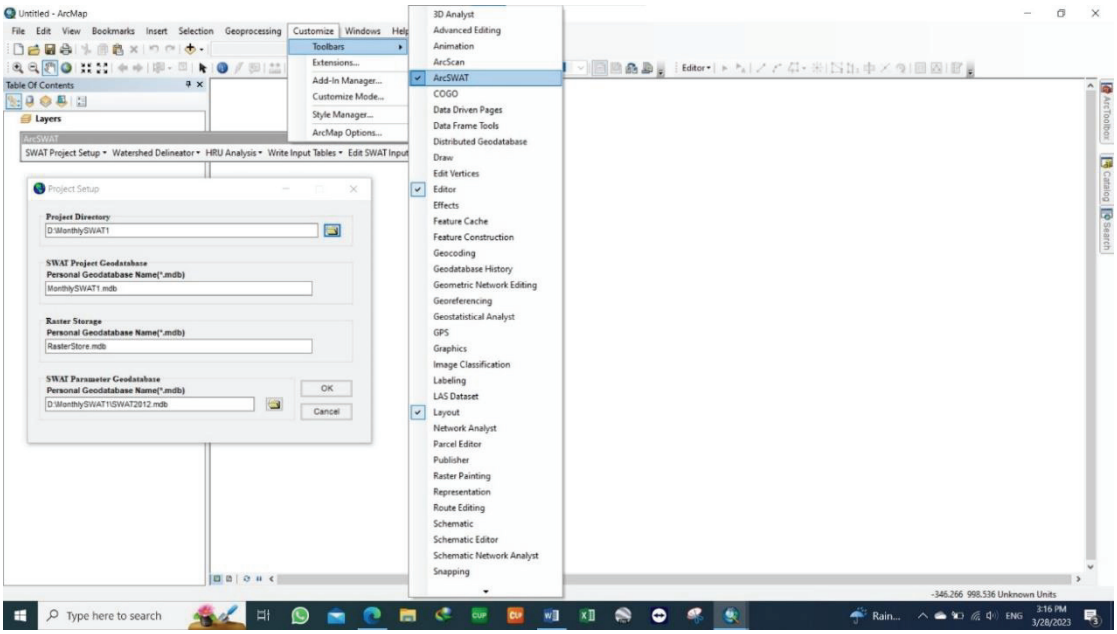

Figure 6.2. ArcSWAT Interface Activation

6.2. Watershed Delineation

The menu to begin the watershed delineation is available on the left corner of the SWAT model menu set, as shown in Figure 6.3. This sub-menu starts with the Digital Elevation Model (DEM) setup. Prior to adding the DEM in its place, DEM in ESRI grid format must be projected, which in this case, the present study area (Porsuk River Basin) DEM is projected into WGS_1984_UTM_Zone_35N. After adding the DEM in raster format and setting the Z-unit in meters, the following options of "Musk and Burn In" become optional in the case of having already clipped the study area DEM into the interest area. Following that, flow directions and accumulation of the watershed are created using the uploaded DEM. This process will create the steams network data for the watershed. If the user already created streams other than the ArcSWAT delineation option, one can also upload the stream network in the delineation box and continue. In this study, the stream network was created by using ArcSWAT's available options.

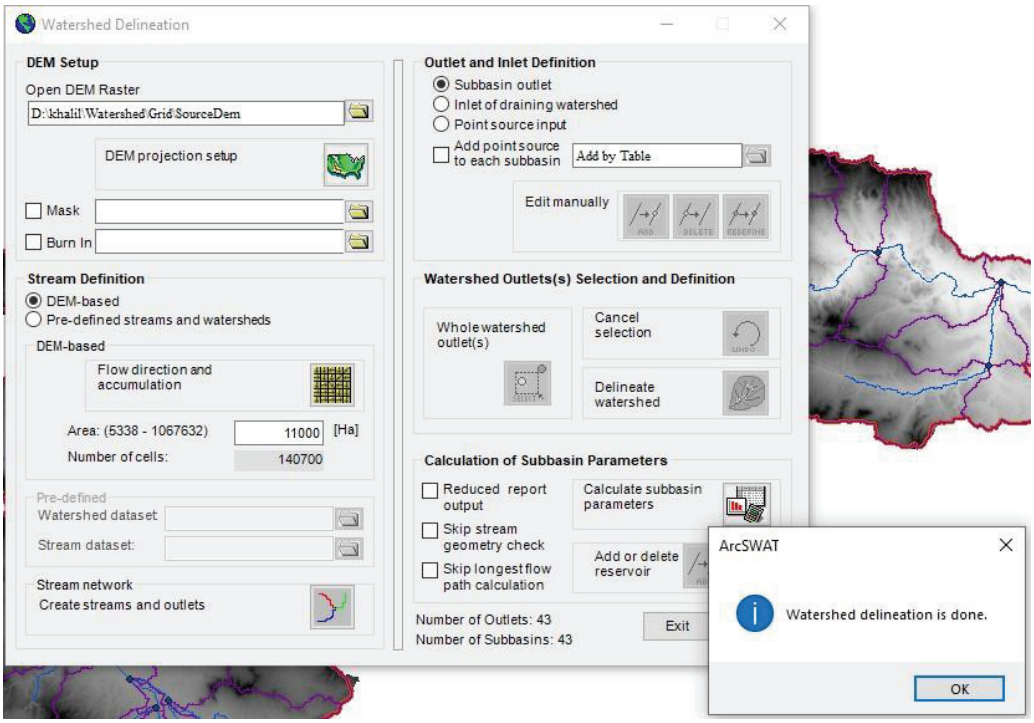

Figure 6.3. Watershed Delineation

A better delineation can be obtained if the user has defined the outlets and inlets of the watershed using accurate coordinate systems. Outlets are an essential part of the watershed delineation where streamflow exits the watershed through them.

A less accurate definition will cause a fatal error in the delineation procedure. For this matter, it is a must to choose a correct and suitable outlet prior to the delineation. In this study, following the main stream channel, 43 outlets are defined and using one accurate main system outlet. This produced 43 sub-basins in one main watershed. Later, the geomorphic characteristics of the sub-basins are calculated using the "Calculate Sub-basin parameters" option in the box. After finishing all the tasks, a Topographic Report appears in the watershed reports.

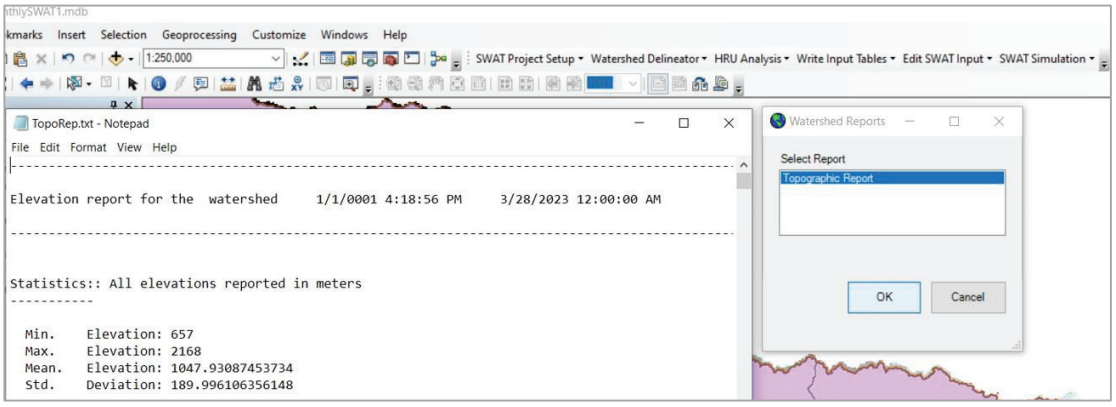

Figure 6.4. Topographic Report

6.3. Hydrological Response Unit (HRU) Analysis

The second essential sub-menu in the ArcSWAT toolbars refers to the HRU analysis, which includes layers of land use class, soil type class, and slope class. In the HRU analysis tools, the created project interface requires the user to upload the land use and soil data to simulate the slope properties for every individual sub-basin one at a time. Before adding the land use and soil datasets into the project, the user must ensure the datasets are projected in a similar coordinate system with the DEM first and then saved in ESRI grid/raster format. Suppose the study area is somewhere not in the USA, in that case, the user must not use the already available land use and soil database after the first SWAT2012 installation. The user is required to create the land use and soil classes individually apart and provide a look-up table in TEXT file format for each (figure 6.5).

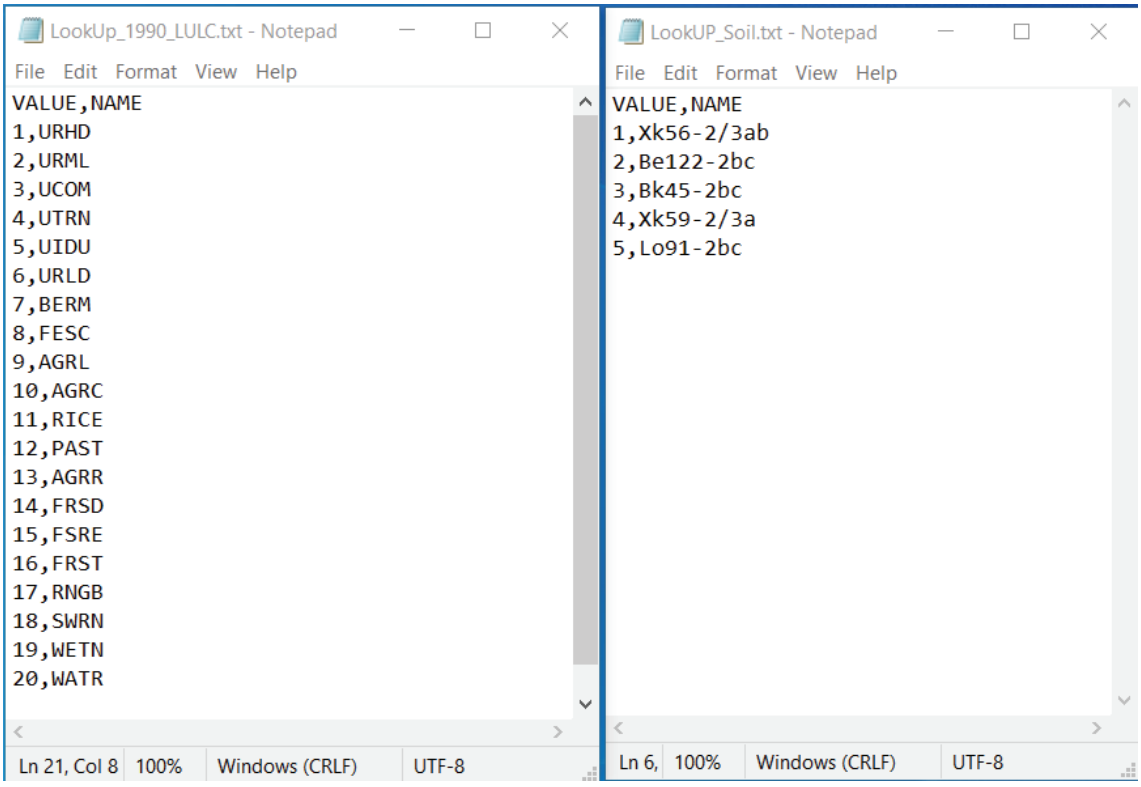

Figure 6.5. Lookup Tables for Land Use and Soil Classes

Once the land use data and the soil data from the user's database are uploaded and the slope in the model with an overlap percentage of over 99% are defined, the three datasets are overlaid and reclassified.

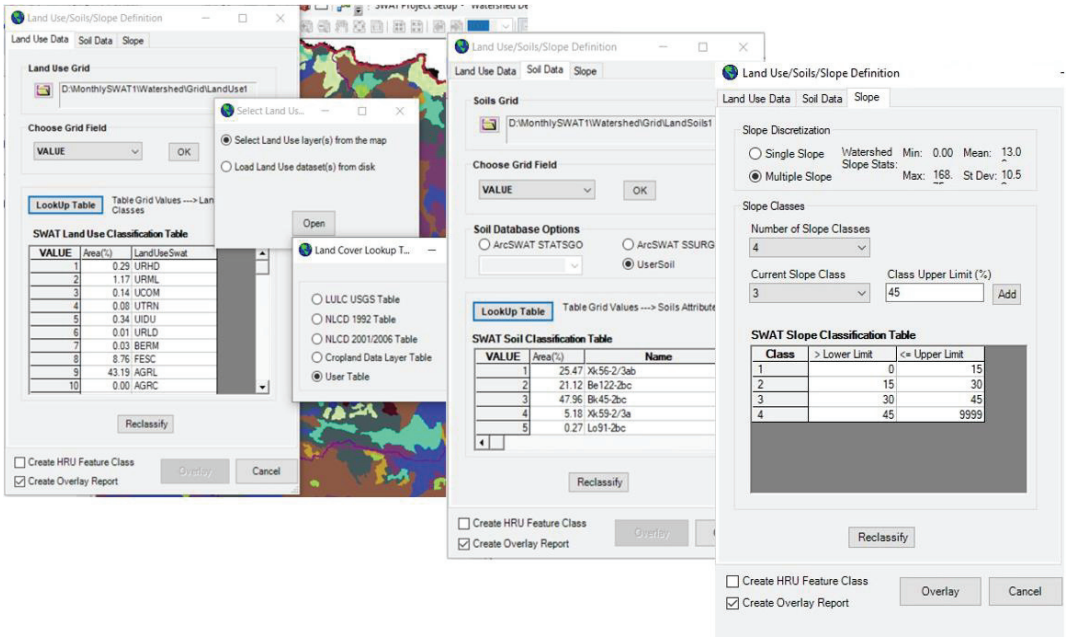

Figure 6.6. Land Use/Soil/Slope Classes Upload

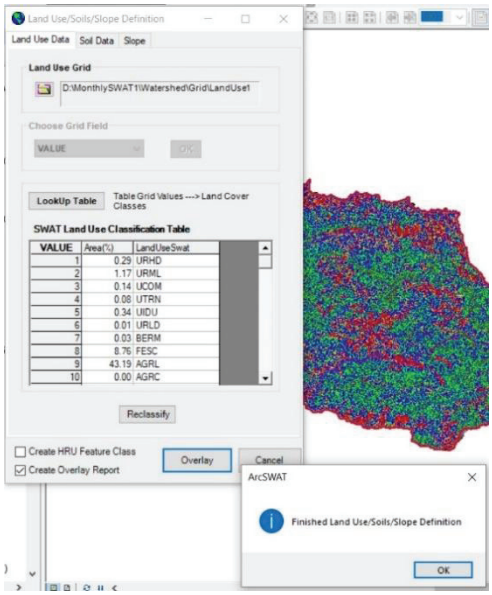

Figure 6.7. Classes Overlay

Right after the overlay is completed, the HRU definition step activates. In this step, HRU thresholds must be defined. In this Porsuk River Basin study, the land use percentage, soil class percentage, and slope class percentage are defined as 5%, 6%, and 6%, respectively, shown in Figure 6.8. In this study, 43 sub-basins are created with 1404 HRUs. Detailed HRU distribution that gives details regarding each sub-basin area is also created after terminating the command.

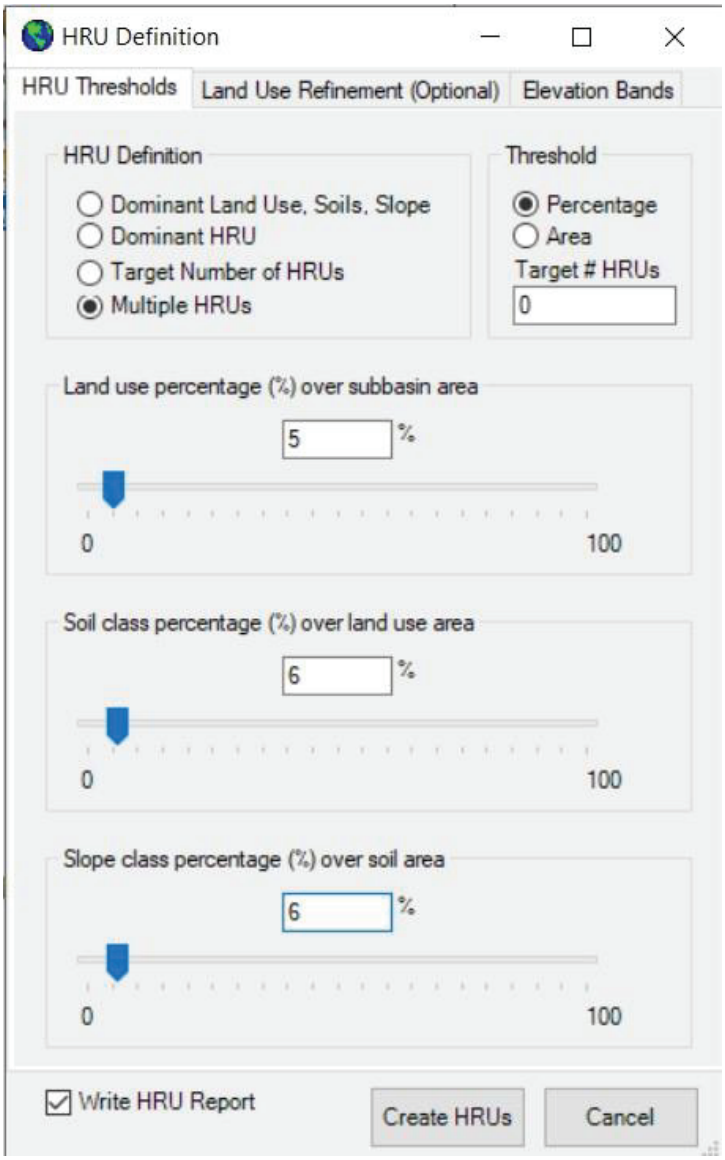

Figure 6.8. HRU Definition

6.4. Write Input Tables

After the HRUs are defined in the Porsuk River Basin, weather stations must be set using the meteorological stations' data from the Write Input tables option. In this study, WGEN_CFSR_World is chosen for the monthly Weather Database. Any other database in the list provides WGEN information for the USA, which exclude the other world. SWAT requires that the weather station location and data be provided in a SWAT readable text file format using the same nomenclature for every station.

In addition, the text files that include station coordinates and data within them must be in the same package folder. It works because the program needs to connect the station locations with related data in them.

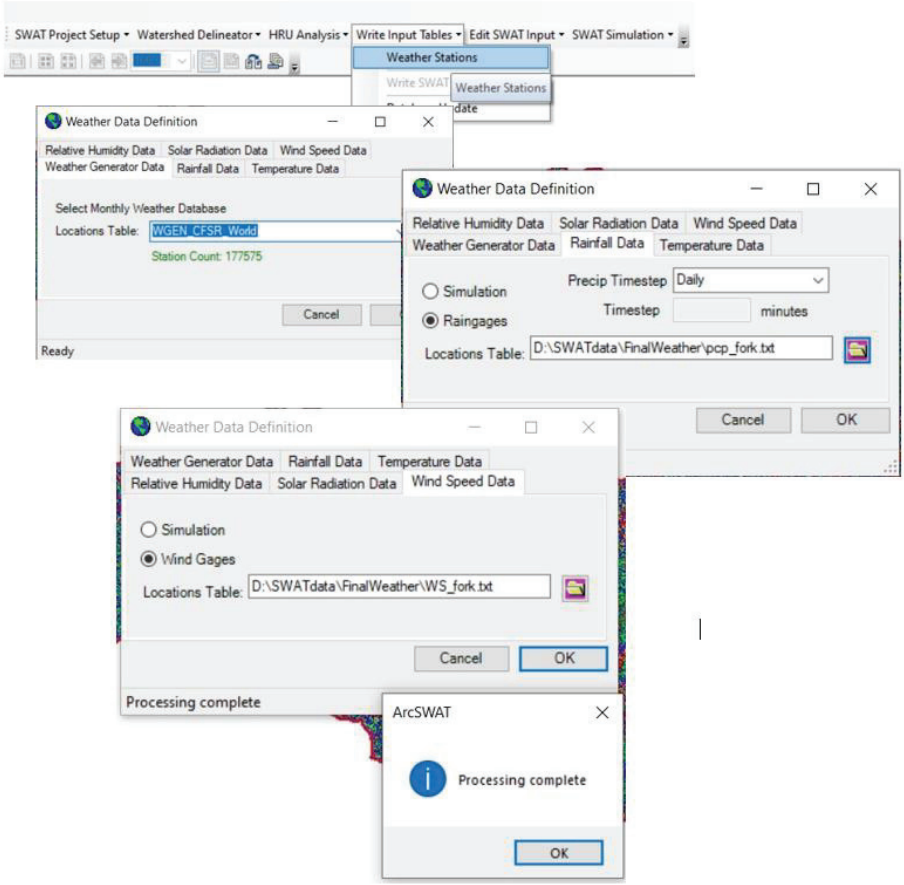

Figure 6.9. Weather Data Definition

The needed data for this task are daily rainfall, maximum and minimum temperature, relative humidity, solar radiation, and wind speed. The files that contain the data for rainfall, maximum and minimum temperature, relative humidity, solar radiation, and wind speed must have the same naming as they are written in the stations coordinate list file that will be uploaded in the SWAT weather data definition environment (Figure 6.10 & Figure 11). Every station must be uploaded and read successfully by the model.

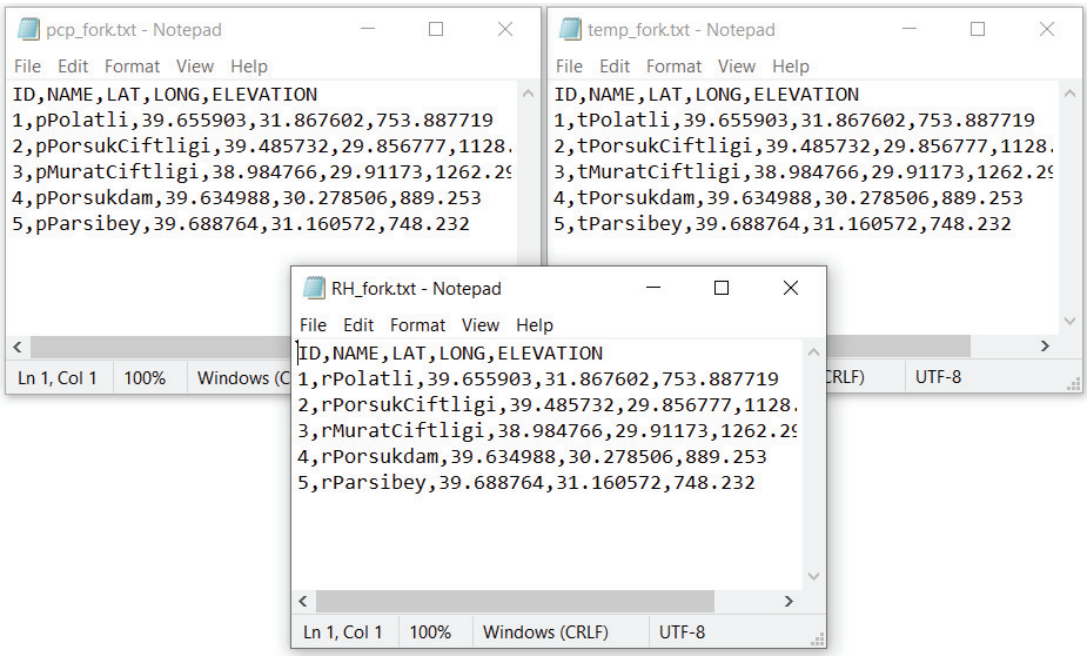

Figure 6.10. Weather Stations SWAT Format

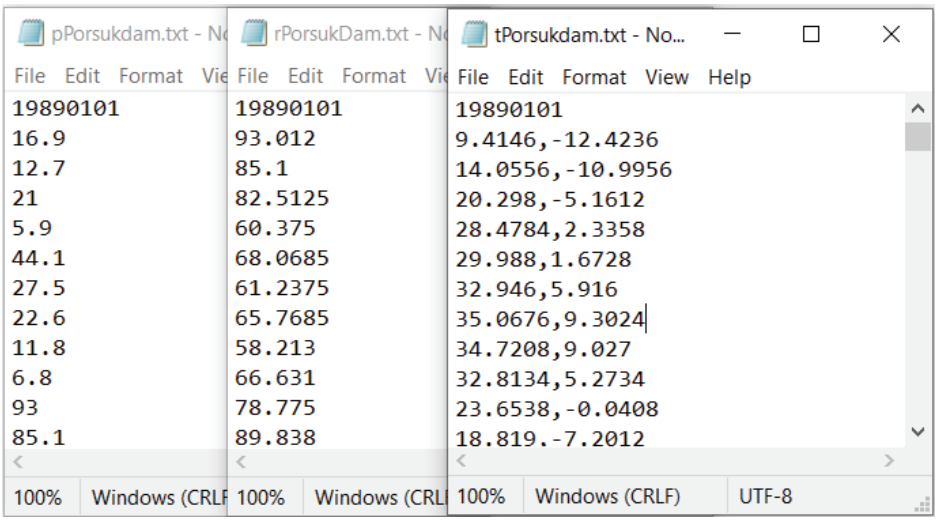

Figure 6.11. Weather Data Format Illustration for PorsukDam Station

The next step is to write SWAT input tables in a database created by the SWAT automatically. This task is done using the Write Input Table's Write All command. Upon finishing the weather data definition, the Edit SWAT Input option activates, giving the user access to manually change some parameters in his/her favor prior to the model run. A before and after writing an illustration of SWAT input files are depicted in Figure 6.12.

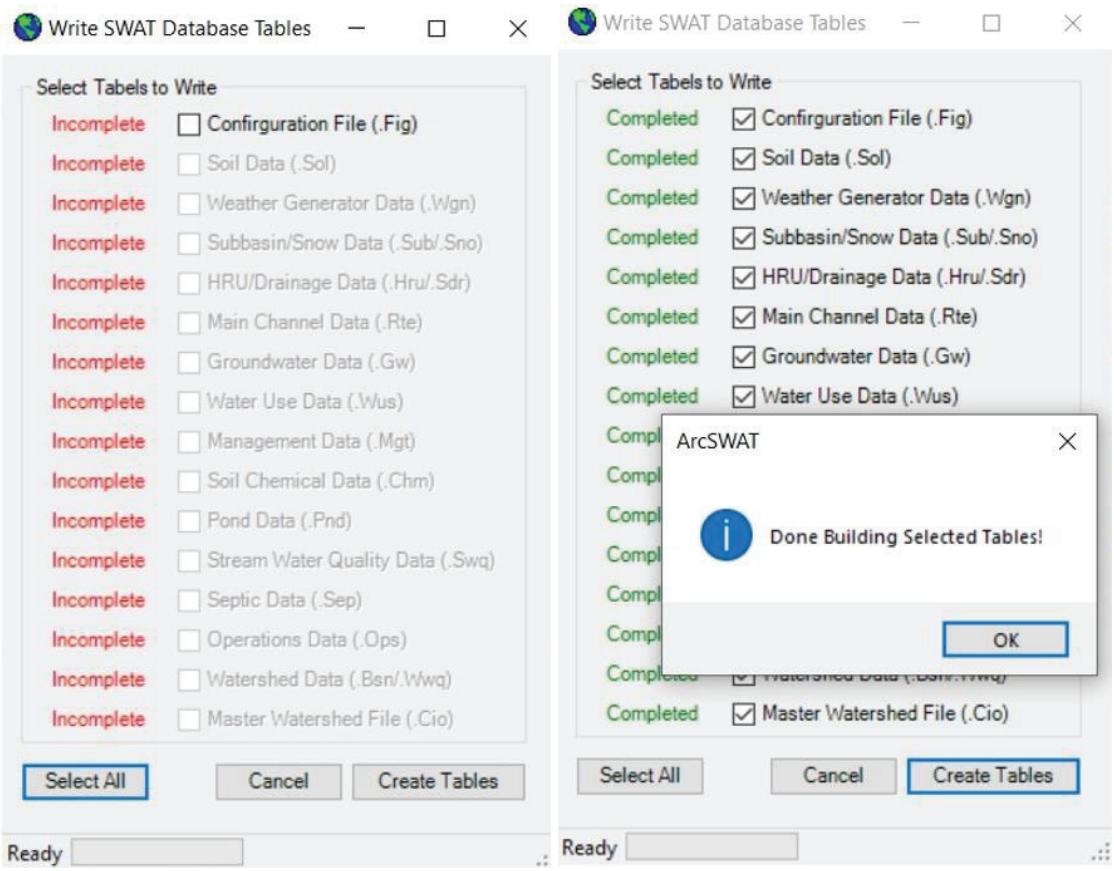

Figure 6.12. Building SWAT Database Tables Before and After Screenshots

Building the SWAT database tables is a time-consuming task, and can sometimes give errors that would require rechecking the uploaded weather datasets. Fortunately, in this study, no error was received at this step.

6.5. SWAT Model Simulation

SWAT simulation is considered to be the last of the model setup processes. Following carefully the tasks explained in sections 6.2 to 6.4, the next step is to go for the SWAT model simulation. SWAT2012 model environment provides a SWAT simulation menu which comes into the picture after all the steps for the model are done. The first input is to check if the period of simulation is taken correctly by the model algorithm, which reads the input data uploaded in the system in the Weather Data Definition (Figure 6.13). In this study, the period of simulation is from 01.01.1989 – 31.12.2010. The second step is to select the rainfall distribution method, which in this study, is selected as skewed normal with rainfall data in daily units. The third thing to consider prior to running the simulation is printout settings. In this study, the monthly data output is selected with a number of years skipped (KYSKIP) of 6 years for the warm-up period. In this case, the model does not print the results for the 6-year warmup. In the next step, "All" is chosen to print out the whole output files. SWAT model simulation run is working in both available SWAT2012 versions for 64-bit computing machines, 64-bit debug, and 64-bit release, respectively. For the current study, 64-bit debug is utilized. It is because that 64-bit debug version will report any the problems and the reason why the model crushed or

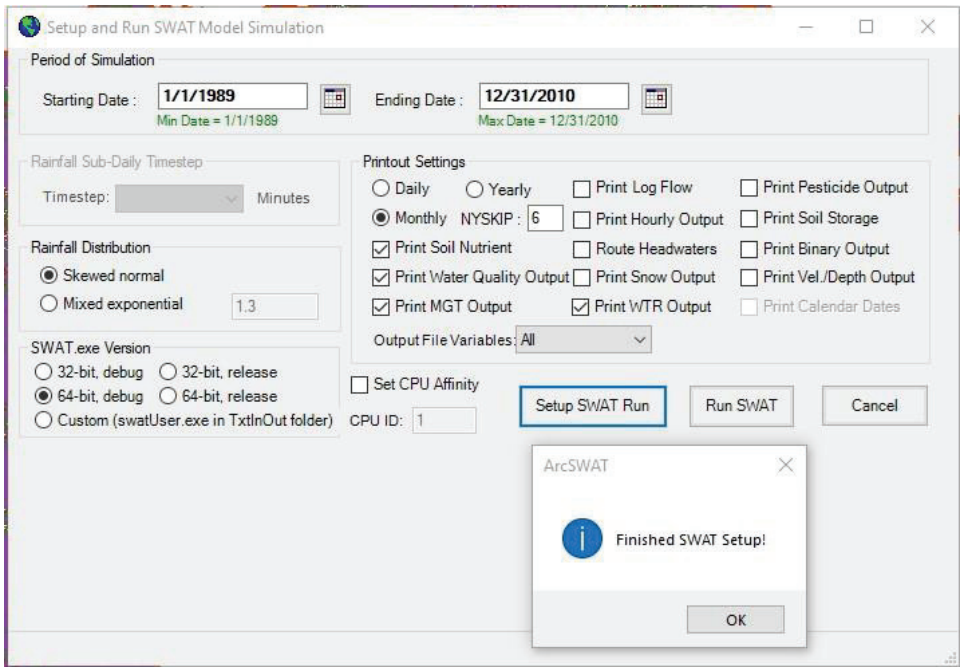

Figure 6.13. SWAT Model Simulation Menu

stop working. 64-bit release version runs faster than 64-bit debug, however, in case any problem happens, the model does not provide a report. By activating and clicking on the "Setup SWAT run" button, it sets the model up and creates a file named 'master control file', file.cio (Figure 6.14) which provides a piece of general information for the simulation model setup.

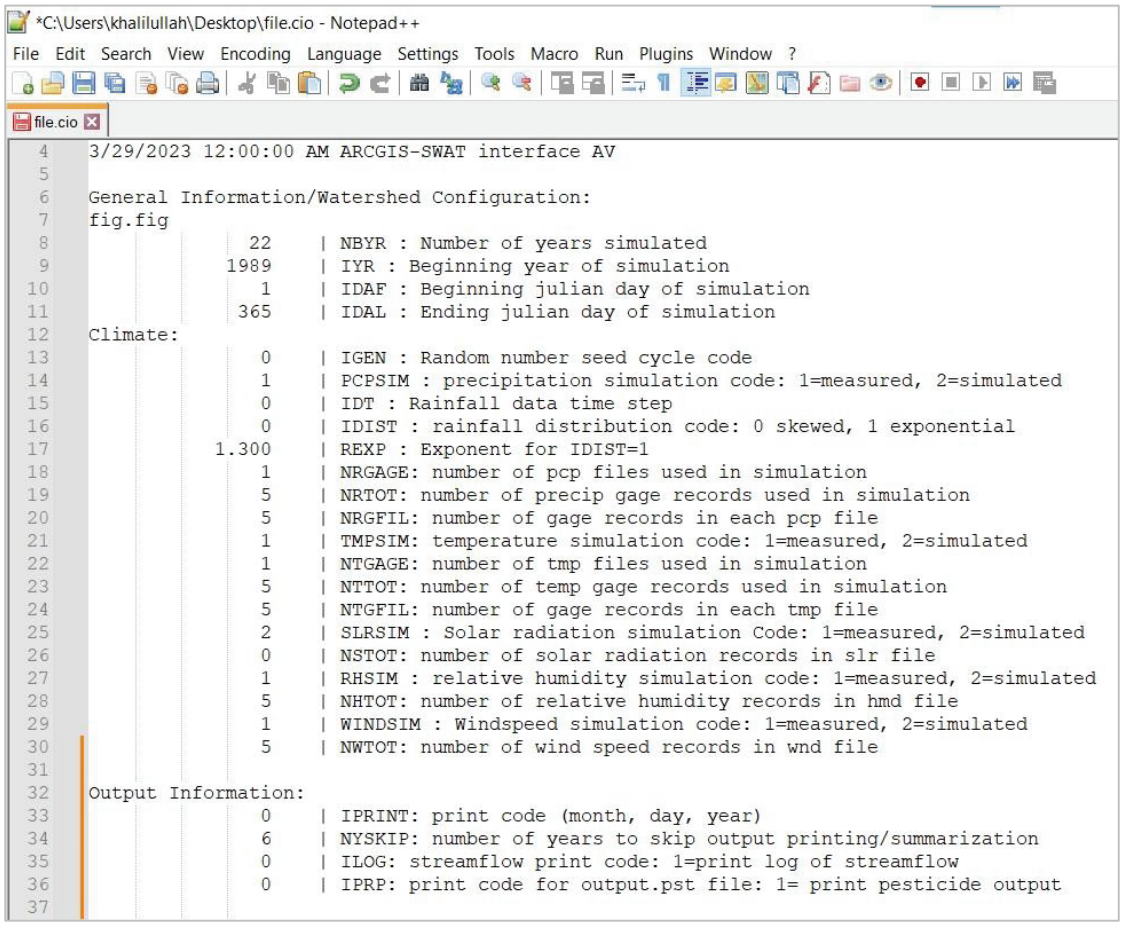

Figure 6.14. Watershed Master Control file (file.cio)

6.6. Sensitivity Analysis

Sensitivity analysis is a post-SWAT model simulation step. It is performed by SWAT Calibration and Uncertainty Program (SWAT-CUP) in order to evaluate the suitable model parameters. Prof. Dr. Karim Abbaspour developed the program with the aim of checking the sensitivity analysis, calibration, and validation of the simulated SWAT model-produced data. SWAT-CUP program contains the following methods:

I. Sequential Uncertainty Fitting version 2 (SUFI2)
II. Generalized Likelihood Uncertainty Estimation (GLUE)
III. Particle Swarm Optimization (PSO)
IV. Parameter Solution (ParaSol),
V. Markov Chain Monte Carlo (MCMC)

SUFI-2 takes into account all potential sources of uncertainty, including model input, observation data inaccuracy, and model structure. Twenty-one sensitive parameters controlling the output variable were found using the sensitivity analysis results (Table 6.1) (Güngör and Göncü, 2013; Abbaspour et al., 2015). SWAT-CUP employs an inner sensitivity analysis method, Latin hypercube, one factor at a time to identify the parameters (Griensven et al., 2006). The parameters were changed simultaneously to fit the ranges until a good match between the observed and SWAT model simulated flows for each sub-basin in Porsuk River Basin was found.

Three distinct ways (v, a, and r) are available in SWAT-CUP to specify the kind of change to be made to the parameter. Where ("v_") denotes replacing the current parameter value with the supplied value, ("a_") denotes adding the specified value to the current parameter value, and ("r_") denotes multiplying the current parameter value by (1 + a given value).

Table 6.1. List of Sensitive Parameters

No.	SWAT-CUP Parameter Name	Parameter Name
1	R__CN2.mgt	SCS runoff curve number II
2	V__PLAPS.sub	Precipitation lapse rate
3	V__TLAPS.sub	Temperature lapse rate
4	V__GWQMN.gw	Threshold depth of water in the shallow aquifer required for return flow to occur (mm)
5	V__SFTMP.bsn	Snow melt base temperature
6	V__SMFMN.bsn	Minimum melt rate for snow during the year (occurs on winter solstice)
7	R__HRU_SLP.hru	Average slope steepness
8	R__SLSUBBSN.hru	Average slope length
9	V__GW_DELAY.gw	Groundwater delay (days)
10	V__TIMP.bsn	Snow pack temperature lag factor
11	V__REVAPMN.gw	Threshold depth of water in the shallow aquifer for "revap" to occur (mm)
12	R__SOL_K(..).sol	Saturated hydraulic conductivity
13	R__ESCO.hru	Soil evaporation compensation factor
14	V__SMFMX.bsn	Maximum melt rate for snow during year (occurs on summer solstice)
15	V__SURLAG.bsn	Surface runoff lag time
16	R__SOL_AWC.sol	Available water capacity of the soil layer
17	R__OV_N.hru	Manning's "n" value for overland flow
18	V__ALPHA_BF.gw	Baseflow alpha factor (days)
19	V__GW_REVAP.gw	Groundwater "revap" coefficient

6.7. Calibration and Validation

In response to the findings of the sensitivity analysis, model calibration was carried out to determine the best values for the sensitive parameters. SWAT offers three calibration options: automatic calibration, manual calibration, and a combination of the two. For this study, some of the parameters were initially manually calibrated. Then, manual calibration was used to tweak several model parameters. In this technique, parameter values were changed by altering one or two parameters at a time while staying within the permissible ranges, either by replacing the starting value or by adding to or multiplying the initial value as per the interface's design.

The model calibration and validation were completed using the Sequential Uncertainty Fitting (SUFI-2) technique in the SWAT-CUP program (Abbaspour et al., 2004, 2007). In this study, the calibrating software (SWAT-CUP) uses the previously simulated discharge from the SWAT model and the time series of discharge at the five different sub-outlets basins as inputs to calibrate and validate outputs under the specified sensitive parameters. The rankings of the most sensitive and effective parameters will be sorted in the coming chapter under Table 7. The real observed data that is set to be calibrated and validated need to be portioned into two sub-categories, one for each, respectively. The portioned data should be homogenous, meaning it must contain data for all the year's seasons. The calibration data in this study covers the period of (1996-2005).

The same procedure is conducted for the observed data validation case. The identical input parameters with the same value ranges utilized for the calibration procedure held true during the data validation step. The validation data is from (2006-2010).

6.8. Model Performance Evaluation

The assessment of the model's performance is required to evaluate the simulation outputs in relation to the observed data. There are several techniques to assess the model's effectiveness during the calibration and validation phases. Coefficient of determination (R^2), Nash Sutcliffe simulation efficiency (NSE), and Percent Bias (PBIAS) were the three techniques used in this research. The ranges to follow along with these parameters are given in Table 6.3. R^2 is a measure of how much of the overall variance in the observed data can be accounted for by the model. R^2 has a range of 0.0 to 1.0. Greater values indicate improved performance.

$$R^2 = \frac{\left[\sum_{i=1}^{n}\left(Q_{sim} - Q_{sim_m}\right) * \left(Q_{obs} - Q_{obs_m}\right)\right]^2}{\sum_{i=1}^{n}\left(Q_{sim} - Q_{sim_m}\right)^2 * \sum_{i=1}^{n}\left(Q_{obs} - Q_{obs_m}\right)^2} \quad (6.1)$$

where Q_{obs} is the observed flow data, Q_{sim} is the simulated flow data, Q_{obsm} is the mean observed flow data and Q_{simm}shows the mean simulated flow data.

The plots of real versus simulated data are compared to see how well they fit the 1:1 line using the Nash-Sutcliffe simulation efficiency (NSE). NSE can have a value between 0 and 1, with a value of 0 indicating that the observed data mean is a better predictor than the simulated values and a value of 1 indicating a perfect match between the two.

$$NSE = 1 - \frac{\sum_{i=1}^{n}\left(Q_{obs} - Q_{sim}\right)^2}{\sum_{i=1}^{n}\left(Q_{obs} - Q_{obs_m}\right)^2} \quad (6.2)$$

Where Q_{obs} is the observed flow data, Q_{sim} is the simulated flow data and $Q_{obsm}$is the mean observed flow data.

Table 6.2. Performance ranges for calibration and validation processes.

Performance	R^2	NSE	PBIAS
Very Good	0.75 - 1.00	0.75 - 1.00	0 - $\pm$10
Good	0.65 - 0.75	0.65 - 0.75	$\pm$10 - $\pm$ 15
Sufficient	0.50 - 0.65	0.50 - 0.65	$\pm$15 - $\pm$25
Not Good	0.50 - 0.00	0.50 - 0.00	> $\pm$25

Percentage bias (PBIAS) calculates the mean inclination of the simulated data to differ from the observed values by a certain amount. Positive numbers indicate model underestimation, whereas negative values indicate model overestimation. The ideal value is zero for PBIAS.

$$\text{PBIAS} = \frac{\sum_{i=1}^{n} \left(\left(Q_{obs} - Q_{sim} \right) * 100 \right)}{\sum_{i=1}^{n} \left(Q_{obs} \right)} \tag{6.3}$$

where $Q_{obs}$is the observed flow data and Q_{sim} is the simulated flow data.

CHAPTER 7

RESULT AND DISCUSSION

This analysis in Porsuk River Basin is divided into two major sections: i) the Impact of 1990 Land Use (Scenario 1) and ii) 2006 Land Use changes on the hydrology and water balance of the basin (Scenario 2). The study analysis is discussed based on the chronological order, which starts from SWAT model watershed delineation, calibration, and validation of the simulated SWAT model data and finally, discussing the parameters with their respective ranges that are found to be the most sensitive and reading the two scenarios impacts on hydrological parameters surface runoff, evapotranspiration, groundwater, and lateral flow, respectively.

7.1. Land Use

The water cycle is impacted by changes in land use and vegetation, and the impact depends on the species' morphology and plant cover density. The water cycle is impacted by changes in land use and vegetation, and the impact depends on the species' morphology and plant cover density. The Porsuk River Basin's reaction to several hydrological parameters was examined using likely changes in two distinct land use change scenarios, 1990 and 2006, respectively. The study's objective is to examine the temporal evolution of surface runoff, evapotranspiration, groundwater, and lateral flow rates due to changes in land uses, mostly due to urban development.

7.1.1. 1990 CORINE Land Use (Scenario 1)

There are 20 distinct land use classifications identified based on the 1990 CORINE land use, as indicated in Table 7.1. 43% of the land is used for agriculture (AGRL), which is the main land use, followed by rangeland, forests, urban areas, and wetlands.

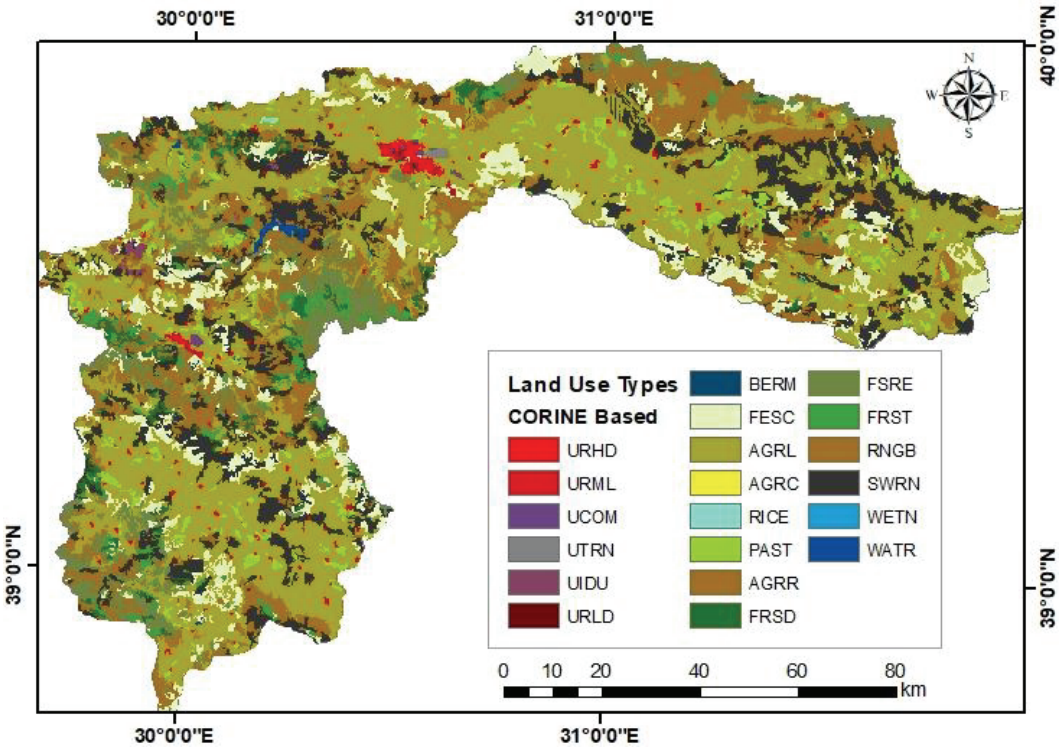

Figure 7.1. 1990 CORINE Land Use Classification

Based on the Porsuk River Basin 1990 CORINE land use and SWAT model classification, there are 20 different land-use classes (Figure 7.1). The dominating classes are agricultural land, shrub-land, and sparsely vegetated areas with coverage percentages of 43.19, 13.81, and 13.8, respectively.

Table 7.1. 1990 Land Use Classification Table

CORINE Code	Class Name	SWAT Code	SWAT Class	Area (km^2)	Area (%)
212	Permanently irrigated land	AGRC	Small Grains	0.4	0.0
211	Non-irrigated arable land	AGRL	Agricultural Land Generic	4611.11	43.19
243	Agricultural Land-Row Crops	AGRR	Row Crops	440.1	4.12
141	Green Urban Areas	BERM	Bermuda Grass	2.95	0.03
321	Natural Grass Land	FESC	Tall Fescue	935.17	8.76
311	Broad-leaved forest	FRSD	Deciduous Forest	223.12	2.09

(cont. on next page)

Table 7.1. (Cont.)

231	Pastures	PAST	Pasture	329.32	3.1
313	Mixed Forest	FRST	Forest-Mix	211.9	2.0
312	Coniferous Forest	FRSE	Evergreen Forest	753.7	7.0
213	Rice Fields	RICE	Rice	3.85	0.01
132	Dump Sites	RNGB	Range Shrub-land	1447.16	13.81
333	Sparsely Vegetated Areas	SWRN	Bare Rock	1495.6	13.80
121	Industrial Units	UCOM	Urban Commercial	15.01	0.14
131	Mineral Sites	UIDU	Urban Industrial	36.11	0.34
111	Continuous Urban Fabric	URHD	Urban High Density	30.43	0.29
133	Construction Sites	URLD	Residential, Low Density	1.36	0.01
112	Discontinuous Urban Fabric	URML	Urban Medium Density	124.93	1.17
122	Road and rail networks	UTRN	Urban Transportation	8.52	0.08
512	Water Bodies	WATR	Water	27.38	0.26
411	Inland Marshes	WETN	Wetlands-Non-Forested	1.8	0.02

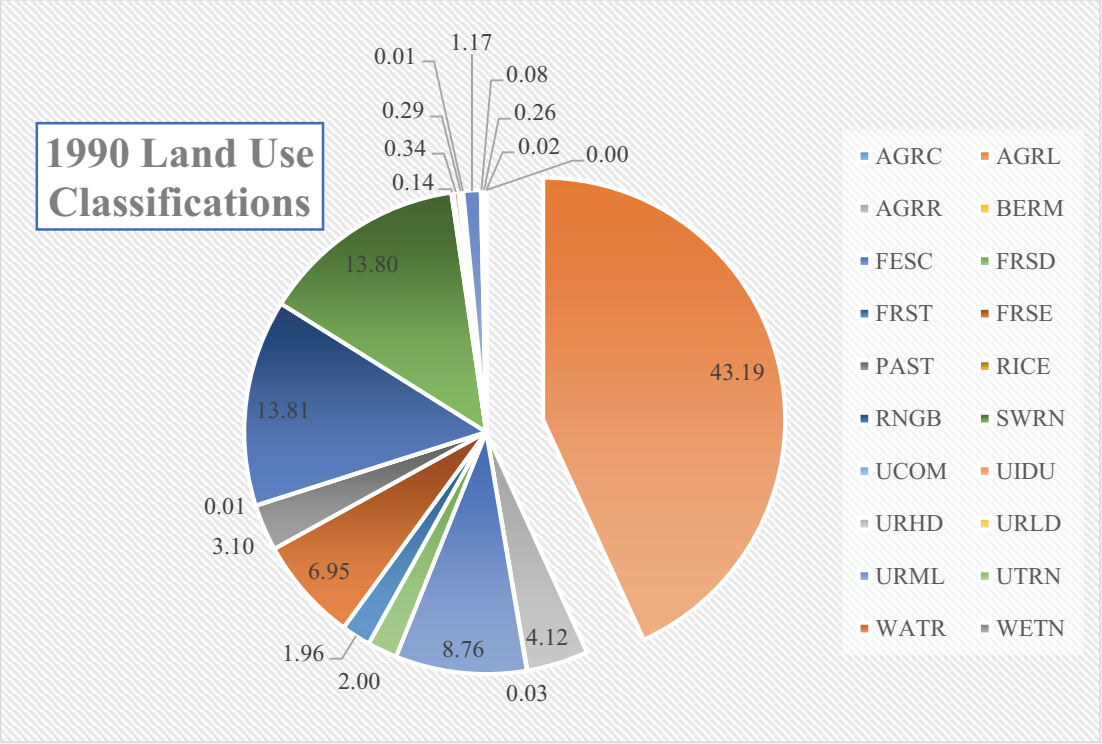

Figure 7.2. 1990 Land Use Classification Pie Chart

7.1.2. 2006 CORINE Land Use (Scenario 2)

There are 21 distinct land use classifications identified based on the 2006 CORINE land use, as indicated in Table 7.2. 32% of the land is used for agriculture (AGRL), which is the main land use, followed by rangeland, forests, urban areas, and wetlands.

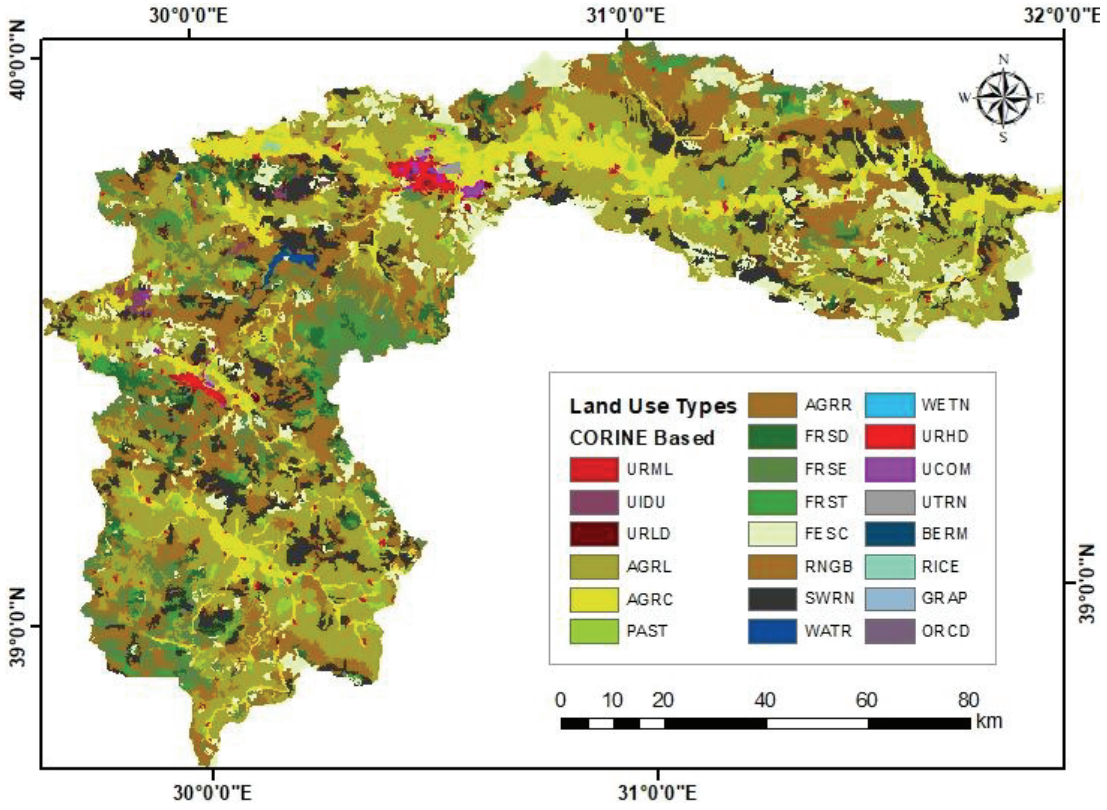

Figure 7.3. 2006 CORINE Land Use Classification

It is clear that over the past 22 years, there has been a rise in residential and industrial areas and rangelands with a loss in agricultural land, forest, grass, and marshy terrain. As shown in Figure 7.2, the land use and land cover map from 1990 reveals that the entire cultivated land comprised around 43.19% of the watershed's total area. In 2006, it quickly decreased to about 32.16% of the watershed (Figure 7.3). This is primarily due to population growth, which increased the need for new settlement areas and agricultural land, leading to a decline in the area's different kinds of land use and land cover.

Table 7.2. 2006 Land Use Classification Table

CORINE Code	CLASS NAME	SWAT Code	SWAT CLASS	Area (km^2)	Area (%)
212	Permanently irrigated land	AGRC	Agricultural Land-Close-grown	1122.8	10.52
211	Non-irrigated arable land	AGRL	Agrıcultural Land Generic	3434.1	32.16
243	Agricultural Land-Row Crops	AGRR	Row Crops	540.6	5.10
141	Green Urban Areas	BERM	Bermuda Grass	2.5	0.02
321	Natural Grass Land	FESC	Tall Fescue	910.2	8.53
311	Broad-leaved forest	FRSD	Deciduous Forest	255.1	2.39
313	Mixed Forest	FRST	Forest-Mix	222.6	2.08
312	Coniferous Forest	FRSE	Evergreen Forest	736.6	6.90
231	Pastures	PAST	Pasture	302.9	2.84
213	Rice Fields	RICE	Rice	3.9	0.04
132	Dump Sites	RNGB	Range Shrub-land	1701.2	15.93
333	Sparsely Vegetated Areas	SWRN	Bare Rock	1146.5	10.74
121	Industrial Units	UCOM	Urban Commercial	32.5	0.30
131	Mineral Extraction Sites	UIDU	Urban Industrial	62.0	0.58
111	Continuous Urban Fabric	URHD	Urban High Density	42.9	0.40
133	Construction Sites	URLD	Residential, Low Density	6.9	0.06
112	Discontinuous Urban Fabric	URML	Urban Medium Density	105.4	0.99
122	Road and rail networks	UTRN	Urban Transportation	14.4	0.13
512	Water Bodies	WATR	Water	28.8	0.27
411	Inland Marshes	WETN	Wetlands-Non-Forested	4.4	0.04

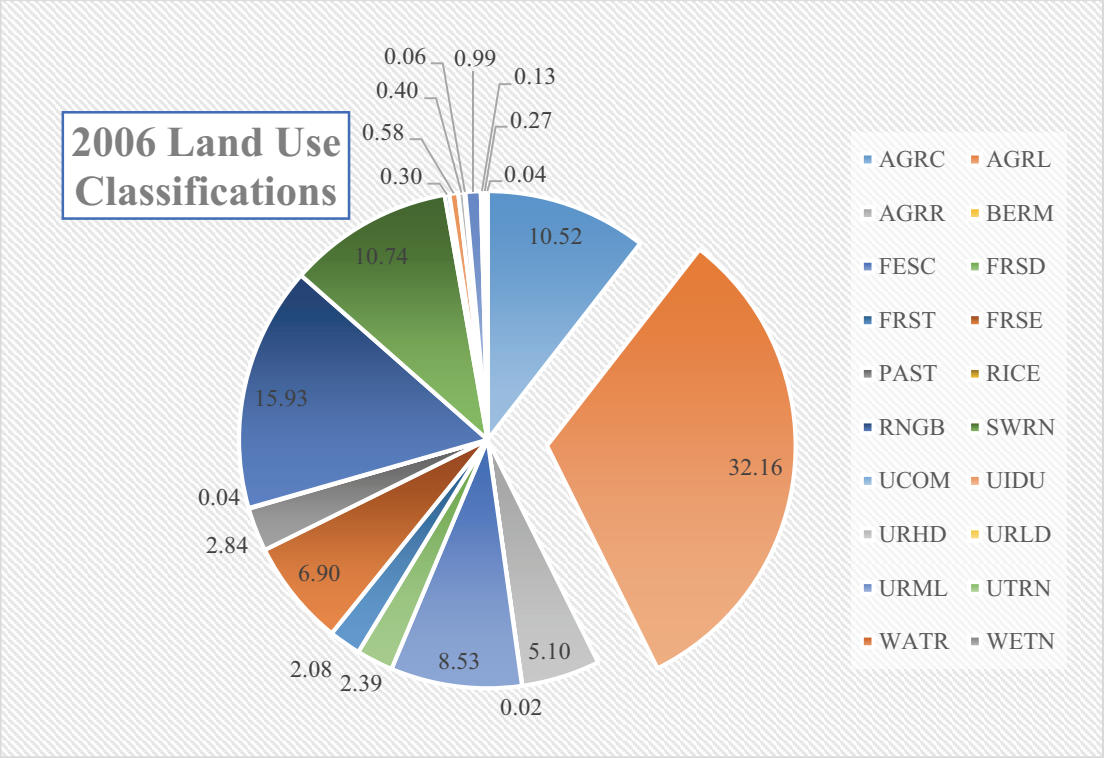

Figure 7.4. Land Use Types (2006) Classification Pie Chart

7.2. Sensitivity Analysis

In general, sensitivity analysis was done to reduce the complexity of the model parameter. A literature review was done to find commonly used characteristics that affect water flow to get around the complexity as shown in Table 7.3. 11 of those parameters crucial to the model's structure were individually checked as part of the screening process.

Table 7.3. The most Sensitive Parameters

No.	Parameter Name	Parameter Name
1	R__CN2.mgt	SCS runoff curve number II
2	V__PLAPS.sub	Precipitation lapse rate
3	V__TLAPS.sub	Temperature lapse rate
4	V__GWQMN.gw	Threshold depth of water in the shallow aquifer required for return flow to occur (mm)
5	V__SMTMP.bsn	Snow melt base temperature
6	V__SMFMN.bsn	Minimum melt rate for snow during the year (occurs on winter solstice)
7	R__HRU_SLP.hru	Average slope steepness
8	R__SLSUBBSN.hru	Average slope length
9	V__GW_DELAY.gw	Groundwater delay (days)
10	V__TIMP.bsn	Snow pack temperature lag factor
11	V__REVAPMN.gw	Threshold depth of water in the shallow aquifer for "revap" to occur (mm)
12	R__SOL_K(..).sol	Saturated hydraulic conductivity
13	R__ESCO.hru	Soil evaporation compensation factor
14	V__SMFMX.bsn	Maximum melt rate for snow during year (occurs on summer solstice)
15	V__SURLAG.bsn	Surface runoff lag time
16	R__SOL_AWC.sol	Available water capacity of the soil layer
17	R__OV_N.hru	Manning's "n" value for overland flow
18	V__ALPHA_BF.gw	Baseflow alpha factor (days)
19	V__GW_REVAP.gw	Groundwater "revap" coefficient
20	V__CH_N2.rte	Manning's "n" value for the main channel
21	V__CH_K2.rte	Effective hydraulic conductivity in main channel alluvium
22	V__SOL_ZMX.sol	Maximum rooting depth of soil profile
23	V__RCHRG_DP.gw	Deep aquifer percolation fraction

The hydrological parameters were then configured using the global sensitivity analysis approach for the SWAT-CUP with the SUFI-2 algorithm. The SWAT-CUP (SUFI-2) technique measures and indicates the significance of sensitivity using two variables (Figure 7.5), namely t-stat, and p-value (Van Griensven and Meixner 2006). When the t-state and p-value are close to zero, a sensitive parameter will have a higher absolute value based on the Nash-Sutcliffe objective function.

The t-Stat and P-values of the parameters that are entered are used to determine how sensitive they are. The more absolute t-Stat value is bigger and P-value is smaller, the more sensitive the model parameters are (Figure 7.6). The sensitivity of each parameter is calculated using the Latine Hypercube Sampling one-at-a-time approach. Data on observed monthly discharges from several stations are specified as the process's inputs. For a period of 22 years (1989–2010), the model's simulated monthly discharge data were acquired based on the upper and lower bounds of each sensitive parameter that were initially defined. Eighteen of the twenty-two hydrological parameters that were assessed for sensitivity were used to calibrate the model.

Parameter Name	t-Stat	P-Value
11:V__TIMP.bsn	0.037314363	0.970261038
18:R__OV_N.hru	0.162689549	0.870880646
2:V__SFTMP.bsn	0.171585649	0.863887675
7:R__SLSUBBSN.hru	-0.294114035	0.768889457
6:V__SMFMN.bsn	0.322540441	0.747284874
15:V__SMFMX.bsn	0.543124358	0.587477826
8:V__SFTMP.bsn	0.547001701	0.584814803
10:V__TLAPS.sub	0.731641374	0.465001565
16:V__SURLAG.bsn	-1.154418869	0.249316329
14:R__ESCO.hru	1.191457176	0.234486711
4:V__PLAPS.sub	-1.338634020	0.181779602
13:R__SOL_K(..).sol	1.641501374	0.101820096
19:V__ALPHA_BF.gw	1.668055867	0.096426523
12:V__REVAPMN.gw	1.898331155	0.058684331
17:R__SOL_AWC(.....	-2.161641829	0.031496187
5:R__HRU_SLP.hru	2.398874097	0.017102033
20:V__GW_REVAP.gw	-10.764984974	0.000000000
3:R__CN2.mgt	14.872811663	0.000000000
9:V__GW_DELAY.gw	-20.186556016	0.000000000
1:V__GWQMN.gw	-23.105485779	0.000000000

Figure 7.5. t-value and p-value of Sensitive Parameters

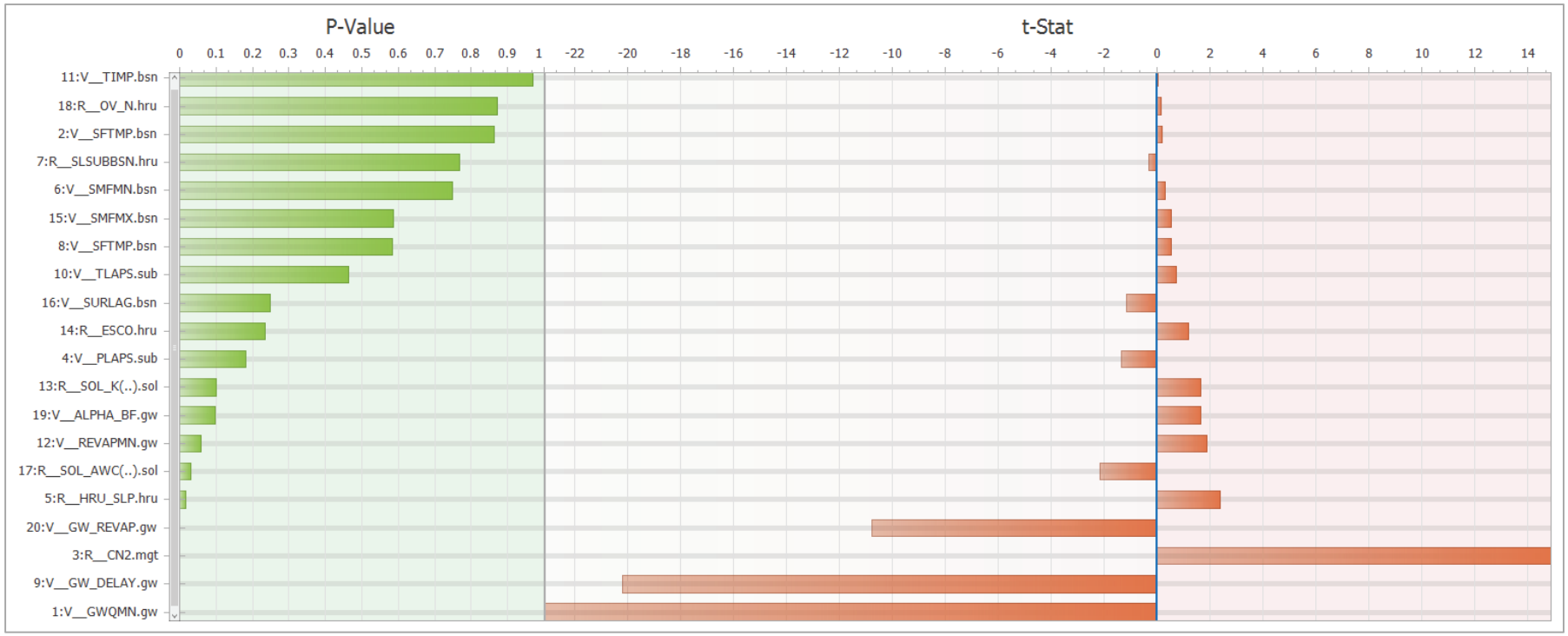

Figure 7.6. Most Sensitive Parameters Schematic Description

The sensitive parameters are ranked using the Nash-Sutcliffe (NS) objective function in SUFI 2 algorithm; in the results, bigger values in the t-state and lower P-values indicate the most sensitive status of the parameter. The parameters arrangement in (Figure 7.6) show that groundwater, sub-basins, and management characteristics in the research area influence the results the highest. Based the ranking and sensitivity of the results, it can be inferred that the research area has a highly complicated hydrological variability. The most sensitive parameters were found to be the threshold depth of water in the shallow aquifer required for return flow to occur (GWQMN.gw), groundwater delay (GW_DELAY), runoff curve number for moisture condition II (CN2.mgt), groundwater revap coefficient (GW_REVAP), and Average slope steepness (HRU_SLP.hru).

7.3. Calibration and Validation

Distributed watershed models with a physical foundation should be calibrated before being used to simulate hydrological parameters. It is for the cause of lessening the degree of uncertainty surrounding the model's prediction. The observed and simulated flow data were compared in calibration and validation approaches. Monitoring data were only used to confirm the model's general range and magnitude of results in the SWAT-CUP as inputs. In this study, the model was run for calibration and validation based on 1990 and 2006 dated CORINE land use land cover (LULC) maps with constant DEM, soil, and meteorological data from January 1989 to December 2010 in the Porsuk River Basin to evaluate the effects of LCLU changes on hydrological parameters. The observed discharge data between (1995-2004) has been selected for calibration with six years of model warm-up. Simulations were started in 1989 because hydrological models require a warm-up period to be as independent from initial circumstances as possible. The rest of the observed discharge data (2005-2010) is used for validation. SWAT-CUP is run based on a monthly time scale considering the first available parameter values to stay the same. Basin and sub-basin scale analyses were done using the simulation results from previous analyses in the SWAT model. To assess the effects of LCLU changes on hydrological components, the evaluation in cumulative pattern was done at the sub-basin scale. The sub-basin scale LCLU changes together with specific hydrological parameter changes, were assessed to see how sensitive these components were to various LCLU changes.

7.3.1. Parameter Calibration for Five Sub-basins: Scenario 1

The calibration processes aimed at the comparison of the observed runoff data and SWAT simulated runoff data in accordance with the 1990 CORINE land use data and considering the other datasets constant, every sub-basin parameter considered (Table 7.4) in calibration in the Porsuk River Basin is provided in the following tables individually. The calibration is done between 1995-2004 years.

The calibration process is carried out on the 19 parameters that have the highest sensitivity status discovered during the sensitivity study (section 7.2), and their values are repeatedly modified to an acceptable range. During the calibration phase, coefficients of determination (R^2) for the hydrological stations (Kiranharmani, Parsibey, Porsuk Dam,

Porsuk Ciftligi, and Murat Ciftligi) were found to be 0.74, 0.78, 0.77, 0.79, and 0.86, respectively. The SWAT-Cup model is run multiple times to generate better calibrated results with a number of 350 simulations on every run set. The initial parameter ranges and fitted values during calibration period are shown in Table 7-4, Table 7-5, Table 7-6, Table 7-7, and Table 7-8. The scatter plot for the comparison between the simulated and observed discharge during calibration phase in monthly timescale is shown in Figure 7.7.

Table 7.4. Parameter Ranges and fitted values during calibration period for Kiranharmani Catchment

Calibrated Parameter Range Values			
SWAT-CUP Parameter Name	**Monthly Time Scale**		
	Min Value	**Max Value**	**Fitted Value**
R__CN2.mgt	-0.19233	0.18725	-0.00461
V__PLAPS.sub	-245.625	285.62502	-101.302
V__TLAPS.sub	-16.0000	0.0580012	-8.2117
V__GWQMN.gw	-1434.857	2934.847	-407.969
V__SFTMP.bsn	-2.16085	3.827512	-0.75358
V__SMFMN.bsn	-4.318838	1.985504	0.461955
R__HRU_SLP.hru	0.167374	0.732626	0.332239
R__SLSUBBSN.hru	-0.166130	0.282796	-0.09056
V__GW_DELAY.gw	40.54243	450.284	65.2833
V__TIMP.bsn	0.12875	0.865754	0.585000
V__REVAPMN.gw	-154.257	267.8625	29.2667
R__SOL_K(..).sol	-0.20452	0.28365	0.199333
R__ESCO.hru	0.48350	1.16355	0.638333
V__SMFMX.bsn	0.58247	8.5418	5.916667
V__SURLAG.bsn	-8.25879	15.5983	2.458333
R__SOL_AWC.sol	0.55418	1.25815	0.665000
V__RCHRG_DP.gw	0.55326	1.15456	0.174500
V__ALPHA_BF.gw	0.24658	1.34158	0.275000
V__GW_REVAP.gw	0.01247	0.18574	0.044900

Table 7.5. Parameter Ranges and fitted values during calibration period for Parsibey Catchment

Calibrated Parameter Range Values			
SWAT-CUP Parameter Name	**Monthly Time Scale**		
	Min Value	**Max Value**	**Fitted Value**
R__CN2.mgt	-0.338378	0.021044	-0.222764
V__PLAPS.sub	24.972897	516.760437	502.82644
V__TLAPS.sub	-17.550842	-5.690357	-7.449663
V__GWQMN.gw	1921.88415	5778.11523	3869.281006
V__SFTMP.bsn	-3.956185	2.022853	-3.388176
V__SMFMN.bsn	3.480216	10.473117	4.797213
R__HRU_SLP.hru	0.421053	1.265613	0.588557
R__SLSUBBSN.hru	0.218861	0.657805	0.358592
V__GW_DELAY.gw	242.630508	649.169495	527.885376
V__TIMP.bsn	0.261039	0.785627	0.379071
V__REVAPMN.gw	-182.8218	272.821106	117.143341
R__SOL_K(..).sol	-0.194247	0.068913	-0.178019
R__ESCO.hru	0.381071	1.145595	0.914964
V__SMFMX.bsn	-1.056231	6.322897	0.161325
V__SURLAG.bsn	-7.139552	14.306218	-0.884536
R__SOL_AWC.sol	0.404401	1.215599	0.595033
R__OV_N.hru	-0.147923	0.284589	-0.063583
V__ALPHA_BF.gw	0.464370	1.395630	0.900510
V__GW_REVAP.gw	0.086182	0.219018	0.192229

Table 7.6. Parameter Ranges and fitted values during calibration period for Porsuk Dam Catchment

Calibrated Parameter Range Values			
SWAT-CUP Parameter Name	**Monthly Time Scale**		
	Min Value	**Max Value**	**Fitted Value**
R__CN2.mgt	-0.338378	0.021044	0.013556
V__PLAPS.sub	24.972897	516.760437	199.147644
V__TLAPS.sub	-17.550842	-5.690357	-6.728149
V__GWQMN.gw	1921.884155	5778.115234	4123.149414
V__SFTMP.bsn	-9.156266	0.289600	-7.227735
V__SMFMN.bsn	3.480216	10.473117	5.374126
R__HRU_SLP.hru	0.421053	1.265613	0.473838
R__SLSUBBSN.hru	0.218861	0.657805	0.506004
V__GW_DELAY.gw	242.630508	649.169495	349.346985
V__TIMP.bsn	0.261039	0.785627	0.516776
V__REVAPMN.gw	-182.821121	272.821106	65.883591
R__SOL_K(..).sol	-0.194247	0.068913	-0.142712
R__ESCO.hru	0.381071	1.145595	1.097812
V__SMFMX.bsn	-1.056231	6.322897	4.754832
V__SURLAG.bsn	-7.139552	14.306218	-4.905618
R__SOL_AWC.sol	0.404401	1.215599	0.617340
R__OV_N.hru	-0.147923	0.284589	-0.066827
V__ALPHA_BF.gw	0.464370	1.395630	1.236540
V__GW_REVAP.gw	0.086182	0.219018	0.189683

Table 7.7. Parameter Ranges and fitted values during calibration period for Porsuk Ciftligi Catchment

Calibrated Parameter Range Values			
SWAT-CUP Parameter Name	**Monthly Time Scale**		
	Min Value	**Max Value**	**Fitted Value**
R__CN2.mgt	-0.163059	0.190171	0.185756
V__PLAPS.sub	39.919292	358.37601	54.51522
V__TLAPS.sub	-12.149611	-1.306687	-1.622939
V__GWQMN.gw	3019.2095	5227.0893	4941.9047
V__SFTMP.bsn	-10.994484	-3.460986	-4.308505
V__SMFMN.bsn	2.818778	7.929474	3.904801
R__HRU_SLP.hru	0.077221	0.870455	0.787826
R__SLSUBBSN.hru	0.362054	0.649954	0.399241
V__GW_DELAY.gw	199.09308	499.60089	448.26413
V__TIMP.bsn	0.381879	0.651673	0.511155
V__REVAPMN.gw	-58.85142	190.618607	85.633293
R__SOL_K(..).sol	-0.248757	-0.036667	-0.092341
R__ESCO.hru	0.738816	1.456808	0.999088
V__SMFMX.bsn	1.842776	7.666888	2.886263
V__SURLAG.bsn	-14.53031	4.719078	-10.11899
R__SOL_AWC.sol	0.317513	0.917167	0.594853
R__OV_N.hru	-0.24289	0.109240	0.025608
V__ALPHA_BF.gw	0.849643	1.623437	1.162385
V__GW_REVAP.gw	0.137813	0.241553	0.239392

Table 7.8. Parameter Ranges and fitted values during calibration period for Murat Ciftligi Catchment

Calibrated Parameter Range Values			
SWAT-CUP Parameter Name	**Monthly Time Scale**		
	Min Value	**Max Value**	**Fitted Value**
R__CN2.mgt	0.009123	0.362389	0.357973
V__PLAPS.sub	-97.683372	206.713821	-83.7318
V__TLAPS.sub	-6.895735	3.649857	3.342278
V__GWQMN.gw	3978.7209	5905.0884	5656.266
V__SFTMP.bsn	-7.658043	-0.958967	-1.712613
V__SMFMN.bsn	1.888157	5.921445	2.745231
R__HRU_SLP.hru	0.431860	1.143792	1.069632
R__SLSUBBSN.hru	0.273639	0.524843	0.306086
V__GW_DELAY.gw	323.41327	573.1149	530.45764
V__TIMP.bsn	0.440652	0.581658	0.508217
V__REVAPMN.gw	13.178275	158.08833	97.105331
R__SOL_K(..).sol	-0.170735	-0.013947	-0.055104
R__ESCO.hru	0.769644	1.228532	0.935991
V__SMFMX.bsn	0.490853	5.281672	1.349208
V__SURLAG.bsn	-17.554844	-2.683142	-14.14674
R__SOL_AWC.sol	0.433181	0.756525	0.582728
R__OV_N.hru	-0.108937	0.160153	0.096244
V__ALPHA_BF.gw	0.931175	1.393595	1.118070
V__GW_REVAP.gw	0.188514	0.290270	0.288150

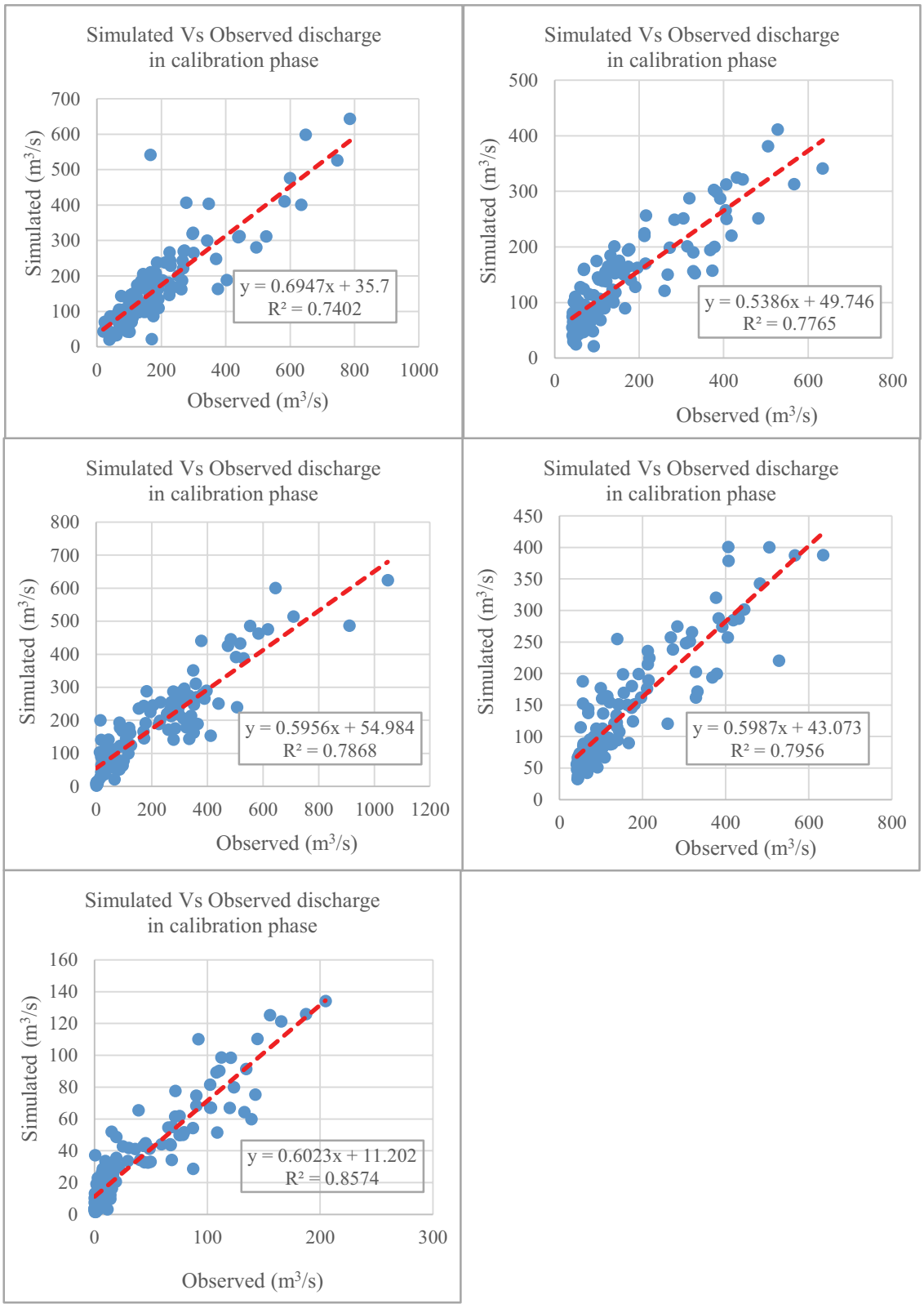

Figure 7.7. The comparison between the calibrated model and observed monthly discharge results for Kiranharmani, Parsibey, Porsuk Dam, Porsuk Ciftligi, and Murat Ciftligi sub-basins.

7.3.2. Parameter Validation for Five Sub-basins: Scenario 1

For the validation step, after the calibration process, the model's performance was assessed using the same calibrated parameters to mimic the watershed's hydrological operation during a different time period not included in the calibration process which is (2005-2010). Based on observed flow data gathered by DSI at five distinct gauge stations along the Porsuk River Basin, flow calibration and validation were performed using the SWAT-CUP following the exact same 350 number of simulations that was set for the calibration process. In order to evaluate the effectiveness of the SWAT simulation, existing measurements were compared with the anticipated outcomes on a monthly timescale. As discussed in the previous chapter, outflow data between 1995 and 2004 were used for calibration, and the parameters were then confirmed from 2004 to 2010. The statistics of the model performance (R^2, NSE, and PBIAS) for the observed and simulated discharge are shown in Table 7.9.

Table 7.9. Model performance statistics for the Porsuk River Basin

Calibration (1995- 2004)				**Validation (2005- 2010)**			**Model Performance**
Station	R^2	NSE	PBIAS	R^2	NSE	PBIAS	Satisfaction Status
Kiranharmani	0.74	0.78	11	0.67	0.70	-16	Satisfactory
Parsibey	0.78	0.84	6	0.72	0.75	12	Satisfactory
Porsuk Dam	0.77	0.73	15	0.89	0.84	10	Satisfactory
Porsuk Ciftligi	0.79	0.77	-8	0.85	0.79	8	Satisfactory
Murat Ciftligi	0.86	0.84	12	0.91	0.77	14	Satisfactory

In the calibration phase (Figure 7.7), the R^2 values were found as 0.74, 0.78, 0.77, 0.79, and 0.86 for Kiranharmani, Parsibey, Porsuk Dam, Porsuk Ciftligi, and Murat Ciftligi sub-basins, respectively. The values of R^2 in the validation phase (Figure 7.8) were found as 0.67, 0.72, 0.89, 0.85, and 0.91 for the above five sub-basins, respectively. Of which, only the Porsuk Dam sub-basin is found to have low R^2 in calibration compared to the validation step.

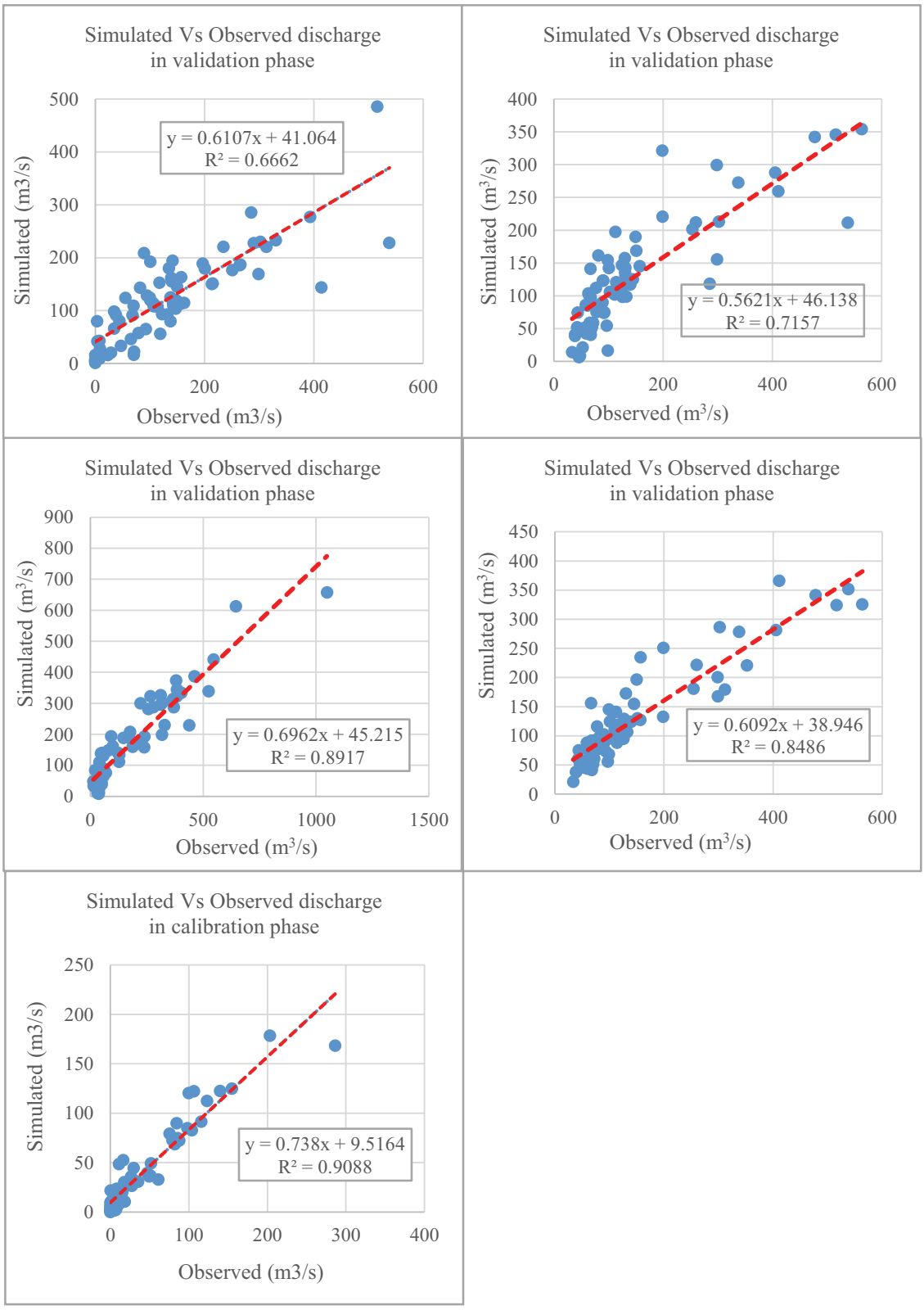

Figure 7.8. The comparison between the validated model and observed monthly discharge results for Kiranharmani, Parsibey, Porsuk Dam, Porsuk Ciftligi, and Murat Ciftligi sub-basins.

When the outputs of the model are compared to the observations at the monitoring stations, as shown in the graphical representations (Figure 7.7 to 7.8), it can be observed that, on the monthly scale, the model satisfactorily simulates the flows. Meanwhile, observing the simulation outcomes for the five sub-basin within the Porsuk River Basin, the increase in the number of simulation (max. 500 and min. 300 simulations checked in this study) inside the SWAT-CUP software does not affect the wellness of NSE and R^2 drastically.

Figures 7.9 to 7.13 depict visual/graphical representation of the comparison of observed and simulated discharge during calibration period (1996-2004) and validation (2005-2010) period. In some circumstances, the model-simulated base flows come too high, the modelled peaks are too low, and the simulated flows shift to the left. To resolve this problem, (Abbaspour et al., 2015) recommends some parameter modifications within the SWAT-Cup model. Among the 19 sensitive parameters in this study, treshold depth of water in the shallow aquifer (GWQMN.gw), runoff curve number II (CN2.mgt), groundwater "revap" coefficient (GW_REVAP.gw), available water capacity of the soil layer (SOL_AWC(..).sol), soil evaporation compensation factor (ESCO.hru), threshold depth of water in the shallow aquifer for "revap" to occur (REVAPMN.gw) are modified.

In case of having a low peak simulated flow, it is suggested to decrease CN2.mgt, increase SOL_AWC.sol, and increase ESCO.hru parameter values within the acceptable range. In case of having a high base flow, it is suggested to increase the parameter values for GWQMN.gw and GW_REVAP.gw, and decrease the parameter value for REVAPMN.gw.

Modification in range values of HRU_SLP, OV_N.hru, and SLSUBBSN.hru will help the shift amid the simulated and observed discharge values.

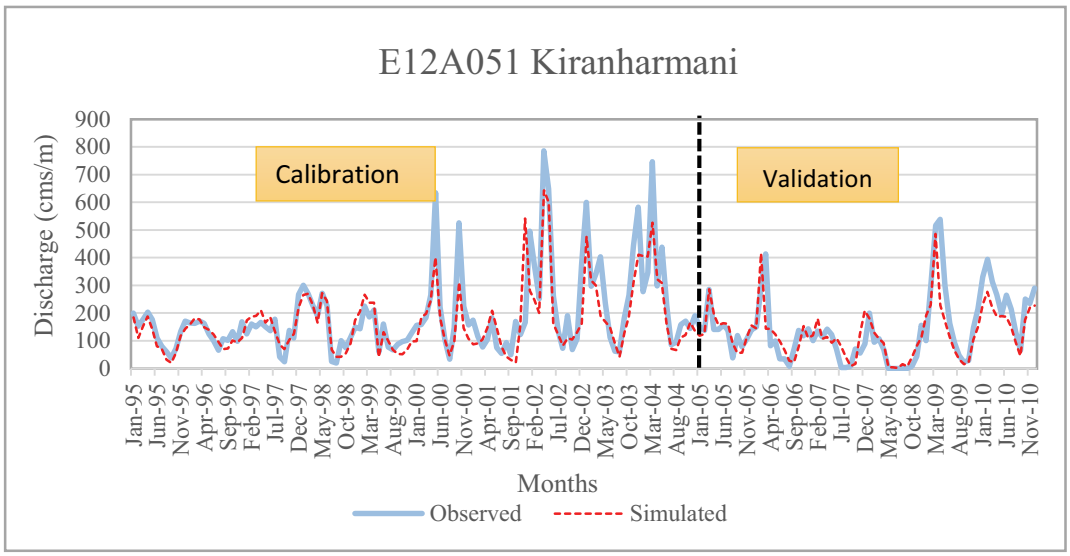

Figure 7.9. Kiranharmani subbasin observed and simulated discharge data comparison during calibration and validation

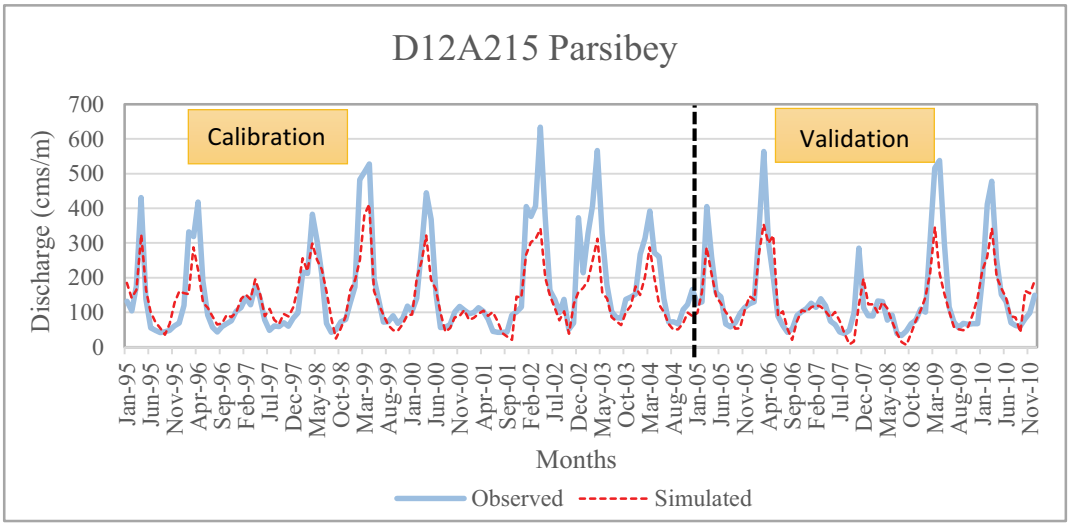

Figure 7.10. Parsibey subbasin observed and simulated discharge data comparison during calibration and validation

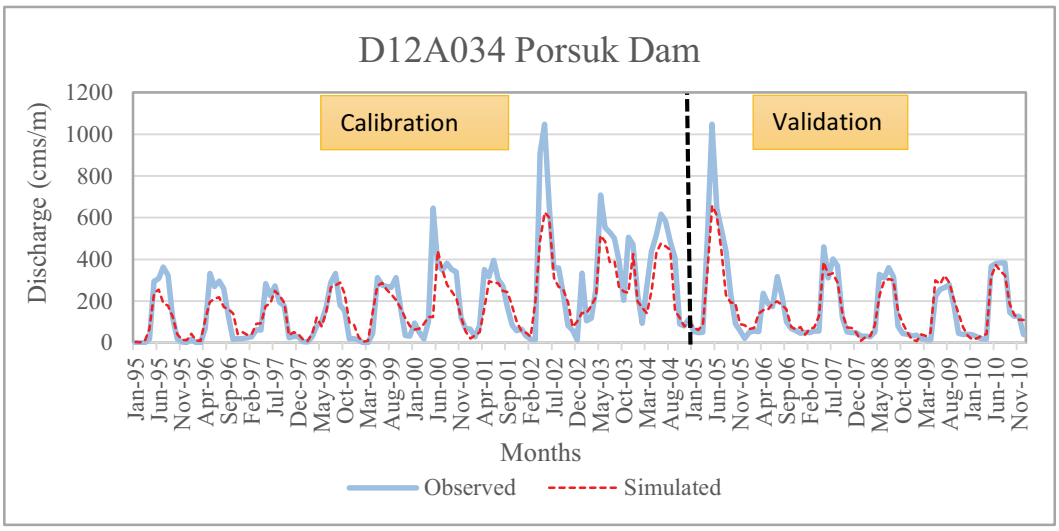

Figure 7.11. Porsuk Dam subbasin observed and simulated discharge data comparison during calibration and validation

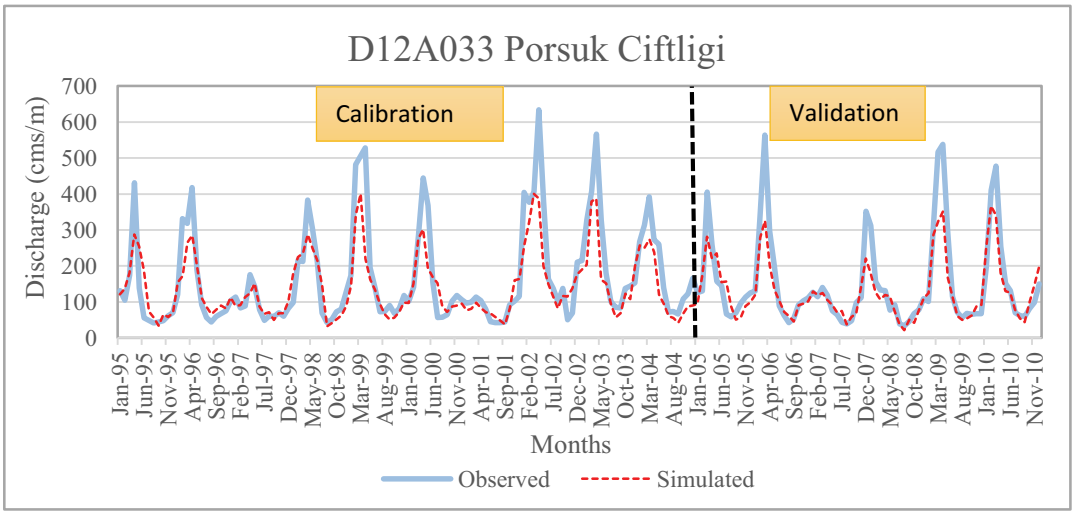

Figure 7.12. Porsuk Ciftligi subbasin observed and simulated discharge data comparison during calibration and validation

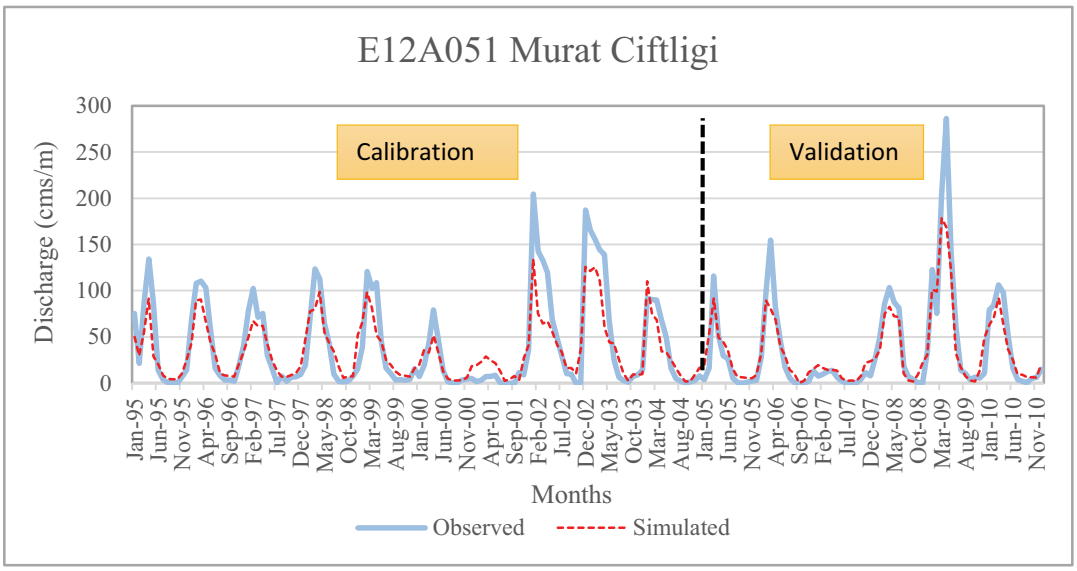

Figure 7.13. Murat Ciftligi subbasin observed and simulated discharge data comparison during calibration (1995-2004) and validation (2005-2010)

7.3.3. Parameter Calibration for Five Sub-basins: Scenario 2

In the second scenario of the analysis, which is to evaluate the land use change impacts on the hydrological processes of the Porsuk River Basin, the calibration process aims to compare the observed runoff data and SWAT simulated runoff data based on the 2006 CORINE land use data and considering the other datasets (discharge precipitation, soil, relative humidity, and solar radiation) constant, every sub-basin parameter considered in calibration phase in the Porsuk River Basin is shown in the following tables individually (Table 7.10).

The calibration process is carried out on the 19 parameters that have the highest sensitivity status discovered during the sensitivity analysis (section 7.2), and their values are repeatedly modified to an acceptable range. During the calibration phase, coefficients of determination (R^2) for the hydrological stations (Kiranharmani, Parsibey, Porsuk Dam, Porsuk Ciftligi, and Murat Ciftligi) were found to be 0.73, 0.81, 0.84, 0.77, and 0.71, respectively. The SWAT-Cup model is run multiple times to generate better calibrated results with a number of 350 simulations on every run set. The initial parameter ranges and fitted values during calibration period are shown in Table 7-10, Table 7-11, Table 7-12, Table 7-13, and Table 7-14. The scatter plot for the comparison between the simulated and observed discharge during calibration phase in monthly timescale is shown in Figure 7.14.

Table 7.10. Parameter Ranges and fitted values during calibration period for Kiranharmani Catchment

Calibrated Parameter Range Values			
SWAT-CUP Parameter Name	**Monthly Time Scale**		
	Min Value	**Max Value**	**Fitted Value**
R__CN2.mgt	-6.12452	5.2475	-3.4252
V__PLAPS.sub	-187.5456	246.87	-87.427
V__TLAPS.sub	-20.4755	0.09245	-5.4756
V__GWQMN.gw	-1234.77	2734.857	-307.981
V__SFTMP.bsn	-3.16085	4.827645	-0.64525
V__SMFMN.bsn	-0.45235	2.86523	0.65278
R__HRU_SLP.hru	0.15235	0.68576	0.77853
R__SLSUBBSN.hru	-0.25478	0.25633	0.06852
V__GW_DELAY.gw	35.4527	450.8524	55.2834
V__TIMP.bsn	0.22653	0.75824	0.47501
V__REVAPMN.gw	-42.6528	385.1427	5.12457
R__SOL_K(..).sol	-0.11253	0.19582	0.16934
R__ESCO.hru	-0.45285	0.98572	0.538374
V__SMFMX.bsn	2.57193	10.04582	4.85371
V__SURLAG.bsn	2.004824	23.2458	7.52468
R__SOL_AWC.sol	0.058723	0.86524	0.63785
V__RCHRG_DP.gw	0.115472	0.68248	0.374421
V__ALPHA_BF.gw	0.212586	0.87524	0.241581
V__GW_REVAP.gw	0.012983	0.17682	0.099002

Table 7.11. Parameter Ranges and fitted values during calibration period for Parsibey Catchment

Calibrated Parameter Range Values			
SWAT-CUP Parameter Name	**Monthly Time Scale**		
	Min Value	**Max Value**	**Fitted Value**
R__CN2.mgt	-12.2545	45.8573	9.6528
V__PLAPS.sub	-156.6257	415.485	58.524
V__TLAPS.sub	-8.45393	7.15272	5.2587
V__GWQMN.gw	552.72	4817.754	287.971
V__SFTMP.bsn	0.24835	5.7588	1.65219
V__SMFMN.bsn	0.58248	4.45758	3.25879
R__HRU_SLP.hru	0.22145	0.95544	0.67344
R__SLSUBBSN.hru	-0.45834	0.24656	-0.18574
V__GW_DELAY.gw	18.2587	358.625	48.2589
V__TIMP.bsn	0.35258	0.87455	0.68.475
V__REVAPMN.gw	0.03587	52.148	2.35878
R__SOL_K(..).sol	1.28575	125.785	10.2587
R__ESCO.hru	0.35874	0.88352	0.55273
V__SMFMX.bsn	3.15247	16.2533	6.25790
V__SURLAG.bsn	0.33785	18.47635	7.25489
R__SOL_AWC.sol	0.11248	0.85748	0.62548
V__RCHRG_DP.gw	0.21247	0.77485	0.59586
V__ALPHA_BF.gw	0.38574	0.88547	0.45258
V__GW_REVAP.gw	0.24158	0.98548	0.78362

Table 7.12. Parameter Ranges and fitted values during calibration period for Porsuk Dam Catchment

Calibrated Parameter Range Values			
SWAT-CUP Parameter Name	**Monthly Time Scale**		
	Min Value	**Max Value**	**Fitted Value**
R__CN2.mgt	-18.8457	35.2568	10.6415
V__PLAPS.sub	-144.2533	318.2547	62.1524
V__TLAPS.sub	-6.25377	8.28865	3.24863
V__GWQMN.gw	225.635	3562.875	445.851
V__SFTMP.bsn	0.18245	6.23547	1.45275
V__SMFMN.bsn	0.44257	4.25877	3.25863
R__HRU_SLP.hru	0.19457	0.88574	0.77452
R__SLSUBBSN.hru	-0.1374	0.33254	-0.2235
V__GW_DELAY.gw	16.2875	300.258	52.6879
V__TIMP.bsn	0.44256	0.96355	0.72158
V__REVAPMN.gw	0.12549	48.2633	3.25849
R__SOL_K(..).sol	1.00254	122.336	9.25841
R__ESCO.hru	0.44172	0.93274	0.71244
V__SMFMX.bsn	2.58331	21.3849	8.24968
V__SURLAG.bsn	0.15241	23.5877	8.96588
R__SOL_AWC.sol	0.65241	0.99658	0.81247
V__RCHRG_DP.gw	0.13256	0.86358	0.72354
V__ALPHA_BF.gw	0.16325	0.78548	0.53296
V__GW_REVAP.gw	0.24158	0.89635	0.61245

Table 7.13. Parameter Ranges and fitted values during calibration period for Porsuk Cifltigi Catchment

Calibrated Parameter Range Values			
SWAT-CUP Parameter Name	**Monthly Time Scale**		
	Min Value	**Max Value**	**Fitted Value**
R__CN2.mgt	9.12452	42.1563	13.2548
V__PLAPS.sub	1.25454	412.125	73.2566
V__TLAPS.sub	0.12457	10.25484	4.23585
V__GWQMN.gw	185.248	2541.124	356.158
V__SFTMP.bsn	0.14257	7.25825	2.15247
V__SMFMN.bsn	0.35269	8.1247	4.25848
R__HRU_SLP.hru	0.13254	0.91254	0.75485
R__SLSUBBSN.hru	-0.14725	0.78548	0.12433
V__GW_DELAY.gw	10.2547	298.147	52.1244
V__TIMP.bsn	0.24112	0.82154	0.81247
V__REVAPMN.gw	0.11289	54.1272	4.86329
R__SOL_K(..).sol	0.92457	85.2477	15.2486
R__ESCO.hru	0.29588	0.86325	0.68547
V__SMFMX.bsn	3.66247	25.4273	10.4789
V__SURLAG.bsn	0.14255	16.24732	10.2415
R__SOL_AWC.sol	0.44153	0.93147	0.77458
V__RCHRG_DP.gw	0.12352	0.91238	0.62325
V__ALPHA_BF.gw	0.51241	0.89305	0.61254
V__GW_REVAP.gw	0.14284	0.91025	0.40824

Table 7.14. Parameter Ranges and fitted values during calibration period for Murat Cifltigi Catchment

Calibrated Parameter Range Values			
SWAT-CUP Parameter Name	**Monthly Time Scale**		
	Min Value	**Max Value**	**Fitted Value**
R__CN2.mgt	2.01245	56.2548	22.1457
V__PLAPS.sub	2.12458	513.012	96.3256
V__TLAPS.sub	0.22325	12.1547	5.3206
V__GWQMN.gw	100.2588	1896.96	415.209
V__SFTMP.bsn	0.12354	12.1247	3.25476
V__SMFMN.bsn	0.21547	6.2358	3.2658
R__HRU_SLP.hru	0.22145	0.89326	0.61247
R__SLSUBBSN.hru	0.02154	0.91247	0.35124
V__GW_DELAY.gw	12.25475	385.102	66.3258
V__TIMP.bsn	0.17521	0.87058	0.72155
V__REVAPMN.gw	0.24518	16.3289	12.3688
R__SOL_K(..).sol	6.32588	92.0524	42.0178
R__ESCO.hru	0.21358	0.99405	0.58041
V__SMFMX.bsn	2.92547	24.0005	16.20153
V__SURLAG.bsn	0.12309	19.04127	8.15242
R__SOL_AWC.sol	0.35016	0.931247	0.77458
V__RCHRG_DP.gw	0.22305	0.98012	0.81425
V__ALPHA_BF.gw	0.41025	0.92104	0.77124
V__GW_REVAP.gw	0.22301	0.83144	0.66014

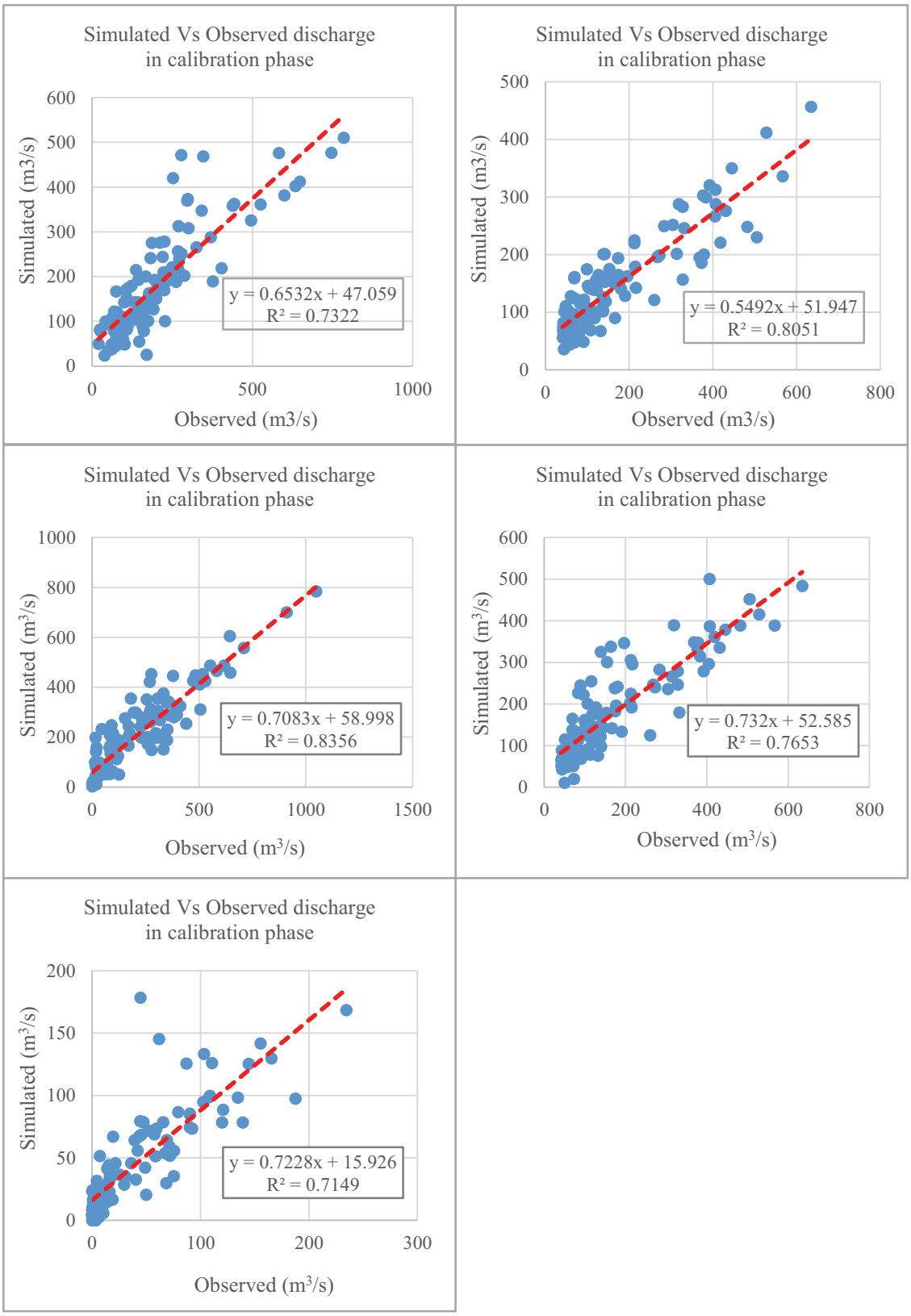

Figure 7.14. The comparison between calibrated and observed monthly discharge results for Kiranharmani, Parsibey, Porsuk Dam, Porsuk Ciftligi, and Murat Ciftligi sub-basins.

7.3.4. Parameter Validation for Five Sub-basins: Scenario 2

The parameter validation process of the 2006 CORINE Land Use dataset-based discharge produced by the SWAT-model is analyzed following the exact same approaches considered in section 7.3.2. The dataset used in the validation of Scenario 2 includes the years between (2005-2010). Parallel to Scenario 1, the number of simulations considered in SWAT-CUP is 350 for the same five hydrological stations (Kiranharmani, Parsibey, Porsuk Dam, Porsuk Ciftligi, and Murat Ciftligi). The model outcome performance is assessed with R^2, NSE, and PBIAS statistics given in Table 7.15.

Based on observed flow data gathered by DSI at five distinct gauge stations along the Porsuk River Basin, validation phase was performed using the SWAT-CUP following the exact same number of simulations that was set for the calibration process. In order to evaluate the effectiveness of the SWAT simulation, existing measurements were compared with the anticipated outcomes on a monthly timescale. The statistics of the model performance (R^2, NSE, and PBIAS) for the observed and simulated discharge are shown in Table 7.15.

Table 7.15. Model performance statistics for the Porsuk River Basin

Calibration (1995- 2004)				**Validation (2005- 2010)**			**Model Performance**
Station	R^2	NSE	PBIAS	R^2	NSE	PBIAS	Satisfaction Status
Kiranharmani	0.73	0.78	13	0.70	0.64	-14	Satisfactory
Parsibey	0.81	0.83	4	0.76	0.74	11	Satisfactory
Porsuk Dam	0.84	0.75	17	0.89	0.84	8	Satisfactory
Porsuk Ciftligi	0.77	0.71	-3	0.85	0.79	9	Satisfactory
Murat Ciftligi	0.71	0.79	10	0.78	0.71	13	Satisfactory

In the calibration phase (Figure 14), the R^2 values were found as 0.73, 0.81, 0.84, 0.77, and 0.72 for Kiranharmani, Parsibey, Porsuk Dam, Porsuk Ciftligi, and Murat Ciftligi sub-basins, respectively. The values of R^2 (Figure 15) were found as 0.70, 0.76, 0.89, 0.85, and 0.78 for the above five sub-basins in validation case, respectively. Of which, only the Porsuk Dam sub-basin is found to have low R^2 in calibration compared to the validation step.

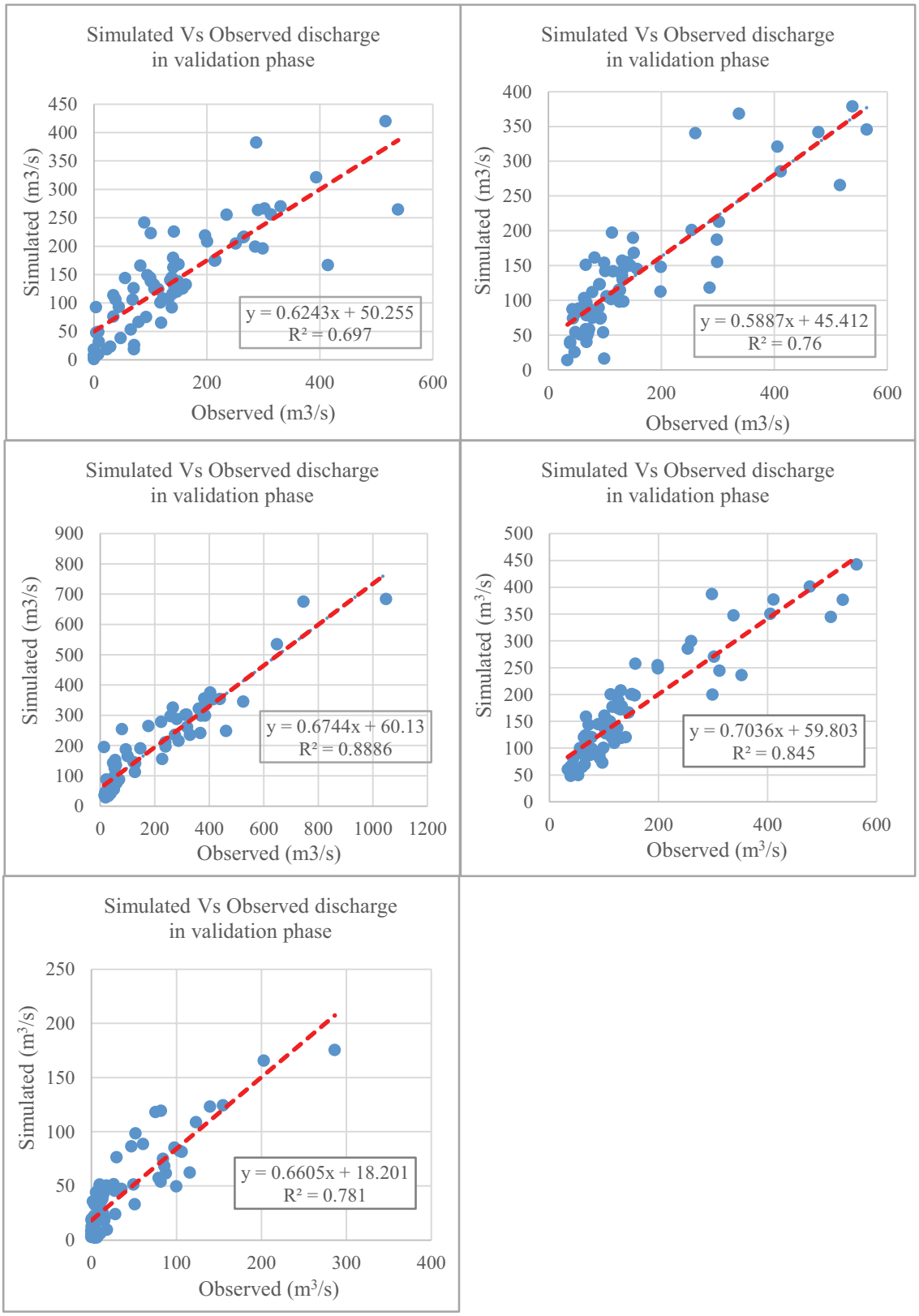

Figure 7.15. The comparison between validated and observed monthly discharge results for Kiranharmani, Parsibey, Porsuk Dam, Porsuk Ciftligi, and Murat Ciftligi sub-basins.

Figures 7.16 to 7.20 show a visual depiction of the observed and simulated discharge for the calibration (1996–2004) and validation (2005–2010) periods. Under certain conditions, the model-simulated base flows are too high, the model-simulated peaks are too low, and the simulated flows shift to the left. To address this issue, (Abbaspour et al., 2015) suggests modifying some parameters in the SWAT-Cup model. In between the 19 sensitive parameters in this study, the shallow aquifer depth threshold (GWQMN.gw), runoff curve number II (CN2.mgt), groundwater "revap" coefficient (GW_REVAP.gw), available water capacity of the soil layer (SOL_AWC(..).sol), soil evaporation compensation factor (ESCO.hru), and shallow aquifer depth threshold for "revap" to occur (REVAPMN.gw). If the peak simulated flow is low, it is recommended to lower CN2.mgt, increase SOL_AWC.sol, and increase ESCO.hru parameter values within the acceptable range. If the base flow is high, it is recommended to increase the parameter values for GWQMN.gw and GW_REVAP.gw while decreasing the parameter value for REVAPMN.gw. Changes to the range values of HRU_SLP, OV_N.hru, and SLSUBBSN.hru will aid in the transition between simulated and observed discharge values.

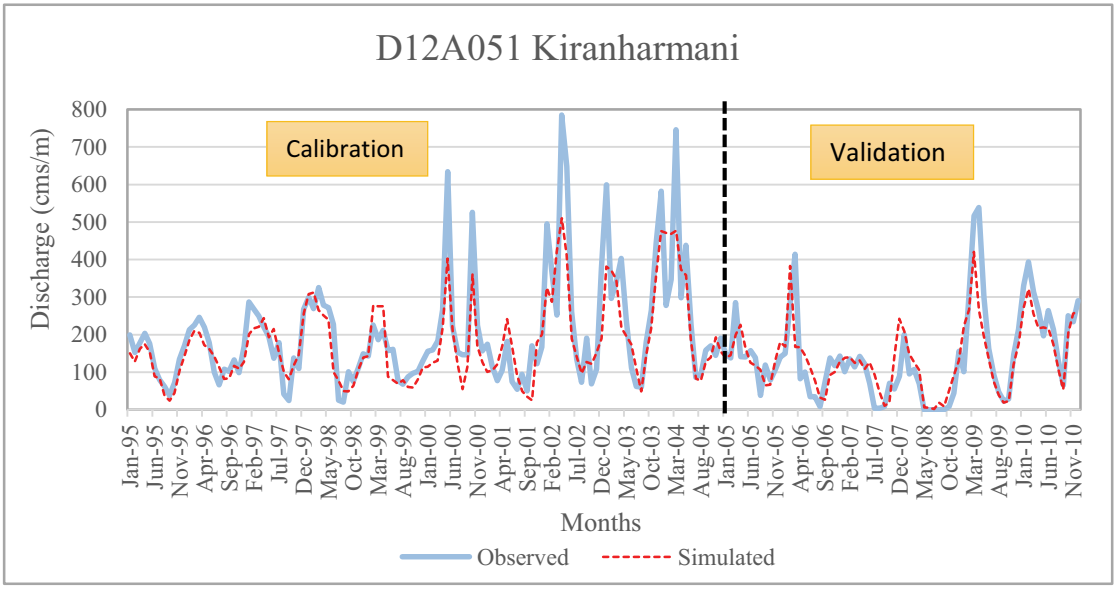

Figure 7.16. Kiranharmani subbasin observed and simulated discharge data comparison during calibration and validation

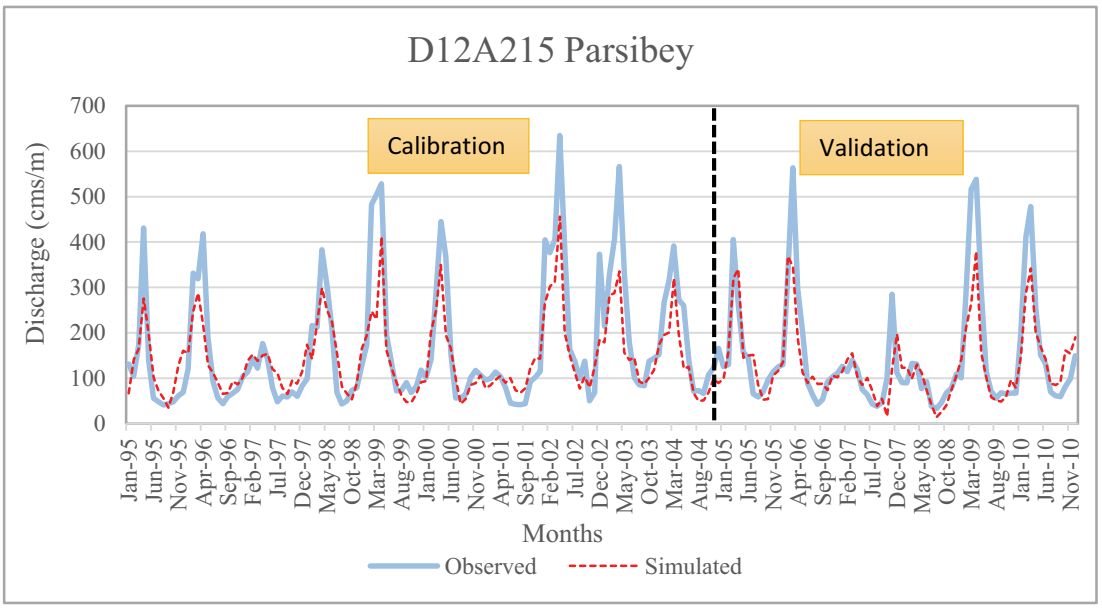

Figure 7.17. Parsibey subbasin observed and simulated discharge data comparison during calibration and validation

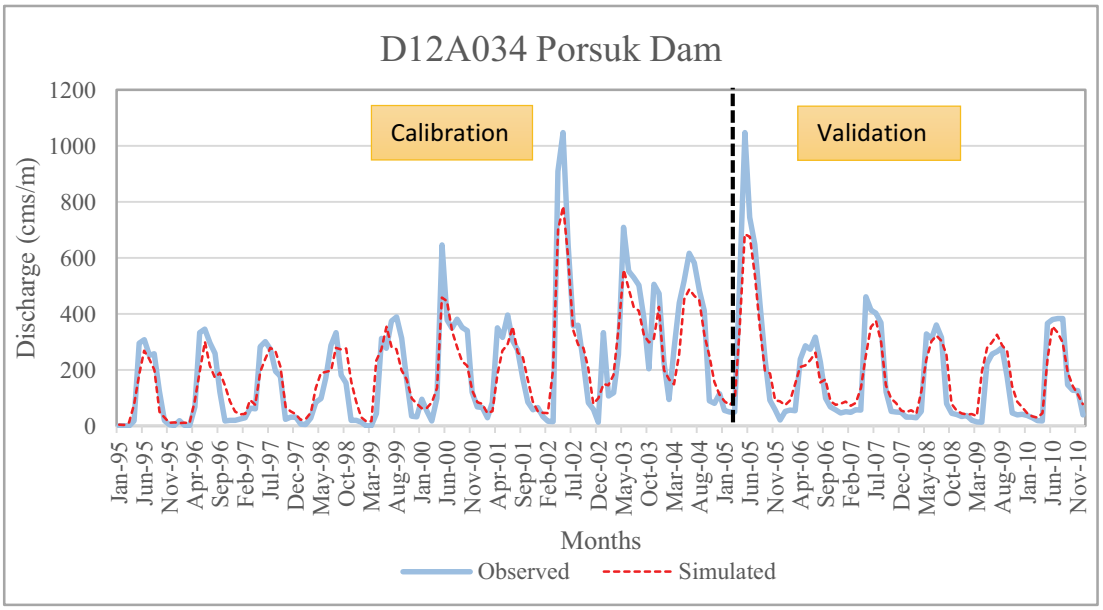

Figure 7.18. Porsuk Dam subbasin observed and simulated discharge data comparison during calibration and validation

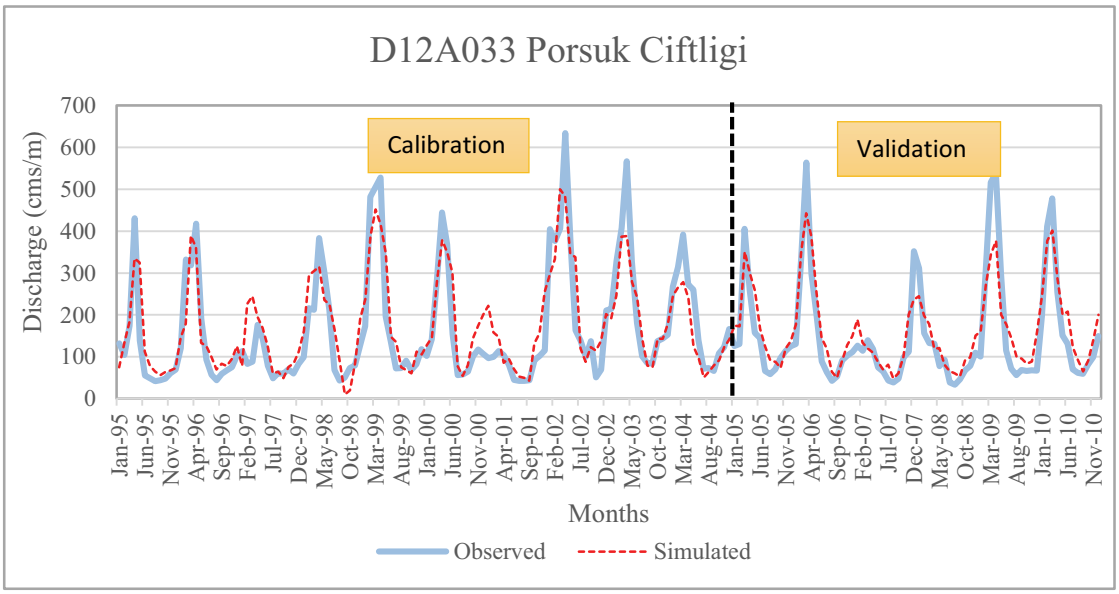

Figure 7.19. Porsuk Ciftligi subbasin observed and simulated discharge data comparison during calibration and validation

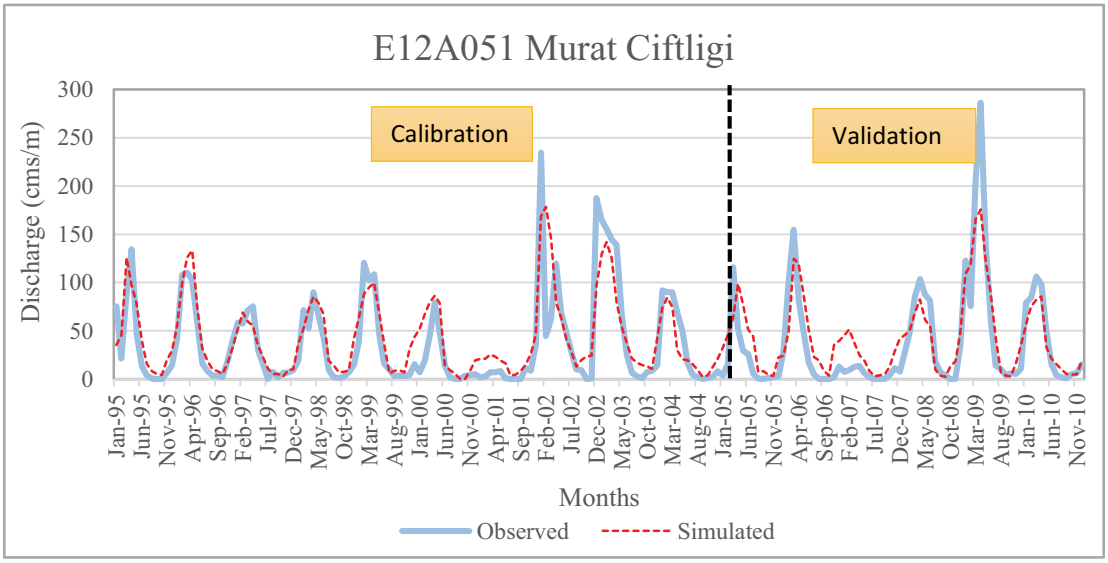

Figure 7.20. Murat Ciftligi subbasin observed and simulated discharge data comparison during calibration and validation

7.4. Hydrological Processes Change Evaluation Based on Two Different Land Use and land Cover Change Scenarios

The SWAT model assessed the hydrological impact analysis of land use disputes. To measure the effects of various land use changes on the key hydrological components, such as surface runoff, groundwater, evapotranspiration, and lateral flow, the implications of land use at the sub-basin level were examined. In order to evaluate the overall impact of the CORINE 1990 and 2006 land use scenarios, we analyzed the long-term (1989–2010) annual average values of surface runoff, groundwater, evapotranspiration, and lateral flow for five sub-basins (Kiranharmani, Parsibey, Porsuk Dam, Porsuk Ciftligi, and Murat Ciftligi). Then, the annual average value differences were determined by subtracting the Scenario 2 average output values from Scenario 1.

7.4.1. Surface Runoff (mm)

The surface runoff simulated considering the impacts of the scenario one land use changes has seen an increase in all sub-basins (Kiranharmani, Parsibey, Porsuk Dam, Porsuk Ciftligi, and Murat Ciftligi) except Porsuk Dams catchment compared to scenario 2 (Figure 7.21). The mean annual surface runoff for the five sub-basins in different years is given in Table 7.16. Infiltration and evapotranspiration would be reduced by the greater amount of impermeable cover in the high-intensity development areas, resulting in an increase in surface runoff generation.

Table 7.16. Mean annual Surface Runoff (mm) variation in 2 scenarios

Surface Runoff (mm)				
Sub-basin	**Scenario 1**	**Scenario 2**	**Difference (mm)**	**Percentage (%)**
Kiranharmani	160.76	201.19	40.43	+ 25.15
Parsibey	182.93	215.91	32.99	+ 18.03
Porsuk Dam	337.69	331.74	-5.95	- 1.76
Porsuk Ciftligi	265.02	299.23	34.21	+ 12.91
Murat Ciftligi	114.58	131.84	17.27	+ 15.07

As shown in Figure 7.21, except Porsuk Dam sub-basin the other four sub-basins have seen clear changes in the amount of surface runoff.

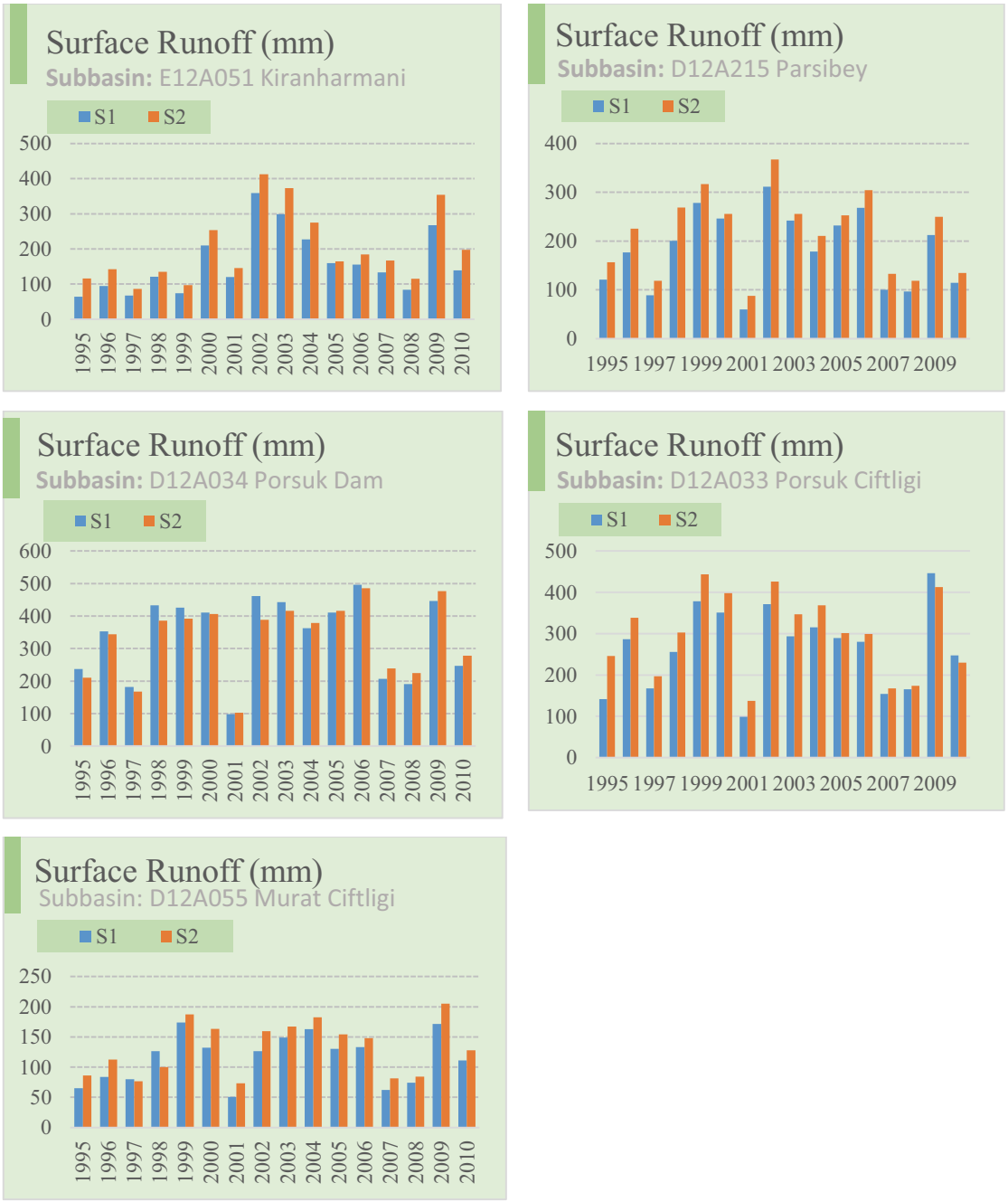

Figure 7.21. Annual Surface Runnoff (mm) parameter values in sub-basins (Kiranharmani, Parsibey, Porsuk Dam, Porsuk Ciftligi, and Murat Ciftligi)

7.4.2. Groundwater (mm)

The findings related to groundwater show an increase in the sub-basins of Kiranharmani and Porsuk Dam in the first nine years of the analysis in scenario one compared to scenario two by a mean annual value of 128.25 and 184.58, respectively. On the other hand, the sub-basins of Parsibey, Porsuk Ciftligi, and Murat Ciftligi have shown a slight decrease in scenario one compared to scenario two by a mean annual values difference of 118.42, 216.34, and 112.15, respectively as seen in Table 7.17.

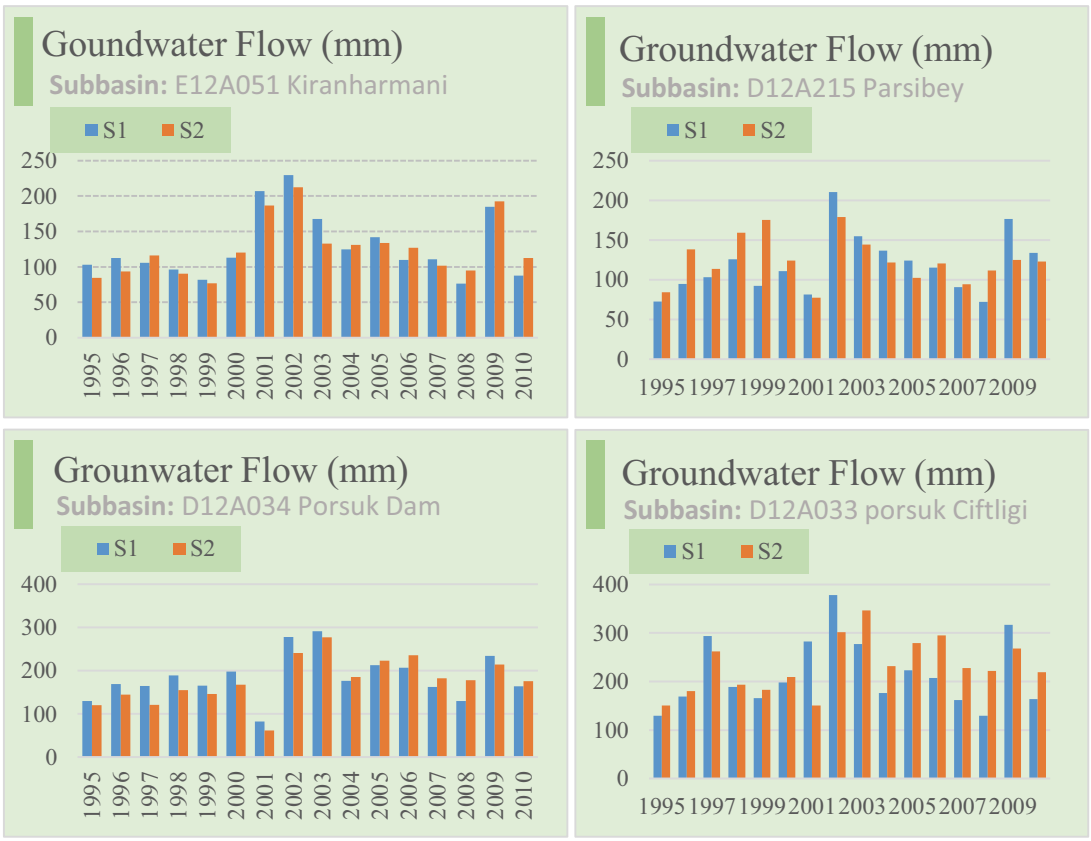

Figure 7.22. Annual Groundwater (mm) parameter values in sub-basins (Kiranharmani, Parsibey, Porsuk Dam, Porsuk Ciftligi, and Murat Ciftligi)

(cont. on next page)

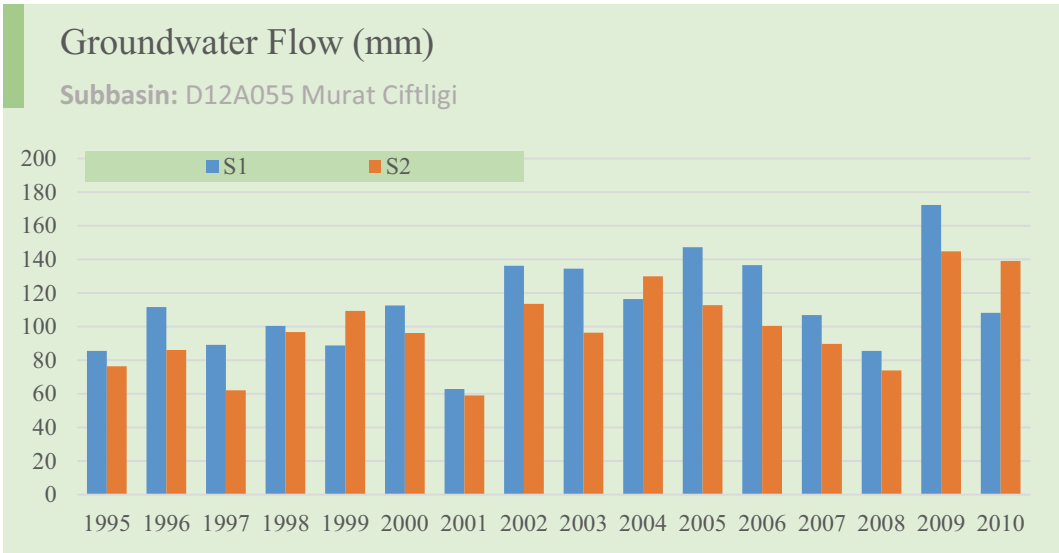

Figure 7.22 (cont.)

Table 7.17. Mean annual groundwater (mm) variation

Groundwater (mm)				
Sub-basin	**Scenario 1**	**Scenario 2**	**Difference (mm)**	**Percentage (%)**
Kiranharmani	128.25	125.36	- 2.89	- 2.26
Parsibey	118.42	124.60	6.18	+ 5.22
Porsuk Dam	184.58	176.73	- 7.84	- 4.26
Porsuk Ciftligi	216.34	232.48	16.14	+ 7.46
Murat Ciftligi	112.15	99.14	-13.01	- 11.6

7.4.3. Evapotranspiration (mm)

The findings related to evapotranspiration show an increase in the sub-basin of Kiranharmani in scenario two compared to scenario one by a mean annual value of 247.57. On the other hand, the remaining sub-basins of Parsibey, Porsuk Dam, Porsuk Ciftligi, and Murat Ciftligi do not show an increase in scenario 2 compared to scenario one, as seen in Table 7.18.

Table 7.18. Mean annual evapotranspiration (mm) variation

Evapotranspiration (mm)				
Sub-basin	**Scenario 1**	**Scenario 2**	**Difference (mm)**	**Percentage (%)**
Kiranharmani	234.07	247.57	13.50	+ 5.77
Parsibey	226.66	202.77	-23.90	- 10.54
Porsuk Dam	278.15	271.65	-6.50	- 2.34
Porsuk Ciftligi	265.09	234.39	-30.70	- 11.28
Murat Ciftligi	83.84	69.88	-13.96	- 16.65

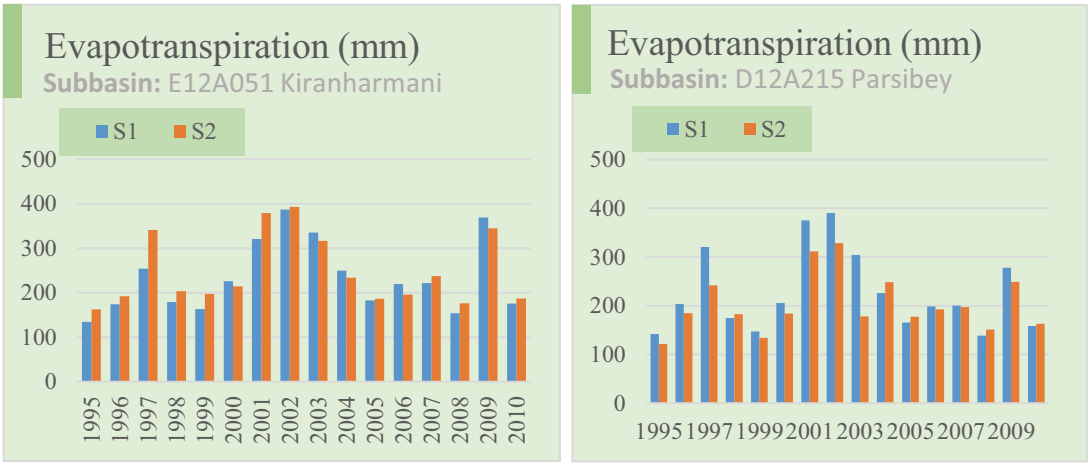

Figure 7.23. Annual Evapotranspiration (mm) parameter values in sub-basins (Kiranharmani, Parsibey, Porsuk Dam, Porsuk Ciftligi, and Murat Ciftligi)

(cont. on next page)

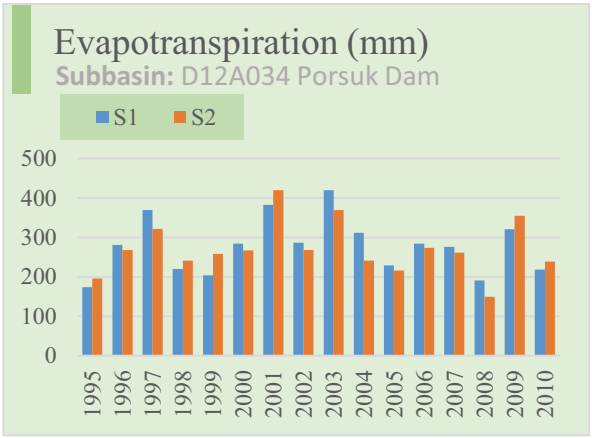

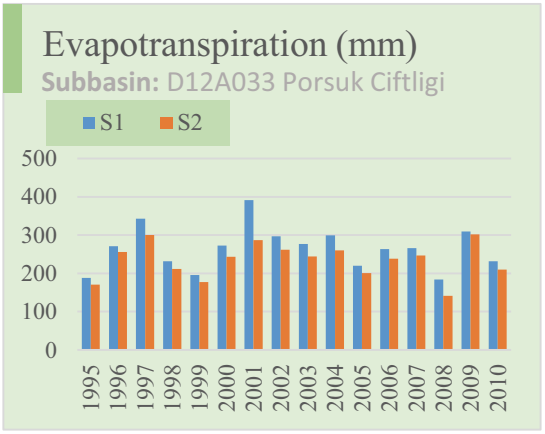

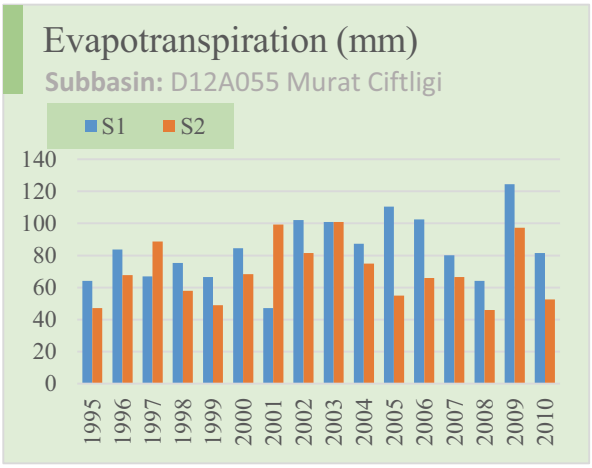

Figure 7.23 (cont.)

7.4.4. Lateral Flow (mm)

Based on the results related to lateral flow, the Kiranharmani, Porsuk Dam, and Murat Ciftligi sub-basins showed a decrease of -8.20 %, -7.58%, -12.70% in scenario 2. The remaining sub-basins (Parsibey, Porsuk Ciftligi) did not demonstrate an increase in their annual lateral flow amount in scenario 2.

Table 7.19. Mean annual lateral (mm) variation

Lateral Flow (mm)				
Subbasin	**Scenario 1**	**Scenario 2**	**Difference (mm)**	**Percentage (%)**
Kiranharmani	29.43	27.02	-2.41	- 8.20
Parsibey	25.97	26.66	0.69	+ 2.67
Porsuk Dam	47.88	44.25	-3.63	- 7.58
Porsuk Ciftligi	59.16	72.11	12.94	+ 21.87
Murat Ciftligi	40.01	34.90	-5.11	- 12.70

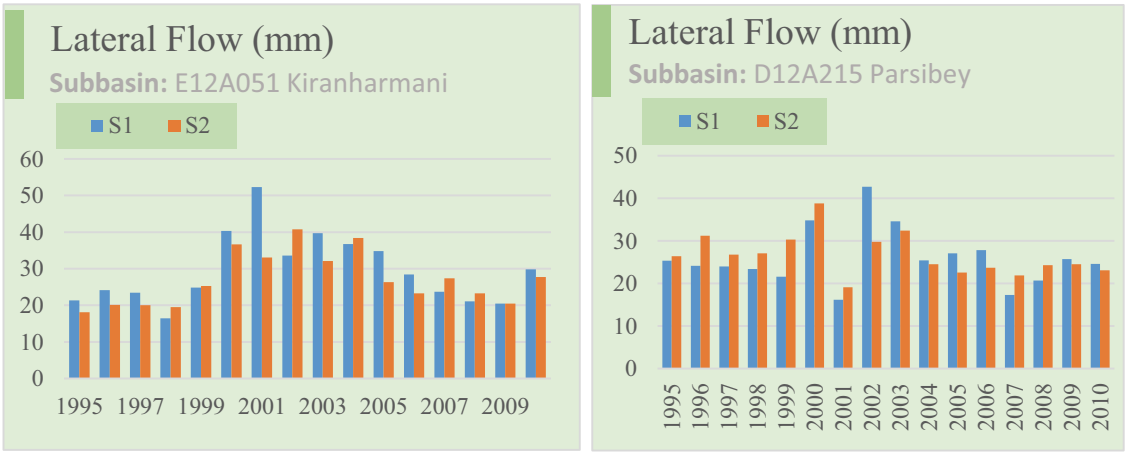

Figure 7.24. Annual Lateral flow (mm) parameter values in sub-basins (Kiranharmani, Parsibey, Porsuk Dam, Porsuk Ciftligi, and Murat Ciftligi)

(cont. on next page)

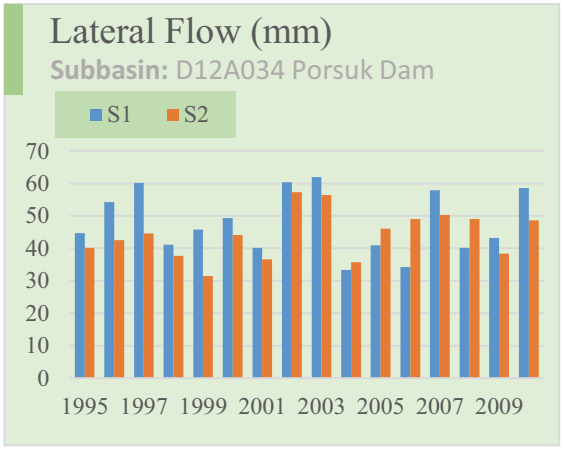

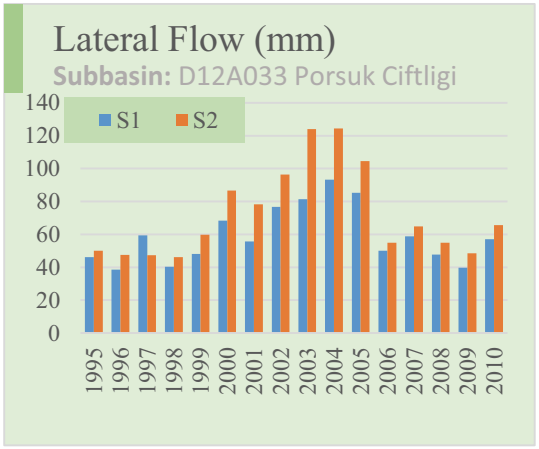

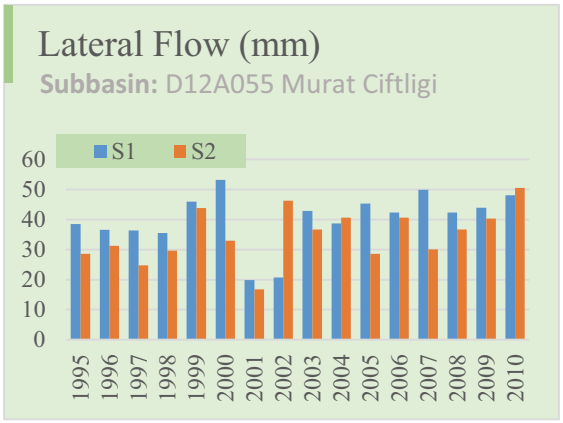

Figure 7.24 (cont.)

CHAPTER 8

CONCLUSION AND RECOMMENDATIONS

This research study was conducted to assess and investigate the different LULC development scenario impacts on the hydrological parameters in Porsuk river basin, Turkey using SWAT2012 model in ArcGIS environment. An integrative GIS and SWAT model algorithm method has proven to be great tools for mapping diverse categories of land cover as well as detecting and analyzing spatiotemporal LULC alterations. These methodologies were used to enable and assess the dynamic effects of land cover on the basin hydrology. To conduct the analysis, first of all, the changes in LULC during previous 16 years between 1990 - 2006 were analyzed with the CORINE Land use 1990 and 2006.

Prior to LULC analysis, preparations of the model data, process of sensitivity analysis, the calibration and validation steps, and the SWAT output model performance were done within ArcGIS atmosphere. ArcGIS software is the core platform to process and visually display the necessary data including, digital elevation model (DEM), LULC, soil data, and slope analysis within the basin. Based on the study results, the below conclusions are note taken:

Agricultural land and forest classes were reduced in Parsibey, Porsuk Dam, Porsuk Ciftligi, and Murat Ciftligi basins by 11.61 %, 1.77 %, 5.5 %, and 6.7 %, respectively. Rapid urbanization and heavy anthropogenic activities in these sub-basins are considered to be the main reasons for a decrease in agricultural land cover area. The ratio of urban settlement in the Porsuk river basin has increased by (31.11%, 200.76%, 129.4%, 6072.92%, and 1285.6%) in Kiranharmani, Parsibey, Porsuk Dam, Porsuk Ciftligi, and Murat Ciftligi, respectively.

The 19 most crucial parameters that govern the stream flow of the investigated river basin were identified by the sensitivity analysis performed using the SWAT-CUP model.

Additionally, the results in model calibration and validation also revealed that the SWAT model satisfactorily simulated the discharge flow.

In Scenario 1, the Nash-Sutcliffe coefficients (NSE) values were found to be 0.78, 0.84, 0.73, 0.77, 0.84 and coefficients of determination (R^2) were 0.74, 0.78, 0.77, 0.79, 0.86 during calibration; and 0.70, 0.75, 0.84, 0.79, 0.77 and 0.67, 0.72, 0.89, 0.85, 0.91 during validation, in the sub-basins of Kiranharmani, Parsibey, Porsuk Dam, Porsuk Ciftligi, and Murat Ciftligi, respectively.

In Scenario 2, (NSE) values were found to be 0.78, 0.83, 0.75, 0.71, 0.79 and (R^2) values were 0.73, 0.81, 0.84, 0.77, 0.71 during calibration; and 0.64, 0.74, 0.84, 0.79, 0.71 and 0.70, 0.76, 0.89, 0.85, 0.78 during validation in the sub-basins of Kiranharmani, Parsibey, Porsuk Dam, Porsuk Ciftligi, and Murat Ciftligi, respectively. Based on the performance range list, it was determined that the model's performance for the calibration and validation fell well within their ranges and was generally satisfactory.

This study concludes that increase in runoff, decrease in groundwater recharge, and in evapotranspiration (ET) and as well as in lateral flow all have an adverse effect on water resources in the Porsuk River basin; thus, urbanization and enlarging in the area of grey infrastructure appear to be significant environmental stressors affecting the basin's hydrology over a decade of land use change in the studied area.

To evaluate the effects of various scenarios for changing LCLU on hydrological components, future LCLU projections have the potential to be modeled utilizing remote sensing technology, land use models, and simulated future LULC. In order to plan and manage water resources sustainably, it is crucial to prepare and assess various predictions of the future availability of water with regard to various land cover/use developments. Another recommendation on the betterment of the future studies in this current research area is to improve the quality and quantity of the available weather stations. This study could have definitely better results if the available weather stations data in the Porsuk River basin was monitored consistently and recorded the other climatic datasets such as wind speed, solar radiation, and humidity.

With the results in this study, it was shown that the deforestation has been one of the major impacts on the amount of surface runoff and consequently, the floods. To prevent this, planting more trees and local water absorbing plants could be of huge benefit.

REFERENCES

Abbaspour, K. C., Rouholahnejad, E., Vaghefi, S., Srinivasan, R., Yang, H., & Kløve, B. (2015). A continental-scale hydrology and water quality model for Europe: Calibration and uncertainty of a high-resolution large-scale SWAT model. *Journal of Hydrology*, *524*, 733-752.

Aghsaei, H., Dinan, N. M., Moridi, A., Asadolahi, Z., Delavar, M., Fohrer, N., & Wagner, P. D. (2020). Effects of dynamic land use/land cover change on water resources and sediment yield in the Anzali wetland catchment, Gilan, Iran. *Science of The Total Environment*, *712*, 136449.

Anand, J., Gosain, A. K., & Khosa, R. (2018). Prediction of land use changes based on Land Change Modeler and attribution of changes in the water balance of Ganga basin to land use change using the SWAT model. *Science of The Total Environment*, *644*, 503-519.

Arceo, M. (2017). Predicting the hydrologic responses to land cover and climate changes of selected watersheds in the Philippines using Soil and Water Assessment Tool (SWAT) model.

Arceo, M., Cruz, R. V. O., Tiburan Jr, C. L., Balatibat, J. B., & Alibuyog, N. R. (2018). Modeling the hydrologic responses to land cover and climate changes of selected watersheds in the Philippines using soil and water assessment tool (SWAT) model. *DLSU Bus. Econ. Rev*, *28*, 84-101.

Arnold, J. G., Moriasi, D. N., Gassman, P. W., Abbaspour, K. C., White, M. J., Srinivasan, R., Santhi, C., Harmel, R., Van Griensven, A., & Van Liew, M. W. (2012). SWAT: Model use, calibration, and validation. *Transactions of the ASABE*, *55*(4), 1491-1508.

Arnold, J. G., Srinivasan, R., Muttiah, R. S., & Williams, J. R. (1998). Large area hydrologic modeling and assessment part I: model development 1. *JAWRA Journal of the American Water Resources Association*, *34*(1), 73-89.

Arnold Jr, C. L., & Gibbons, C. J. (1996). Impervious surface coverage: the emergence of a key environmental indicator. *Journal of the American planning Association*, *62*(2), 243-258.

Arnold, T. W. (2010). Uninformative parameters and model selection using Akaike's Information Criterion. *The Journal of Wildlife Management*, *74*(6), 1175-1178.

ASTER, N. M. A. J. S. a. U. S. J. (2023). *ASTER Global Digital Elevation Model V003. 2019, distributed by NASA EOSDIS Land Processes DAAC*. Retrieved 28 February 2023 from https://lpdaac.usgs.gov/products/astgtmv003/

Bewket, W., & Sterk, G. (2005). Dynamics in land cover and its effect on stream flow in the Chemoga watershed, Blue Nile basin, Ethiopia. *Hydrological Processes: An International Journal*, *19*(2), 445-458.

Brabec, E., Schulte, S., & Richards, P. L. (2002). Impervious Surfaces and Water Quality: A Review of Current Literature and Its Implications for Watershed Planning. *Journal of Planning Literature*, *16*(4), 499-514. https://doi.org/10.1177/088541202400903563

Bucak, T., Trolle, D., Tavşanoğlu, Ü. N., Çakıroğlu, A. İ., Özen, A., Jeppesen, E., & Beklioğlu, M. (2018). Modeling the effects of climatic and land use changes on phytoplankton and water quality of the largest Turkish freshwater lake: Lake Beyşehir. *Science of The Total Environment*, *621*, 802-816.

Cherkauer, K. A., & Sinha, T. (2010). Hydrologic impacts of projected future climate change in the Lake Michigan region. *Journal of Great Lakes Research*, *36*, 33-50.

Chien, H., Yeh, P. J.-F., & Knouft, J. H. (2013). Modeling the potential impacts of climate change on streamflow in agricultural watersheds of the Midwestern United States. *Journal of Hydrology*, *491*, 73-88.

Cibin, R., Sudheer, K., & Chaubey, I. (2010). Sensitivity and identifiability of stream flow generation parameters of the SWAT model. *Hydrological Processes: An International Journal*, *24*(9), 1133-1148.

Costa, M. H., Botta, A., & Cardille, J. A. (2003). Effects of large-scale changes in land cover on the discharge of the Tocantins River, Southeastern Amazonia. *Journal of Hydrology*, *283*(1-4), 206-217.

Coutu, G. W., & Vega, C. (2007). Impacts of landuse changes on runoff generation in the east branch of the Brandywine creek watershed using a GIS-based hydrologic model. *Middle States Geographer*, *40*, 142-149.

Cuceloglu, G., Abbaspour, K. C., & Ozturk, I. (2017). Assessing the water-resources potential of Istanbul by using a soil and water assessment tool (SWAT) hydrological model. *Water*, *9*(10), 814.

Cuceloglu, G., & Ozturk, I. (2019). Assessing the impact of CFSR and local climate datasets on hydrological modeling performance in the mountainous Black sea catchment. *Water*, *11*(11), 2277.

Cüceloğlu, G., SEKER, D. Z., TANIK, A., & Öztürk, İ. (2021). Analyzing effects of two different land use datasets on hydrological simulations by using SWAT model. *International Journal of Environment and Geoinformatics*, *8*(2), 172-185.

DeFries, R., & Eshleman, K. N. (2004). Land-use change and hydrologic processes: a major focus for the future. *Hydrological Processes*, *18*(11), 2183-2186.

Diriba, B. T. (2021). Surface runoff modeling using SWAT analysis in Dabus watershed, Ethiopia. *Sustainable Water Resources Management*, *7*, 1-11.

Dougherty, M., Dymond, R. L., Grizzard Jr, T. J., Godrej, A. N., Zipper, C. E., & Randolph, J. (2007). Quantifying long-term hydrologic response in an urbanizing basin. *Journal of Hydrologic Engineering*, *12*(1), 33-41.

Du, J., Qian, L., Rui, H., Zuo, T., Zheng, D., Xu, Y., & Xu, C.-Y. (2012). Assessing the effects of urbanization on annual runoff and flood events using an integrated hydrological modeling system for Qinhuai River basin, China. *Journal of Hydrology*, *464*, 127-139.

Dunne, T., & Leopold, L. B. (1978). *Water in environmental planning*. Macmillan.

El-Sadek, A., & Irvem, A. (2014). Evaluating the impact of land use uncertainty on the simulated streamflow and sediment yield of the Seyhan River basin using the SWAT model. *Turkish Journal of Agriculture and Forestry*, *38*(4), 515-530.

Emam, A. R., Kappas, M., & Hosseini, S. Z. (2015). Assessing the impact of climate change on water resources, crop production and land degradation in a semi-arid river basin. *Hydrology Research*, *46*(6), 854-870.

EU_CORINE, E. E. A. (2022). *CORINE LAND USE LAND COVER*. CORINE LAND USE LAND COVER. Retrieved 28 February 2023 from https://www.eea.europa.eu/publications/COR0-landcover

Ghoraba, S. M. (2015). Hydrological modeling of the Simly Dam watershed (Pakistan) using GIS and SWAT model. *Alexandria Engineering Journal*, *54*(3), 583-594.

Glavan, M., Pintar, M., & Volk, M. (2013). Land use change in a 200-year period and its effect on blue and green water flow in two Slovenian Mediterranean catchments—lessons for the future. *Hydrological Processes*, *27*(26), 3964-3980.

Gleick, P. H. (1996). Water resources. *Encyclopedia of climate, weather*, 817-823.

Grey, O. P., Webber, D. F. S. G., Setegn, S. G., & Melesse, A. M. (2014). Application of the soil and water assessment tool (SWAT model) on a small tropical island (Great River watershed, Jamaica) as a tool in integrated watershed and coastal zone management. *Revista de Biología Tropical*, *62*, 293-305.

Güngör, Ö., & Göncü, S. (2013). Application of the soil and water assessment tool model on the Lower Porsuk Stream Watershed. *Hydrological Processes*, *27*(3), 453-466.

Guo, H., Hu, Q., & Jiang, T. (2008). Annual and seasonal streamflow responses to climate and land-cover changes in the Poyang Lake basin, China. *Journal of Hydrology*, *355*(1-4), 106-122.

Hay, L. E., Markstrom, S. L., & Ward-Garrison, C. (2011). Watershed-scale response to climate change through the twenty-first century for selected basins across the United States. *Earth Interactions*, *15*(17), 1-37.

Hjelmfelt, A., Group, N. A. C. N. W., & Moody, H. (2004). Estimation of direct runoff from storm rainfall. *Part 630 Hydrology National Engineering Handbook*.

Hollis, G. (1975). The effect of urbanization on floods of different recurrence interval. *Water resources research*, *11*(3), 431-435.

Hörmann, G., Horn, A., & Fohrer, N. (2005). The evaluation of land-use options in mesoscale catchments: prospects and limitations of eco-hydrological models. *Ecological Modelling*, *187*(1), 3-14.

Hussainzada, W., & Lee, H. S. (2021). Hydrological modelling for water resource management in a semi-arid mountainous region using the soil and water assessment tool: A case study in northern Afghanistan. *Hydrology*, *8*(1), 16.

Jha, M., Arnold, J. G., Gassman, P. W., Giorgi, F., & Gu, R. R. (2006). CLIMATE CHHANGE SENSITIVITY ASSESSMENT ON UPPER MISSISSIPPI RIVER BASIN STREAMFLOWS USING SWAT 1. *JAWRA Journal of the American Water Resources Association*, *42*(4), 997-1015.

Kalnay, E., & Cai, M. (2003). Impact of urbanization and land-use change on climate. *Nature*, *423*(6939), 528-531.

Kang, B., & Ramírez, J. A. (2007). Response of streamflow to weather variability under climate change in the Colorado Rockies. *Journal of Hydrologic Engineering*, *12*(1), 63-72.

Koltsida, E., Mamassis, N., & Kallioras, A. (2023). Hydrological modeling using the Soil and Water Assessment Tool in urban and peri-urban environments: the case of Kifisos experimental subbasin (Athens, Greece). *Hydrology and Earth System Sciences*, *27*(4), 917-931.

Koycegiz, C., & Buyukyildiz, M. (2019). Calibration of SWAT and two data-driven models for a data-scarce mountainous headwater in semi-arid Konya closed basin. *Water*, *11*(1), 147.

Lee, S.-J., & Berbery, E. H. (2012). Land cover change effects on the climate of the La Plata Basin. *Journal of Hydrometeorology*, *13*(1), 84-102.

Leopold, L. B. (1968). *Hydrology for urban land planning: A guidebook on the hydrologic effects of urban land use* (Vol. 554). US Geolgoical Survey.

Li, Y., & Wang, C. (2009). Impacts of urbanization on surface runoff of the Dardenne Creek watershed, St. Charles County, Missouri. *Physical Geography*, *30*(6), 556-573.

Li, Z., Lyu, S., Chen, H., Ao, Y., Zhao, L., Wang, S., Zhang, S., & Meng, X. (2021). Changes in climate and snow cover and their synergistic influence on spring runoff in the source region of the Yellow River. *Science of The Total Environment*, *799*, 149503.

Lundin, M., Bengtsson, M., & Molander, S. (2000). Life cycle assessment of wastewater systems: influence of system boundaries and scale on calculated environmental loads. *Environmental Science & Technology*, *34*(1), 180-186.

McGinn, A. J., Wagner, P. D., Htike, H., Kyu, K. K., & Fohrer, N. (2021). Twenty years of change: Land and water resources in the Chindwin catchment, Myanmar between 1999 and 2019. *Science of The Total Environment*, *798*, 148766.

Mengistu, T. D., Chung, I.-M., Kim, M.-G., Chang, S. W., & Lee, J. E. (2022). Impacts and Implications of Land Use Land Cover Dynamics on Groundwater Recharge and Surface Runoff in East African Watershed. *Water*, *14*(13), 2068.

Miller, S. N., Kepner, W. G., Mehaffey, M. H., Hernandez, M., Miller, R. C., Goodrich, D. C., Kim Devonald, K., Heggem, D. T., & Miller, W. P. (2002). Integrating landscape assessment and hydrologic modeling for land cover change analysis 1. *JAWRA Journal of the American Water Resources Association*, *38*(4), 915-929.

Mirchi, A., Watkins Jr, D., & Madani, K. (2010). Modeling for watershed planning, management, and decision making. *Watersheds: Management, restoration and environmental impact*, 354-392.

Mirchi, A., Watkins Jr, D., & Madani, K. (2010). Modeling for watershed planning, management, and decision making. Chapter 6 In: Vaughn JC (ed) Watersheds: management, restoration and environmental impact. In: Nova Science Publishers, Hauppauge, NY, USA.

Neitsch, S. L., Arnold, J. G., Kiniry, J. R., & Williams, J. R. (2011). *Soil and water assessment tool theoretical documentation version 2009*.

Ogden, F. L., Raj Pradhan, N., Downer, C. W., & Zahner, J. A. (2011). Relative importance of impervious area, drainage density, width function, and subsurface storm drainage on flood runoff from an urbanized catchment. *Water resources research*, *47*(12).

Pagano, T., & Sorooshian, S. (2002). Hydrologic cycle. *Encyclopedia of Global Environment Change*.

Paudel, M. (2010). *An examination of distributed hydrologic modeling methods as compared with traditional lumped parameter approaches*. Brigham Young University.

Paul, M. J., & Meyer, J. L. (2001). Streams in the urban landscape. *Annual review of Ecology and Systematics*, *32*(1), 333-365.

Rose, S., & Peters, N. E. (2001). Effects of urbanization on streamflow in the Atlanta area (Georgia, USA): a comparative hydrological approach. *Hydrological Processes*, *15*(8), 1441-1457.

Schueler, T. R., & Galli, J. (1992). Environmental impacts of stormwater ponds. *Watershed Restoration Source Book*, 159-180.

Sertel, E., Imamoglu, M. Z., Cuceloglu, G., & Erturk, A. (2019). Impacts of land cover/use changes on hydrological processes in a rapidly urbanizing mid-latitude water supply catchment. *Water*, *11*(5), 1075.

Sertel, E., Robock, A., & Ormeci, C. (2010). Impacts of land cover data quality on regional climate simulations. *International Journal of Climatology*, *30*(13), 1942-1953.

Shukla, S., Meshesha, T. W., Sen, I. S., Bol, R., Bogena, H., & Wang, J. (2023). Assessing Impacts of Land Use and Land Cover (LULC) Change on Stream Flow and Runoff in Rur Basin, Germany. *Sustainability*, *15*(12), 9811.

Smith, J. A., Baeck, M. L., Meierdiercks, K. L., Nelson, P. A., Miller, A. J., & Holland, E. J. (2005). Field studies of the storm event hydrologic response in an urbanizing watershed. *Water resources research*, *41*(10).

Smith, M. B. (1993). A GIS-based distributed parameter hydrologic model for urban areas. *Hydrological Processes*, *7*(1), 45-61.

Twisa, S., Kazumba, S., Kurian, M., & Buchroithner, M. F. (2020). Evaluating and predicting the effects of land use changes on hydrology in Wami River Basin, Tanzania. *Hydrology*, *7*(1), 17.

Vieux, B. E., Cui, Z., & Gaur, A. (2004). Evaluation of a physics-based distributed hydrologic model for flood forecasting. *Journal of Hydrology*, *298*(1-4), 155-177.

Vorosmarty, C. J., Green, P., Salisbury, J., & Lammers, R. B. (2000). Global water resources: vulnerability from climate change and population growth. *science*, *289*(5477), 284-288.

Watson, J. E., Dudley, N., Segan, D. B., & Hockings, M. (2014). The performance and potential of protected areas. *Nature*, *515*(7525), 67-73.

Wei, X., & Zhang, M. (2010). Quantifying streamflow change caused by forest disturbance at a large spatial scale: A single watershed study. *Water resources research*, *46*(12).

Westenbroek, S. M., Kelson, V., Dripps, W., Hunt, R., & Bradbury, K. (2010). *SWB--a modified Thornthwaite-Mather Soil-Water-Balance Code for estimating groundwater recharge*. US Department of the Interior, US Geological Survey, Ground Resources ….

Yan, R., Zhang, X., Yan, S., Zhang, J., & Chen, H. (2018). Spatial patterns of hydrological responses to land use/cover change in a catchment on the Loess Plateau, China. *Ecological Indicators*, *92*, 151-160.

Zeng, Y., Cai, Y., Jia, P., & Jee, H. (2012). Development of a web-based decision support system for supporting integrated water resources management in Daegu city, South Korea. *Expert Systems with Applications*, *39*(11), 10091-10102.

Zhang, D., Zhang, Q., Qiu, J., Bai, P., Liang, K., & Li, X. (2018). Intensification of hydrological drought due to human activity in the middle reaches of the Yangtze River, China. *Science of The Total Environment*, *637*, 1432-1442.

Zhang, H., Wang, B., Li Liu, D., Zhang, M., Leslie, L. M., & Yu, Q. (2020). Using an improved SWAT model to simulate hydrological responses to land use change: A case study of a catchment in tropical Australia. *Journal of Hydrology*, *585*, 124822.

APPENDIX A

Potential surface runoff CN2 values obtained for every HRU available.

SBBSN	LULC	CN2	SBBSN	LULC	CN2	SBBSN	LULC	CN2
1	FESC	53.4	2	AGRR	69.9	4	FESC	53.4
1	FESC	53.4	2	AGRR	76.3	4	FESC	53.4
1	FESC	53.4	2	AGRR	76.3	4	FESC	53.4
1	FESC	53.4	2	AGRR	76.3	4	AGRL	67
1	FESC	61.7	2	AGRR	76.3	4	AGRL	67
1	FESC	61.7	2	FSRE	51.2	4	AGRL	67
1	FESC	61.7	2	FSRE	51.2	4	AGRL	67
1	FESC	61.7	2	FSRE	51.2	4	AGRL	67
1	AGRL	67	2	RNGB	55.7	4	AGRL	67
1	AGRL	67	2	RNGB	55.7	4	AGRL	67
1	AGRL	67	2	RNGB	55.7	4	AGRL	67
1	AGRL	67	2	RNGB	63	4	AGRL	67
1	AGRL	73	2	RNGB	63	5	BERM	73.9
1	AGRL	73	2	RNGB	63	5	BERM	73.9
1	AGRL	73	2	RNGB	63	5	BERM	73.9
1	AGRL	73	2	SWRN	55.7	5	BERM	73.9
1	FSRE	51.2	2	SWRN	55.7	5	BERM	73.9
1	FSRE	51.2	2	SWRN	55.7	5	BERM	78.7
1	FSRE	51.2	2	SWRN	63	5	BERM	78.7
1	RNGB	55.7	2	SWRN	63	5	BERM	78.7
1	RNGB	55.7	2	SWRN	63	5	BERM	78.7
1	RNGB	55.7	2	SWRN	63	5	BERM	59
1	RNGB	63	3	FESC	53.4	5	BERM	59
1	RNGB	63	3	FESC	53.4	5	BERM	59
1	RNGB	63	3	FESC	53.4	5	BERM	59
1	SWRN	55.7	3	FESC	53.4	5	BERM	59
1	SWRN	55.7	3	AGRL	67	5	BERM	77
1	SWRN	55.7	3	AGRL	67	5	BERM	77
1	SWRN	63	3	AGRL	67	5	BERM	77
1	SWRN	63	3	AGRL	67	5	BERM	77
1	SWRN	63	3	AGRL	67	5	BERM	77
2	AGRL	67	3	AGRL	73	5	AGRL	67
2	AGRL	67	3	AGRL	73	5	AGRL	67
2	AGRL	67	3	AGRL	73	5	AGRL	67
2	AGRL	67	3	AGRL	73	5	AGRL	67
2	AGRL	73	3	FRSD	59.3	5	AGRL	73
2	AGRL	73	3	FRSD	59.3	5	AGRL	73
2	AGRL	73	3	FRSD	59.3	5	AGRL	73
2	AGRL	73	3	FRSD	59.3	6	AGRL	67
2	AGRL	73	3	RNGB	55.7	6	AGRL	67

SBBSN	LULC	CN2	SBBSN	LULC	CN2	SBBSN	LULC	CN2
6	AGRL	73	8	AGRL	67	10	AGRL	73
6	AGRL	73	8	AGRL	73	10	AGRL	73
6	AGRL	73	8	AGRL	73	10	SWRN	63
6	AGRL	73	8	AGRL	73	10	SWRN	63
6	RNGB	55.7	8	AGRL	73	10	SWRN	63
6	RNGB	55.7	8	AGRL	73	10	SWRN	63
6	RNGB	55.7	8	AGRL	73	11	AGRL	67
6	RNGB	55.7	8	AGRL	73	11	AGRL	67
6	SWRN	55.7	8	AGRL	73	11	AGRL	67
6	SWRN	55.7	8	AGRL	73	11	AGRL	67
6	SWRN	55.7	8	AGRL	73	11	AGRL	67
6	SWRN	63	8	PAST	61.7	11	AGRL	67
6	SWRN	63	8	PAST	61.7	11	AGRL	67
6	SWRN	63	8	PAST	61.7	11	AGRL	67
6	SWRN	63	8	PAST	61.7	11	AGRL	67
7	FESC	53.4	8	PAST	68.4	11	AGRL	67
7	FESC	53.4	8	PAST	68.4	11	RNGB	55.7
7	FESC	53.4	8	PAST	68.4	11	RNGB	55.7
7	FESC	61.7	8	PAST	68.4	11	RNGB	55.7
7	FESC	61.7	8	PAST	68.4	11	RNGB	55.7
7	FESC	61.7	8	PAST	68.4	11	RNGB	55.7
7	FESC	61.7	8	PAST	68.4	11	RNGB	55.7
7	FESC	61.7	8	PAST	68.4	11	RNGB	55.7
7	FESC	61.7	8	PAST	68.4	11	RNGB	55.7
7	FESC	61.7	8	PAST	68.4	11	SWRN	55.7
7	AGRL	67	8	RNGB	55.7	11	SWRN	55.7
7	AGRL	67	8	RNGB	55.7	11	SWRN	55.7
7	AGRL	67	8	RNGB	55.7	11	SWRN	55.7
7	AGRL	67	8	RNGB	55.7	11	SWRN	55.7
7	AGRL	67	8	SWRN	55.7	11	SWRN	55.7
7	AGRL	73	8	SWRN	55.7	11	SWRN	55.7
7	AGRL	73	8	SWRN	55.7	11	SWRN	55.7
7	AGRL	73	8	SWRN	55.7	12	FESC	53.4
7	AGRL	73	8	SWRN	63	12	FESC	53.4
7	AGRL	73	8	SWRN	63	12	FESC	53.4
7	AGRL	73	8	SWRN	63	12	FESC	53.4
7	AGRL	73	8	SWRN	63	12	FESC	61.7
7	AGRL	73	9	AGRL	73	12	FESC	61.7
7	AGRL	73	9	AGRL	73	12	FESC	61.7
7	AGRL	73	9	AGRL	73	12	FESC	61.7
7	RNGB	55.7	9	AGRL	73	12	FESC	61.7
7	RNGB	55.7	10	AGRL	73	12	FESC	61.7
7	RNGB	55.7	10	AGRL	73	12	FESC	61.7
7	RNGB	63	10	AGRL	73	12	FESC	61.7
7	RNGB	63	10	AGRL	73		AGRL	67

SBBSN	LULC	CN2	SBBSN	LULC	CN2	SBBSN	LULC	CN2
12	AGRL	73	14	SWRN	63	16	RNGB	55.7
12	AGRL	73	14	SWRN	63	16	RNGB	55.7
12	AGRL	73	14	SWRN	63	16	RNGB	55.7
12	AGRL	73	14	SWRN	63	16	RNGB	55.7
12	AGRL	73	15	FESC	61.7	16	RNGB	55.7
12	AGRL	73	15	FESC	61.7	16	RNGB	55.7
12	AGRL	73	15	FESC	61.7	16	RNGB	55.7
12	AGRL	73	15	FESC	61.7	16	SWRN	55.7
12	AGRL	73	15	AGRL	73	16	SWRN	55.7
12	RNGB	55.7	15	AGRL	73	16	SWRN	55.7
12	RNGB	55.7	15	AGRL	73	16	SWRN	55.7
12	RNGB	55.7	15	AGRL	73	16	SWRN	55.7
12	RNGB	55.7	15	AGRL	73	16	SWRN	55.7
12	RNGB	63	15	AGRL	73	16	SWRN	55.7
12	RNGB	63	15	AGRL	73	16	SWRN	55.7
12	RNGB	63	15	AGRL	73	17	AGRL	67
12	RNGB	63	15	AGRL	73	17	AGRL	67
13	FESC	61.7	15	AGRL	73	17	AGRL	67
13	FESC	61.7	15	PAST	68.4	17	AGRL	67
13	FESC	61.7	15	PAST	68.4	17	AGRL	67
13	FESC	61.7	15	PAST	68.4	17	RNGB	55.7
13	FESC	61.7	15	PAST	68.4	17	RNGB	55.7
13	AGRL	73	15	PAST	68.4	17	RNGB	55.7
13	AGRL	73	15	PAST	68.4	17	RNGB	55.7
13	AGRL	73	15	PAST	68.4	17	SWRN	55.7
13	AGRL	73	15	PAST	68.4	17	SWRN	55.7
13	AGRL	73	15	PAST	68.4	17	SWRN	55.7
13	SWRN	63	15	RNGB	63	17	SWRN	55.7
13	SWRN	63	15	RNGB	63	18	AGRL	67
13	SWRN	63	15	RNGB	63	18	AGRL	67
13	SWRN	63	15	SWRN	63	18	AGRL	67
14	FESC	61.7	15	SWRN	63	18	AGRL	67
14	FESC	61.7	15	SWRN	63	18	AGRL	67
14	FESC	61.7	15	SWRN	63	18	AGRL	67
14	FESC	61.7	16	FESC	53.4	18	AGRL	67
14	AGRL	73	16	FESC	53.4	18	AGRL	67
14	AGRL	73	16	FESC	53.4	18	AGRL	67
14	AGRL	73	16	FESC	53.4	18	AGRL	67
14	AGRL	73	16	AGRL	67	18	FSRE	51.2
14	AGRL	73	16	AGRL	67	18	FSRE	51.2
14	RNGB	55.7	16	AGRL	67	18	FSRE	51.2
14	RNGB	55.7	16	AGRL	67	18	FSRE	51.2
14	RNGB	55.7	16	AGRL	67	18	FSRE	51.2
14	RNGB	63	16	AGRL	67	18	FSRE	51.2
14	RNGB	63	16	AGRL	67	18	FSRE	51.2

SBBSN	LULC	CN2	SBBSN	LULC	CN2	SBBSN	LULC	CN2
18	RNGB	55.7	20	SWRN	63	23	FESC	61.7
18	RNGB	55.7	20	SWRN	63	23	AGRL	73
18	RNGB	55.7	20	SWRN	63	23	AGRL	73
18	RNGB	55.7	21	FESC	61.7	23	AGRL	73
18	SWRN	55.7	21	FESC	61.7	23	AGRL	73
18	SWRN	55.7	21	FESC	61.7	23	AGRL	73
18	SWRN	55.7	21	FESC	61.7	23	RNGB	63
18	SWRN	55.7	21	FESC	61.7	23	RNGB	63
18	SWRN	55.7	21	AGRL	73	23	RNGB	63
18	SWRN	55.7	21	AGRL	73	23	RNGB	63
18	SWRN	55.7	21	AGRL	73	23	SWRN	63
18	SWRN	55.7	21	AGRL	73	23	SWRN	63
19	FSRE	51.2	21	AGRL	73	23	SWRN	63
19	FSRE	51.2	21	AGRR	76.3	23	SWRN	63
19	FSRE	51.2	21	AGRR	76.3	24	AGRL	67
19	FSRE	51.2	21	AGRR	76.3	24	AGRL	67
19	RNGB	55.7	21	AGRR	76.3	24	AGRL	67
19	RNGB	55.7	21	AGRR	76.3	24	AGRL	67
19	RNGB	55.7	21	SWRN	63	24	AGRL	67
19	RNGB	55.7	21	SWRN	63	24	AGRL	67
19	RNGB	55.7	21	SWRN	63	24	AGRL	67
19	RNGB	55.7	21	SWRN	63	24	AGRL	67
19	RNGB	55.7	21	SWRN	63	24	AGRL	67
19	RNGB	55.7	22	AGRL	67	24	AGRL	67
19	RNGB	55.7	22	AGRL	67	24	FSRE	51.2
19	SWRN	55.7	22	AGRL	67	24	FSRE	51.2
19	SWRN	55.7	22	AGRL	67	24	FSRE	51.2
19	SWRN	55.7	22	AGRL	67	24	FSRE	51.2
19	SWRN	55.7	22	FSRE	51.2	24	FSRE	51.2
19	SWRN	55.7	22	FSRE	51.2	24	FSRE	51.2
19	SWRN	55.7	22	FSRE	51.2	24	FSRE	51.2
19	SWRN	55.7	22	FSRE	51.2	24	FRST	54.5
19	SWRN	55.7	22	FSRE	51.2	24	FRST	54.5
19	WATR	81.7	22	FSRE	51.2	24	FRST	54.5
20	AGRL	73	22	FSRE	51.2	24	FRST	54.5
20	AGRL	73	22	FRST	54.5	24	FRST	54.5
20	AGRL	73	22	FRST	54.5	24	FRST	54.5
20	AGRL	73	22	FRST	54.5	24	FRST	54.5
20	AGRL	73	22	RNGB	55.7	24	RNGB	55.7
20	PAST	68.4	22	RNGB	55.7	24	RNGB	55.7
20	PAST	68.4	22	RNGB	55.7	24	RNGB	55.7
20	PAST	68.4	22	RNGB	55.7	24	RNGB	55.7
20	PAST	68.4	22	RNGB	55.7	24	RNGB	55.7
20	AGRR	76.3	22	RNGB	55.7	24	RNGB	55.7
20	AGRR	76.3	22	RNGB	55.7	24	RNGB	55.7

SBBSN	LULC	CN2	SBBSN	LULC	CN2	SBBSN	LULC	CN2
24	SWRN	55.7	26	AGRR	69.9	27	RNGB	55.7
24	SWRN	55.7	26	AGRR	69.9	27	RNGB	55.7
24	SWRN	55.7	26	AGRR	69.9	28	FESC	53.4
24	SWRN	55.7	26	AGRR	69.9	28	FESC	53.4
24	SWRN	55.7	26	AGRR	69.9	28	FESC	53.4
25	BERM	85.4	26	AGRR	69.9	28	FESC	53.4
25	BERM	85.4	26	AGRR	69.9	28	AGRL	67
25	BERM	85.4	26	AGRR	69.9	28	AGRL	67
25	BERM	85.4	26	AGRR	69.9	28	AGRL	67
25	FESC	53.4	26	FSRE	51.2	28	AGRL	67
25	FESC	53.4	26	FSRE	51.2	28	AGRL	67
25	FESC	53.4	26	FSRE	51.2	28	AGRR	69.9
25	FESC	53.4	26	FSRE	51.2	28	AGRR	69.9
25	AGRL	67	26	FSRE	51.2	28	AGRR	69.9
25	AGRL	67	26	FSRE	51.2	28	AGRR	69.9
25	AGRL	67	26	FSRE	51.2	28	RNGB	55.7
25	AGRL	67	26	FSRE	51.2	28	RNGB	55.7
25	AGRL	67	26	RNGB	55.7	28	RNGB	55.7
25	AGRR	69.9	26	RNGB	55.7	28	RNGB	55.7
25	AGRR	69.9	26	RNGB	55.7	28	SWRN	55.7
25	AGRR	69.9	26	RNGB	55.7	28	SWRN	55.7
25	AGRR	69.9	26	RNGB	55.7	28	SWRN	55.7
25	RNGB	55.7	26	RNGB	55.7	28	SWRN	55.7
25	RNGB	55.7	26	RNGB	55.7	29	FESC	53.4
25	RNGB	55.7	26	RNGB	55.7	29	FESC	53.4
25	RNGB	55.7	26	SWRN	55.7	29	FESC	53.4
25	SWRN	55.7	26	SWRN	55.7	29	FESC	53.4
25	SWRN	55.7	26	SWRN	55.7	29	FESC	53.4
25	SWRN	55.7	26	SWRN	55.7	29	FESC	53.4
25	SWRN	55.7	26	SWRN	55.7	29	FESC	53.4
26	FESC	53.4	26	SWRN	55.7	29	AGRL	67
26	FESC	53.4	26	SWRN	55.7	29	AGRL	67
26	FESC	53.4	26	SWRN	55.7	29	AGRL	67
26	FESC	53.4	26	SWRN	55.7	29	AGRL	67
26	FESC	53.4	27	FESC	53.4	29	AGRL	67
26	FESC	53.4	27	FESC	53.4	29	RNGB	55.7
26	FESC	53.4	27	FESC	53.4	29	RNGB	55.7
26	FESC	53.4	27	FESC	53.4	29	RNGB	55.7
26	FESC	53.4	27	AGRL	67	29	RNGB	55.7
26	AGRL	67	27	AGRL	67	29	RNGB	55.7
26	AGRL	67	27	AGRL	67	29	RNGB	55.7
26	AGRL	67	27	AGRL	67	29	RNGB	55.7
26	AGRL	67	27	AGRL	67	29	SWRN	55.7
26	AGRL	67	27	AGRR	69.9	29	SWRN	55.7
26	AGRL	67	27	AGRR	69.9	29	SWRN	55.7

SBBSN	LULC	CN2	SBBSN	LULC	CN2	SBBSN	LULC	CN2
30	FESC	53.4	31	RNGB	55.7	32	SWRN	55.7
30	FESC	53.4	31	RNGB	55.7	32	SWRN	55.7
30	FESC	53.4	31	SWRN	55.7	32	SWRN	55.7
30	FESC	53.4	31	SWRN	55.7	32	SWRN	55.7
30	FESC	53.4	31	SWRN	55.7	33	FESC	53.4
30	AGRL	67	31	SWRN	55.7	33	FESC	53.4
30	AGRL	67	32	FESC	53.4	33	FESC	53.4
30	AGRL	67	32	FESC	53.4	33	FESC	53.4
30	AGRL	67	32	FESC	53.4	33	FESC	53.4
30	AGRL	67	32	FESC	53.4	33	FESC	53.4
30	AGRR	69.9	32	FESC	53.4	33	FESC	53.4
30	AGRR	69.9	32	FESC	53.4	33	FESC	53.4
30	AGRR	69.9	32	FESC	53.4	33	AGRL	67
30	AGRR	69.9	32	FESC	53.4	33	AGRL	67
30	AGRR	69.9	32	AGRL	67	33	AGRL	67
30	FSRE	51.2	32	AGRL	67	33	AGRL	67
30	FSRE	51.2	32	AGRL	67	33	AGRL	67
30	FSRE	51.2	32	AGRL	67	33	AGRL	67
30	FSRE	51.2	32	AGRL	67	33	AGRL	67
30	FRST	54.5	32	AGRL	67	33	AGRL	67
30	FRST	54.5	32	AGRL	67	33	RNGB	55.7
30	FRST	54.5	32	AGRL	67	33	RNGB	55.7
30	RNGB	55.7	32	AGRL	67	33	RNGB	55.7
30	RNGB	55.7	32	AGRR	69.9	33	RNGB	55.7
30	RNGB	55.7	32	AGRR	69.9	33	RNGB	55.7
30	RNGB	55.7	32	AGRR	69.9	33	RNGB	55.7
30	SWRN	55.7	32	AGRR	69.9	33	RNGB	55.7
30	SWRN	55.7	32	AGRR	69.9	33	RNGB	55.7
30	SWRN	55.7	32	AGRR	69.9	33	SWRN	55.7
30	SWRN	55.7	32	AGRR	69.9	33	SWRN	55.7
31	FESC	53.4	32	AGRR	69.9	33	SWRN	55.7
31	FESC	53.4	32	FSRE	51.2	33	SWRN	55.7
31	FESC	53.4	32	FSRE	51.2	33	SWRN	55.7
31	FESC	53.4	32	FSRE	51.2	33	SWRN	55.7
31	AGRL	67	32	FSRE	51.2	33	SWRN	55.7
31	AGRL	67	32	FSRE	51.2	33	SWRN	55.7
31	AGRL	67	32	FSRE	51.2	34	FESC	53.4
31	AGRL	67	32	FSRE	51.2	34	FESC	53.4
31	AGRL	67	32	RNGB	55.7	34	FESC	53.4
31	FSRE	51.2	32	RNGB	55.7	34	FESC	53.4
31	FSRE	51.2	32	RNGB	55.7	34	AGRL	67
31	FSRE	51.2	32	RNGB	55.7	34	AGRL	67
31	FSRE	51.2	32	RNGB	55.7	34	AGRL	67
31	FRST	54.5	32	RNGB	55.7	34	AGRL	67
31	FRST	54.5	32	RNGB	55.7	34	SWRN	55.7

SBBSN	LULC	CN2	SBBSN	LULC	CN2	SBBSN	LULC	CN2
35	FESC	53.4	38	AGRL	67	41	FSRE	51.2
35	FESC	53.4	38	AGRL	67	41	FSRE	51.2
35	FESC	61.7	38	FSRE	51.2	41	FRST	54.5
35	FESC	61.7	38	FSRE	51.2	41	FRST	54.5
35	FESC	61.7	38	FSRE	51.2	41	FRST	54.5
35	FESC	61.7	38	FSRE	51.2	41	FRST	54.5
35	AGRL	67	38	FSRE	51.2	41	FRST	54.5
35	AGRL	67	38	FSRE	51.2	41	FRST	54.5
35	AGRL	67	38	RNGB	55.7	41	RNGB	55.7
35	AGRL	67	38	RNGB	55.7	41	RNGB	55.7
35	AGRL	67	38	RNGB	55.7	41	RNGB	55.7
35	RNGB	55.7	38	RNGB	55.7	41	RNGB	55.7
35	RNGB	55.7	38	RNGB	55.7	41	RNGB	55.7
35	RNGB	55.7	38	RNGB	55.7	41	RNGB	55.7
35	RNGB	55.7	38	RNGB	55.7	41	RNGB	55.7
35	SWRN	55.7	38	SWRN	55.7	41	SWRN	55.7
35	SWRN	55.7	38	SWRN	55.7	41	SWRN	55.7
35	SWRN	55.7	38	SWRN	55.7	41	SWRN	55.7
35	SWRN	55.7	38	SWRN	55.7	41	SWRN	55.7
36	FESC	53.4	38	SWRN	55.7	41	SWRN	55.7
36	FESC	53.4	38	SWRN	55.7	41	SWRN	55.7
36	FESC	53.4	38	SWRN	55.7	42	FESC	53.4
36	FESC	53.4	39	AGRL	67	42	FESC	53.4
36	AGRL	67	39	AGRL	67	42	FESC	53.4
36	AGRL	67	39	AGRL	67	42	FESC	53.4
36	AGRL	67	39	PAST	61.7	42	AGRL	67
36	AGRL	67	39	PAST	61.7	42	AGRL	67
36	FSRE	51.2	39	PAST	61.7	42	AGRL	67
36	FSRE	51.2	40	AGRL	67	42	AGRL	67
36	FSRE	51.2	40	AGRL	67	42	AGRL	67
36	SWRN	55.7	40	AGRL	67	42	SWRN	55.7
36	SWRN	55.7	40	AGRL	67	42	SWRN	55.7
36	SWRN	55.7	40	RNGB	55.7	42	SWRN	55.7
36	SWRN	55.7	40	RNGB	55.7	42	SWRN	55.7
37	AGRL	67	40	RNGB	55.7	43	FESC	53.4
37	AGRL	67	40	RNGB	55.7	43	FESC	53.4
37	AGRL	67	40	SWRN	55.7	43	FESC	53.4
37	AGRL	67	40	SWRN	55.7	43	FESC	53.4
37	SWRN	55.7	40	SWRN	55.7	43	AGRL	67
37	SWRN	55.7	40	SWRN	55.7	43	AGRL	67
37	SWRN	55.7	41	AGRL	67	43	AGRL	67
37	SWRN	55.7	41	AGRL	67	43	AGRL	67
38	AGRL	67	41	AGRL	67	43	AGRL	67
38	AGRL	67	41	AGRL	67	43	AGRR	69.9
38	AGRL	67	41	AGRL	67	43	AGRR	69.9

SBBSN	LULC	CN2	SBBSN	LULC	CN2	SBBSN	LULC	CN2
43	RNGB	55.7						
43	RNGB	55.7						
43	SWRN	55.7						
43	SWRN	55.7						
43	SWRN	55.7						
43	SWRN	55.7						

Where SBBSN stands for subbasin, LULC for land use land cover, and CN2 for potential curve number in the appendix A.